Characterization of antagonistic interbacterial pathways at the single-cell level

Michele LeRoux

A dissertation

submitted in partial fulfillment of the

requirements for the degree of

Doctor of Philosophy

University of Washington

2015

Reading Committee:

Joseph D. Mougous, Chair

E. Peter Greenberg

Brad Cookson

Program Authorized to Offer Degree:

Molecular and Cellular Biology

University of Washington

Abstract

Characterization of antagonistic interbacterial pathways at the single-cell level

Michele LeRoux

Chair of the Supervisory Committee:
Associate Professor, Joseph D. Mougous
Department of Microbiology

Antagonistic pathways are nearly universal among free-living bacteria, and may determine which organisms co-exist in polymicrobial communities. Bacteria have also evolved pathways that can sense and respond to assaults from competitors. In this work, I characterize interbacterial interactions mediated by the type VI secretion system (T6SS), and describe the integration of this antagonistic factor into a global regulatory pathway that senses and responds to danger from bacterial competitors. I developed tools to investigate interbacterial antagonism at the single-cell level, and applied these tools to the characterization of interbacterial interactions mediated by the Hcp-secretion Island I T6SS (H1-T6SS) of *Pseudomonas aeruginosa*. This approach revealed that T6S-dependent interactions require direct cell–cell contact and that T6SS

effectors induce recipient cell lysis. Furthermore, I discovered that H1-T6S-mediated intoxication is more likely to occur when the recipient has an active T6SS itself. The mechanistic underpinnings of this observation are two-fold. First, preferential localization of the apparatus towards cells with an active T6SS suggests that assembly of the apparatus is spatiotemporally coordinated between neighboring cells. Second, I found that H1-T6SS expression is induced when cells are in direct contact with a competitor – a form of innate immunity that we term danger sensing. *P. aeruginosa* senses antagonism by detecting lysed kin cells via the Gac/Rsm regulatory pathway. This global regulatory pathway stimulates increased expression of the T6SS, as well as other offensive and defensive factors that collectively promote fitness in co-culture with a competitor. Finally, I utilized the single-cell analysis tools to characterize the outcomes and mechanisms of a potential programmed cell-death pathway of *P. aeruginosa*. This pathway responds to DNA damage, and provides an advantage in an *in vivo* infection model. Utilizing a single-cell approach to study bacteria within communities has uncovered the environmental significance and ramifications of interbacterial pathways.

Table of Contents

List of Figures

List of Tables

Acknowledgements

My parents, Tessa and Johann LeRoux, are both exceptional teachers and scholars who have always encouraged and nurtured my interest in intellectual pursuits, while modeling the importance of work-life balance and family. Their decision to move our family from South Africa to the United States gave me access to an excellent education, but required significant career sacrifices for them. Over the past several years, their support and love has been invaluable. I am also incredibly grateful for my sister, Nicole LeRoux, whose physical distance did not diminish the support and encouragement she provided me throughout this time. Finally, I would like to thank my husband, David Rosen, who has shared in all of my accomplishments and disappointments throughout graduate school and has provided me with incredible day-to-day support.

An exceptional biology teacher, Emily Norton, awakened my passion for biology in high school. This interest in biology was nurtured at Colgate University where I was fortunate to have inspiring teachers and participate in exciting primary research both off-campus at the National Institutes of Health and on campus at Colgate University. I would specifically like to thank Dr. Krista Ingram, whose laboratory I worked in for two years. Her encouragement, support, and scientific training laid the groundwork for my graduate work, and she continues to be an inspiring role model. I would also like to thank Dr. Johanna Daily and Dr. Dyann Wirth, who were my supervisors during my time as a research assistant at the Harvard School of Public Health, where I was first exposed to the study of microbes. Two family friends provided essential advice: Joe Aieta, who wisely nudged me off the path to medical school when I was a

first year in college, and Gavin Barnard, who encouraged me during college and throughout my years in graduate school.

The Mougous lab has been a supportive, fun, and nurturing environment, in large part due to my fantastic colleagues, many of whom have become good friends. I want to thank Julie Silverman, Rachel Hood, Li Mo, Sandra Schwarz, Justin De Leon, Alistair Russell, Seemay Chou, John Whitney, Danielle Agnello, Brittany Harding, Aria Eshraghi, Kaitlyn LaCourse, Snow Brook Peterson, Elena Montauti, Taylor Gardiner, Max Ferrin, and Jungyun (Rachel) Kim. I especially valued the mentorship, support, and friendship of Brook Peterson, Seemay Chou, Julie Silverman, and Sandra Schwarz. I am also grateful to Elena Montauti, an undergraduate who worked with me for two years, for her dedication and enthusiasm, and to Robin Kirkpatrick, a technician who worked closely with me on Chapter 3 of this thesis.

I immensely valued the camaraderie of many graduate students and postdocs in the Microbiology department, including the "Kbac" group who created a welcoming community. In particular, I want to acknowledge Kelly Colvin and Boo Shan Tseng, both of whom guided me and became good friends. Graduate school would not have been the same without my close friend and classmate, Sarah Wilson, who went through many of the ups and downs of grad school with me.

I would like to thank my committee members, Brad Cookson, Pete Greenberg, Pradeep Singh, David Fredricks, and Bill Parks for their advice, scientific input, and support. I would specifically like to thank the members of my reading committee, Brad Cookson and Pete Greenberg.

This work would not have been possible without our long time collaborator, Paul Wiggins, who exposed me to the physicist's perspective on biology, and spent many hours of his

time teaching me fundamental aspects of microscopy, coding in Matlab, and thinking about image data quantitatively. Thanks also to his postdoc, Nathan Kuwada, who is extremely patient and generous with his time, and helped me with many technical aspects of our single-cell analysis software.

Finally, thanks to my graduate advisor, Joseph Mougous. Joseph's mentorship has taken many forms, ranging from hands on training in designing and executing successful experiments, effective science communication, to subtle but critical skills such as determination and confidence. His enthusiasm and drive are infectious, and it has been a privilege to watch the lab evolve and succeed. Throughout my time in the lab, Joseph's commitment to my education and success has been constant and unwavering, and I am incredibly fortunate to have had the opportunity to train in his lab.

Dedication

To my parents, Tessa and Johann le Roux.

Chapter 1. Introduction

Portions of this chapter are currently under review:
LeRoux M., Peterson S.B., and Mougous J.D. Bacterial Danger Sensing. *Journal of Molecular Biology*.

1.1 Bacterial danger sensing

Viewed classically, an immune system relies on specialized cell types to detect the presence of threats and orchestrate a response. The discovery of the CRISPR/CAS system in bacteria has challenged this long-held perspective and demonstrated that even adaptive immunity is feasible in a single-cell organism (1). Given that prokaryotes are among the most ancient and successful life forms, it would be surprising if they had not also evolved the ability to detect more generalized forms of danger and take protective measures, akin to the innate arm of immunity in eukaryotes.

Innate immune systems of multicellular organisms function by detecting molecules associated with invasion by pathogens. One such class of molecules consists of conserved cellular components of the pathogens themselves, termed pathogen-associated molecular patterns (PAMPs). Interaction between PAMPs and pattern recognition receptors (PRR) stimulates an inflammatory response during which effector cells are recruited to eliminate the danger and repair tissue. More recently, this paradigm has been extended to include a class of immunostimulatory molecules termed damage associated molecular patterns (DAMPs) (2). DAMPs arise when endogenous molecules that make up a healthy cell are mislocalized to the extracellular milieu due to necrosis or cell damage. Many of the same PRRs that respond to PAMPs, including Toll- and Nod-like receptors, have the capacity to recognize these so-called danger signals (3, 4). Eukaryotes thus detect exogenous and endogenous molecules that indicate danger and launch appropriate responses.

For a bacterium to sense and respond to danger, these actions must somehow occur within the context of an individual cell or a distributed population of genetically identical cells. This would require the capacity to sense a set of cues that are associated with a threat and

respond with measures that eliminate the source of danger, prevent an attack, or minimize damage resulting from an attack. Here we assemble an assortment of published studies and reevaluate their significance in light of the hypothesis that bacteria – in a process we term danger sensing – recognize exogenous self- and non-self-derived molecules and respond in a concerted fashion with protective measures, akin to the eukaryotic innate immune system.

1.1.1 *Danger sensing in bacteria*

Bacteria face constant threats to their survival, including environmental factors (e.g. extreme temperature, nutrient limitation, ultraviolent radiation) and antagonism by other organisms. For the purposes of this review, we will focus on biotic threats that derive from bacterial competitors. Interbacterial competition has been honed over eons as microbes battle for overlapping niches. Bacteria overtly antagonize each other with diffusible small molecule antibiotics, antimicrobial peptides (AMPs), proteineaceous toxins, and contact-dependent toxin delivery pathways including the type VI secretion system (T6SS) and contact dependent inhibition (CDI), among other mechanims (5-9). Given that genes encoding antibacterial factors are virtually universal within bacterial genomes, it would be surprising if bacteria had not evolved generalized cellular programs, i.e., danger sensing pathways, for counteracting them.

Danger sensing is complementary to, but distinct from concept of "competition sensing", recently put forth by Cornforth and Foster. To explain the observation that toxin production is a component of many general stress responses, these authors propose that bacteria have evolved to recognize generalized cell damage as an indication of competitors (10). In contrast, danger sensing is a multicellular behavior that occurs when bacteria detect exogenous self- and non-self-derived molecules to survey their surroundings for threats. There are three components of the

danger sensing process that we delineate. First are the molecular species that indicate a threat (Figure 1-1). Just as eukaryotes have the ability to sense PAMPs and mislocalized self-derived molecules (DAMPs), we find literature demonstrating that bacteria can also sense self and non-self-derived cues and respond with measures to mitigate the danger. The second component is the signal transduction mechanism that detects these danger signals (Figure 1-2). Where the signal transduction mechanism has been characterized, this is most often a two-component regulatory system (TCS), but other types of regulatory pathways are also employed. Last is the response, which is defined by the factor(s) modulated by the danger-responsive signal transduction pathway(s) (Figure 1-3). In the majority of examples we cite, responses consist of the elaboration of both

1.1.2 *Responses to self-produced molecules resulting from cellular damage*

The PhoPQ pathway has been studied most extensively in the pathogen *Salmonella enterica* (11). The sensor kinase PhoQ recognizes cues associated with the intracellular niche of the bacterium (AMPs, low pH, and low Mg^{2+} concentration), and acting through its cognate response regulator *phoP,* induces a multifaceted cellular program that enhances survival *in vivo* (12-14) (Figure 1B). However, the PhoPQ system is found in many bacteria that are not adapted to an intracellular, or even host-associated, lifestyle. We propose that in these bacteria, PhoPQ could serve as the signal transduction mechanism within a conserved danger sensing pathway. Under certain circumstances, each of known stimuli of PhoPQ could indicate a proximal threat. One consequence of PhoPQ sensitivity to Mg^{2+} is that cells respond to the presence of extracellular DNA (eDNA), which can sequester large quantities of the cation (15, 16). Since eDNA is released when cells lyse, PhoPQ is in effect responsive to intercellular antagonism.

Consistent with a role for this pathway in mediating a response to danger, the PhoPQ regulon induces outer membrane modifications that provide protection from antimicrobials, most notably the AMPs (17). For example, PhoPQ activates the PmrAB TCS, which induces the covalent modification of lipid A with aminoarabinose and ethanolamine. Collectively, these changes prevent the integration of AMPs into the membrane by an overall reduction of the negative charge of lipopolysaccharide. (18).

1.1.3 *Responses to exogenous cues that alert cells to danger*

Sensing and responding to antibacterial molecules. In many tissues of eukaryotes, any sign of the presence of another organism indicates that a barrier has been breached and an immune response is warranted. Eukaryotes have thus evolved the capacity to sense conserved yet intrinsically harmless bacterial structures such as flagellin and lipopolysaccharide. In contrast, free-living bacteria rarely exist in isolation from other microbes and therefore responding to such molecules would lead to a constant state of immune activation. We predict that this is an underlying explanation for prevalence of pathways in bacteria that instead sense the effectors of interbacterial antagonism. Such cues signify the proximity of rival cells while simultaneously allowing bacteria to differentiate between friend and foe. Decades of literature regarding bacterial responses to antibiotics support the supposition that toxins can be detected. However, to assess whether such a detection mechanism constitutes a true danger response, it is important to distinguish between the responses that occur due to antibiotic-induced cellular damage (e.g. general stress responses) and those that occur at sub-inhibitory concentrations in which the antibiotic serves as a signaling molecule.

One type of response to antimicrobials consists of an antibiotic stimulating expression of a single operon encoding a corresponding resistance determinant, a process termed adaptive resistance. The cassettes that encode tetracycline and vancomycin resistance are two of the most well characterized examples of this process. In both cases, a negative regulator directly interacts with the antibiotic to relieve repression of resistance genes encoded in the same operon. Specifically, when tetracycline binds to the repressor, TetR, expression of the tetracycline efflux pump, TetA, is induced (19). Vancomycin is sensed by the VanRS TCS, which induces a modification of the antibiotic target, a precursor for peptidoglycan synthesis (20). Accordingly, these gene clusters can be considered to function as highly specific danger sensing pathways wherein a given antibiotic is sensed by a signal transduction mechanism to mediate resistance.

Antimicrobials at sub-inhibitory concentrations have also been reported to stimulate more complex regulons encompassing diverse protective mechanisms, including antibiotic production, spore formation, exopolysaccharide synthesis, or a combination of these functions (21-23). In one of the first studies of the effects of sub-inhibitory antibiotics on bacterial physiology, it was demonstrated that tobramycin induces production of exopolysaccharides in *P. aeruginosa* (24). This effect is mediated by production of the secondary messenger, cyclic di-GMP, although the sensor responsible for detecting tobramycin has not been identified. Increased exopolysaccharide production by *P. aeruginosa* in turn confers enhanced resistance to tobramycin and other aminoglycoside antibiotics (25). This phenomenon has largely been considered in the clinical context where tobramycin is used to treat cystic fibrosis patients with pulmonary *P. aeruginosa* infections. However, tobramycin is a natural product synthesized by the environmental bacterium *Streptomyces tenebrarius* (26). We thus might view increased production of

exopolysaccharides by *P. aeruginosa* in response to tobramycin as an antibiotic danger sensing pathway that could have evolved in response to interbacterial antagonism in the environment.

Responding to subinhibitory concentrations of antibiotics by increasing exopolysaccharide production is a response to danger also exhibited by Gram-positive organisms. A recent study demonstrated that the thiocillin antibiotics – a class of peptide antibiotics produced by members of the *Streptomyces* and *Bacilli* – induce exopolysaccharide production in *Bacillus subtilis.* The response occurs by an unknown mechanism that does not require KinD, an established regulator of exopolysaccharide production in *B. subtilis.* The authors of this study also elegantly established that the signaling function of thiocillin is independent of its toxicity; non-toxic versions of the peptides generated by genetically modifying the biosynthesis locus retained their exopolysaccharide-stimulatory activity (27).

In other Gram-positive organisms, sub-inhibitory antibiotics can induce a complex developmental program that consists of production of multicellular aggregates, spore formation, and antibiotic synthesis. For example, in *Streptomyces coelicolor*, the angucycline class of antibiotics induces production of the antibiotic undecylprodigiosin along with aerial hyphae that help distribute spores (28). Angucyclines are synthesized by other *Streptomyces* species and are detected in *S. coelicolor* by a gamma-butyrolactone-like receptor, ScBR2, which in turn directly regulates the response (28). A related phenotypic response is induced in *S. coelicolor* in the presence of the predatory bacterium *Myxococcus xanthus*, but the signal and receptor mediating this effect have not been identified (29). *M. xanthus* also induces a range of phenotypic responses in environmental *B. subtilis* strains. This can include production of the antibiotic bacillaene or the formation of spore-filled aggregates, both of which confer protection from predation (29-32).

Many of the above pathways that we have recast as danger sensing pathways were originally studied in the context of virulence. Bacterial pathogenesis has also been the lens through which most studies have viewed the response of bacteria to the diverse group of antimicrobials known as AMPs, no doubt due to the important role these molecules play in eukaryotic innate immunity. However, AMPs are also synthesized by many species of bacteria. For example, lantibiotics such as nisin are ribosomally encoded, post-translationally modified peptide antibiotics that mediate antagonism between Gram-positive organisms. Polymyxin B and colistin are cationic lipopeptides produced by *Bacillus polymyxa* that have been widely adopted for clinical uses.

Although diverse in structure, AMPs are commonly cationic, and exert toxicity by interacting with the negatively charged bacterial cell surface. As a result of this common mechanism of action, responses to AMPs across bacterial species also share a number of common features. In contrast to the pathways that detect specific antibiotics discussed earlier in this section, the sensors that perceive AMPs are generally more promiscuous (33, 34). For example, the *aps* three-component regulator/sensor system in *Staphylococcus* spp. is stimulated by a variety of cationic AMPs, including molecules produced by eukaryotes and others that are bacterially synthesized. AMP recognition in this system is mediated by an interaction between the positively charged peptides and an extracellular acidic loop present on the membrane-associated sensor kinase AmpS (35). In Gram-negative bacteria, a major player in the response to AMPs is the PhoPQ TCS. As in the case of ApsS activation, the positive charge of AMPs is crucial for stimulating activation through PhoPQ (36). Bacteria can also have multiple, partially redundant pathways for detection of AMPs. In *P. aeruginosa*, for example, the TCSs PmrAB

(37), ParRS (38), and CprRS (39) act along with PhoPQ (11, 40) to sense and respond to a wide range of AMPs.

AMP-sensing pathways in both Gram-negative and Gram-positive species respond by inducing modifications to the cell surface that confer enhanced AMP resistance. The PhoPQ system, for instance, induces the synthesis and incorporation into lipid A of the positively charged molecule aminoarabinose. The resulting loss of negative charge on the cell surface can then reduce interaction with AMPs. The Aps system in *Staphyloccocus* spp. also regulates functions that lead to decreased negative charge on the cell surface, in this case D-alanyl group addition to teichoic acids in the cell wall and the substitution of negatively charged lipid phosphatidylglycerol in the cell membrane with the neutral species lysyl-phosphatidylglycerol. Induction of export systems can also contribute to enhanced AMP resistance, as in the case of VraFG upregulation by the Aps system (41).

Owing to the fact that sub-inhibitory concentrations of AMPs induce expression of factors that protect cells from their toxicity, AMP-sensing pathways fall within the danger sensing framework. Indeed, they have previously been likened to a prokaryotic innate immune system (33). Given the prevalence of AMP production by bacteria, we hypothesize that adaptive resistance pathways evolved primarily in response to bacterial AMPs and later contributed to the ability of free-living organisms to become opportunistic pathogens. Future experiments are needed to assess the extent to which AMP-sensing pathways affect fitness during interbacterial competition.

Responding to signaling molecules produced by other species ('eavesdropping').

As described above, direct detection of the effectors of bacterial antagonism is one means by which bacteria could distinguish friend from foe. Quorum sensing signals are a second class

of molecules with several characteristics that make them attractive candidates to serve a PAMP-like function for bacteria. First, most quorum sensing signals are species or even strain-specific, which makes detection of foreign signals a good proxy for the presence of another species. Additionally, by being freely diffusible, their concentration in the environment could be an indication of the population density of a competitor species. Finally, quorum sensing often regulates the production of antagonistic factors, such as diffusible antibiotics (42); signal detection could thus be a means of detecting the presence of a potentially antagonistic neighbor.

A molecule termed diffusible signaling factor (DSF) (cis-2-dodecanoic acid), is a recently characterized quorum sensing signal produced by *Xanthomonas* species, *Stenotrophomonas maltophilia* and *Burkholderia cenocepacia* (43, 44). Ryan and colleagues demonstrated that *P. aeruginosa* detects DSF produced by *Stenotrophomonas maltophilia* (Figure 1C) using a putative sensor kinase that contains a signal binding domain with homology to known DSF receptors (45). Upon detection of DSF, *P. aeruginosa* synthesizes increased quantities of exopolysaccharides and induces expression of the aminoarabinose membrane modification pathway that protects against AMPs. Recasting this pathway from the perspective of danger sensing, DSF is a signal that coincides with the presence of a competitor to stimulate behaviors that can be considered protective, or defensive.

A second example of interspecies signal detection that we propose can be interpreted as danger sensing has been described for the bacterium *Chromobacterium violaceum* (46). The acyl-homoserine lactone (acyl-HSL) receptor (LasR homolog CviR) of this bacterium senses not only its cognate acyl-HSL, but also related signals produced by other species. Upon binding to a signal, CviR induces the production of antibiotics, providing increased fitness in the presence of

antagonistic organisms. This ability to mount an antagonistic response to the detection of a non-self signaling molecule follows the paradigm of bacterial danger sensing we have elaborated.

Finally, a number of so-called “orphan” or “solo” LuxR homologues have been identified that lack a linked quorum sensing signal synthase(47). While the function of these proteins remains largely unclear, it has been previously proposed that a subset of orphan LuxR homologues could function in interspecies signaling (47, 48).We suggest orphan LuxR proteins could function in danger sensing pathways by providing a means of recognizing foreign signals and inducing protective functions, a possibility that remains to be experimentally tested.

1.1.4 *Competence as a response to danger*

Competence and competition among closely related organisms. Along with the strategies described above, bacteria possess another behavior that we argue constitutes a response to danger – the ability to take up foreign DNA and incorporate it into their genomes in a process termed natural competence. One cannot a priori categorize competence as either offensive or defensive, as this designation would depend on the precise function conferred by the incoming DNA. If this genetic material promotes DNA repair by serving as a template, competence would be playing a defensive role. Foreign DNA can also be incorporated into the genome of the recipient organism, a process referred to as horizontal gene transfer (HGT). If the incorporated DNA encodes an immunity determinant to a toxin from a competitor, this would again fulfill a defensive function and promote survival in the presence of competition.

In contrast, competence could be thought of as offensive if it promotes the acquisition of factors such as toxins that directly counter the threat. In certain cases, including T6SS- and CDI-associated toxins, horizontal exchange among divergent bacterial species is almost certainly

facilitated by the placement of modular toxin domains within repetitive flanking sequences. Such regions frequently include multiple immunity proteins, suggesting that HGT may also promote expansion of the immunity repertoire of an organism. Experimental evidence suggests that immunity genes acquired within these clusters can be expressed and provide protection against cognate incoming toxins (49).

We present here two examples in which competence gene expression is incorporated into a complex regulon and is induced in response to detection of potential danger signals. In both cases, the regulon contains at least one instance of a clear antagonistic factor that acts by lysing competitor cells. It is conceivable that these toxins act both to eliminate competitors and also to liberate DNA for acquisition by competence. Furthermore, the co-regulation of competence with factors that we have previously implicated in danger sensing provides additional support for the contention that competence is also a response to danger.

Streptococcus pneumoniae and competence. *S. pneumoniae* senses antibiotics that inhibit DNA replication and responds by inducing competence and bacteriocin production. Through the lens of danger sensing, antibiotics produced by bacterial competitors can be viewed as threats that induce a complex survival response. This mechanism has been likened to an alternate SOS pathway; however, the fact that sub-inhibitory concentrations of antibiotics are sufficient to stimulate the competence regulon distinguishes it from a general stress response (50). Sensing and responding to DNA replication-inhibiting antibiotics occurs by a unique mechanism that exploits the genomic location of competence regulatory genes near the origin of replication. When cells are exposed to antibiotics that induce stalling of the replication fork, there is an increase in the copy number of all origin proximal genes. The increased gene copy number leads to elevated levels of the competence stimulating peptide pheromone (CSP,

encoded by *comC*), the two-component system that senses it (ComDE), the CSP transporter (ComAB), and the sigma factor responsible for late competence gene induction (ComX) (51, 52) (Figure 1D). Secreted CSP is detected by the TCS ComDE in adjacent cells, resulting in elevated expression of alternate sigma factor ComX and stimulation of competence throughout the population. The ComX regulon, which can be thought of as the response to danger, consists of over 100 genes, including competence genes and narrow range bacteriocins that target *Streptococcus* species.

Within *S. pneumoniae* there are at least three different variants of CSP, which only elicit a response from strains expressing the cognate receptor. Expression of proteins that provide immunity to CSP-regulated bacteriocins is also under CSP control. Therefore in a mixed population of multiple pherotypes, stimulation of one population will result in killing of the other due to its lack of constitutive immunity (53). Additionally, even within a single pherotype, response to CSP can be heterogeneous, resulting in lysis of genetically identical siblings, a consequence referred to as fratricide (54). Whether recombination occurs predominantly within or between pherotypes remains a matter of debate (55, 56). In either case, the outcome of co-regulation of competence with antibiotic production is that cells lysing as a result of bacteriocin activity provide a source of DNA for natural transformation. Considered from the perspective of danger sensing, the acquisition of DNA deriving from a different pherotype may provide a source of useful genetic material that encodes loci encoding the incompatible CSP or other co-varying traits. Natural competence may thus facilitate pheroconversion via HGT and ultimately promote survival in the presence of incompatible strains. Furthermore, the ComX regulon contains many components of unknown function, therefore the possibility that toxins with a broad target range are also part of the response cannot be ruled out. The *S. pnumoniae*

competence machinery is promiscuous in its capacity to take up DNA from a range of sources, therefore the possibility that this potential danger response extends to taking up DNA from other species remains a possibility.

***Vibrio cholera* and competence.** It was recently discovered that *V. cholerae* coordinately regulates the production of antagonistic factors with competence in response to chitin. Here we propose that chitin could be a danger signal that is unlike the cues discussed previously in that it does not derive from bacterial competitors, but nonetheless coincides with their proximity. In the marine environment, *Vibrio* species preferentially associate with nutritionally rich microenvironments such as the chitinous surfaces of invertebrates or their debris (57, 58). The resulting elevated bacterial density would necessarily lead to an increase in competition for nutrients and substrate, therefore the presence of chitin may be a cue that indicates a need for increased antagonism and protective measures. Growth on chitin has long been known to induce competence in *Vibrio cholera* via the *tfoX* regulator (59). Recently, characterization of the full TfoX regulon revealed that additionally, expression of the T6SS is induced (60). This led Borgeaud and colleagues to hypothesize that similar to bacteriocin production by *S. pneumoniae*, T6S-dependent lysis of competitors releases DNA that can be taken up by competence machinery. They went on to demonstrate that expression of T6S genes enhanced the frequency of natural transformation during co-culture with a susceptible competitor.

The coordination of antagonism with competence could facilitate the exchange of genes encoding either toxins that mediate competition or immunity determinants that protect from antagonism. Consistent with this hypothesis, T6S-associated effector gene clusters vary among *Vibrio cholerae* strains, whereas the T6SS apparatus is conserved (61). The variability of T6S-associated gene clusters is observed in a wide range of organisms. It will therefore be interesting

to investigate whether toxin or immunity acquisition occurs more rapidly in organisms that are naturally competent and coordinate this property with a lysis pathway.

Conclusions. Here we have reexamined existing literature from the perspective of a danger sensing hypothesis. We find evidence of pathways that function to sense microbial threats and coordinate responses in a range of bacteria, from pathogens (e.g. *S. pneumoniae, V. cholerae, S. enterica, P. aeruginosa*) to environmental organisms (e.g. *S. coelicolor*, *B. subtilis*). Based on the apparent prevalence of danger sensing pathways, we predict that targeted investigations will reveal that the capacity for danger sensing is a widespread and integral part of bacterial physiology.

1.2 The model system: the type VI secretion system of *P. aeruginosa*

P. aeruginosa is a Gram-negative opportunistic pathogen that chronically infects chronic wounds and the lungs of patients with cystic fibrosis. At both infection sites, *P. aeruginosa* frequently becomes untreatable and is strongly associated with increased morbidity and mortality (62, 63). *P. aeruginosa* acquisition often correlates with reduced diversity in these typically polymicrobial environments (63, 64). However, the mechanisms by which *P. aeruginosa* eliminates its competitors have not been determined. We hypothesize that interbacterial antagonistic pathways contribute to the ability of *P. aeruginosa* to compete with other bacteria, and may promote its success in these environments. One antagonistic pathway found in *P. aeruginosa* is the type VI secretion system (T6SS), and is a major focus of this dissertation.

The T6SS, a protein translocation apparatus with structural homology to contractile bacteriophage, delivers toxic effectors between two bacterial cells, which we refer to as the donor and recipient cell. These systems are widespread among Gram-negative bacteria, and are

typically encoded on large gene clusters that contain at least thirteen conserved genes, typically encoding structural components, and a variable number of accessory genes, that often encode regulatory components (65). The substrates of the system vary in number and are antibacterial toxins with a range of enzymatic activities (66). Each toxin is encoded in a bicistron adjacent a cognate immunity determinant; the resulting immunity protein neutralizes each toxin to prevent self-intoxication by kin cells. (67, 68).

The mechanism of effector delivery is not well understood and continues to be an active area of study. The proteins VgrG and Hcp are both secreted structural components that have recently been shown to each directly associate with a subset of substrates and mediate their export (69-72). VgrG is structurally homologous to bacteriophage tailspike and is thought to puncture recipient cells, while Hcp forms homohexameric rings that have been shown to stack in a head to tail configuration *in vitro* in a manner dependent on VgrG (73). There is direct evidence that effectors interact with the inner pore of Hcp rings, and that Hcp stabilizes and chaperones a subset of effectors in the donor cell (70). The proteins TssB and TssC form tubules with homology to the bacteriophage tail sheath. This sheath-like structure is highly dynamic within cells, and cryo-electron micrographs have captured both an extended and contracted state. Because TssB and TssC interact with Hcp, and the inside diameter of the TssB/TssC tubules are wide enough to accommodate Hcp rings, it is thought that contractions of the TssB/C sheath propel effectors into recipient cells. The only conserved ATPase of the system, ClpV, mediates disassembly of the TssB/C tubules and is thus thought to energize the contraction events (74, 75). Taken together, it has been proposed that effector-filled Hcp tubules, capped with a VgrG "spike", are propelled out of donor cells through the action of ClpV-mediated contraction of TssB/C tubules.

The genome of *P. aeruginosa* encodes three non-redundant, functionally distinct T6SSs (67, 76, 77). One of these systems, a model for study of the T6SS and the focus of my dissertation, is termed Hcp secretion island I encoded T6SS (H1-T6SS). The H1-T6SS exports seven antibacterial effectors, including enzymes that target the bacterial cell wall (66). The H1-T6SS is integrated into two global regulatory systems that control its expression. The LasR quorum sensing regulator transcriptionally represses H1-T6SS at quorum thresholds, while the pathway is post-transcriptionally regulated by the Gac/Rsm pathway (78-80). This global regulatory pathway reciprocally regulates traditional virulence factors such as the type III secretion system and flagellar synthesis with bacterial targeting factors such as the T6SS and the hydrogen cyanide biosynthesis genes (80). The activity of the H1-T6SS system is regulated at a post-translational level by the threonine phosphorylation pathway (81, 82). PpkA is a kinase that phosphorylates an H1-T6SS-associated forkhead-domain containing protein, Fha1, to activate the system. This activity is opposed by a phosphatase, PppA. Four additional proteins, TagQRST, act upstream of PpkA and PppA, although their precise functions have not been elucidated (81, 83). This pathway presumably fine-tunes effector delivery based on environmental conditions, although the activating cues are not known. A second, independent post-translational regulatory pathway consists of the negative regulator, TagF that responds to surface-associated growth (78).

1.3 Objectives of this thesis

The role of the T6SS in interbacterial antagonism is widely accepted; however, its impact on bacterial communities is not well understood. Likewise, several regulatory mechanisms have been identified, but the environmental cues that stimulate them are not known. Tools to

investigate interbacterial interactions at the single cell level would provide a means by which to observe and dissect the activity and regulation of the H1-T6SS in real time. My dissertation research had three objectives: 1) to develop tools to investigate interbacterial interactions and bacterial growth in communities quantitatively at the single-cell level; 2) to determine the spatiotemporal requirements of H1-T6SS-dependent intoxication and the outcome of intoxication on a bacterial co-culture; and 3) to investigate the integration of the H1-T6SS into the larger regulatory program of *P. aeruginosa*.

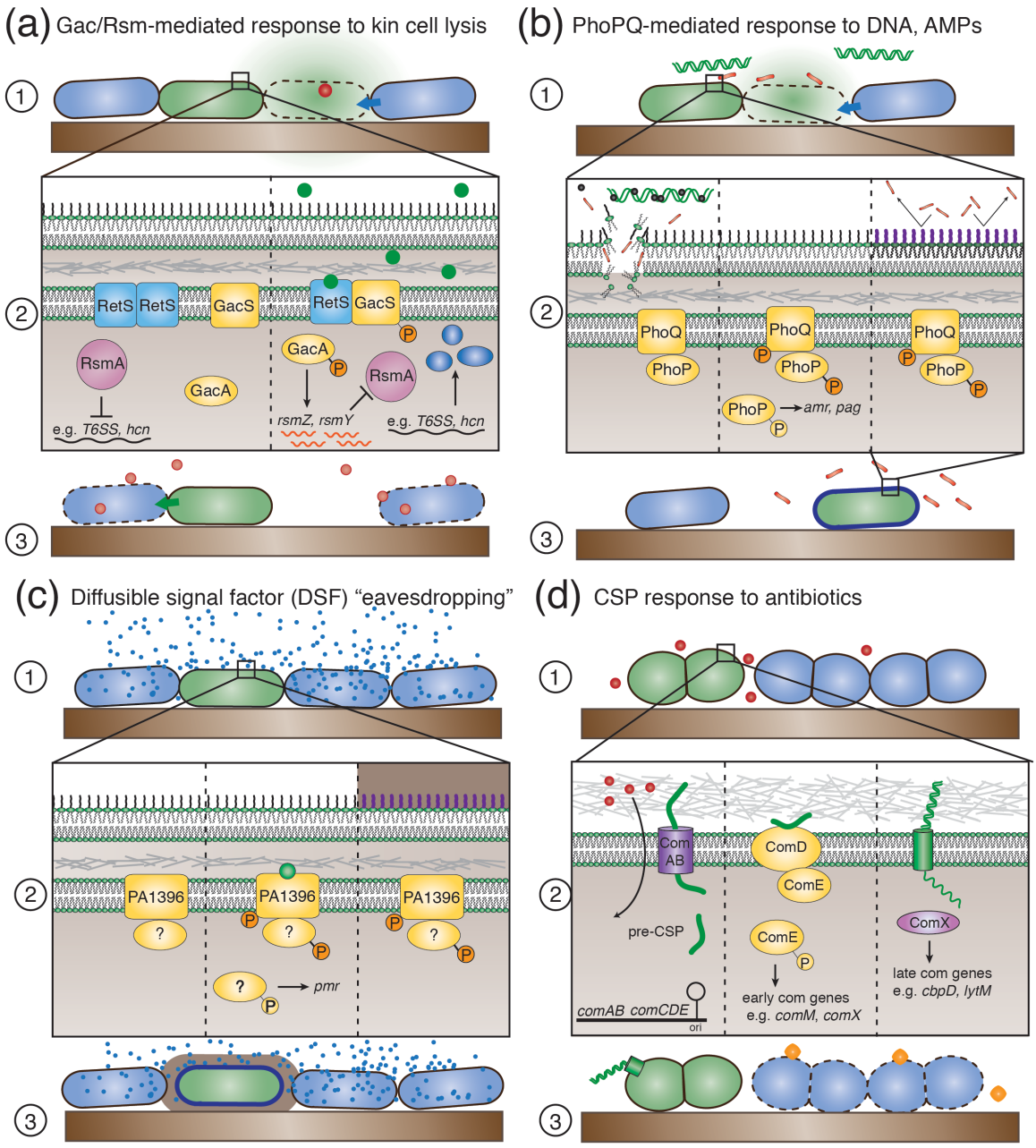

Figure 1.1: Examples of proposed danger sensing pathways Figure 1.
Danger sensing consists of bacteria sensing one or more danger cues (1) via a signal transduction mechanism (2), which stimulates a protective and/or antagonistic response (3).
(a) Gac/Rsm-mediated response to cell lysis. (1) A competitor (blue) lyses a subset of *P. aeruginosa* cells (green). (2) *P. aeruginosa* signal transduction. Left: the signal transduction pathway in the inactive state. Right: A mislocalized self-derived molecular from lysed *P. aeruginosa* stimulates the Gac/Rsm pathway to relieve negative regulation of targets (e.g. T6SS and hydrogen cyanide synthesis) (3) The outcome of this danger sensing mechanism is the increased production of antagonistic and protective factors that mitigate the danger.

(b) PhoPQ-mediated response to DNA and AMPs. (1) Competitor cells (blue) produce AMPs that lyse target cells (green). (2) Target cell signal transduction. Left panel: eDNA from lysed cells chelates cations, reducing the local Mg+ concentration. Middle: Low Mg+ concentrations and/or AMPs stimulate PhoPQ. Right panel: The PhoPQ regulon mediates changes to the outer membrane that reduce its overall negative charge. (3) Resulting membrane alterations protect cells from additional assault by AMPs.
(c) Diffusible signal factor (DSF) "eavesdropping". (1) The quorum sensing signal, DSF, is produced by *S. maltophilia* (blue) and sensed by *P. aeruginosa* (green). (2) *P. aeruginosa* signal transduction. Left: A putative sensor kinase (PA1396) in its inactive state. Middle: PA1396 detects DSF and stimulates its regulon. Right: Gene expression leads to changes in protective behaviors, e.g. outer membrane and increased production of exopolysaccharides. (3) This cellular program is thought to promote survival of *P. aeruginosa* in the presence of *S. maltophilia*.
(d) Response to antibiotics mediated by CSP. (1) *S. pneumoniae* (green) grown in the presence of a competitor (blue) that produces DNA replication targeting antibiotics. (2) Left: Stalling of the replication fork causes an increase in copy number of origin-proximal genes, e.g. ComAB and ComCDE, which leads to production of CSP. Middle: Exogenous CSP stimulates expression of the early Com genes including immunity protein (ComM), and the alternate sigma factor (ComX). Right: ComX producing cells increase expression of competence machinery and bacteriocin production. (3) Bacteriocins lyse susceptible surrounding cells and their DNA is acquired, promoting survival.

Chapter 2. Quantitative single cell characterization of bacterial interactions reveals type VI secretion is a double-edged sword

¶

Published as: LeRoux M., De Leon J. A., Kuwada N. J., Russell A. B., Pinto-Santini D., Hood R. D., Agnello D.M., Robertson S.M., and Mougous J.D. (2012). *Proceedings of the National Academy of Sciences*, *109*(48), 19804–19809.

2.1 Abstract

Interbacterial interaction pathways play an important role in defining the structure and complexity of bacterial associations. A quantitative description of such pathways offers promise for understanding the forces that contribute to community composition. We developed time-lapse fluorescence microscopy (TLFM) methods for quantitation of interbacterial interactions and applied these to the characterization of type VI secretion (T6S) in *Pseudomonas aeruginosa*. Our analyses allowed a direct determination of the efficiency of recipient cell lysis catalyzed by this intercellular toxin delivery pathway and provided evidence that its arsenal extends beyond known effector proteins. Measurement of T6S apparatus localization revealed correlated activation among neighboring cells, which, taken together with genetic data, implicate the elaboration of a functional T6S apparatus with a marked increase in susceptibility to intoxication. This possibility was supported by the identification of T6S-inactivating mutations in a genome-wide screen for resistance to T6S-mediated intoxication and by TLFM analyses showing a decreased lysis rate of recipient cells lacking T6S function. Our discoveries highlight the utility of single cell approaches for measuring interbacterial phenomena and provide a foundation for studying the contribution of a widespread bacterial interaction pathway to community structure.

2.2 Introduction

Though bacteria are often considered single-celled organisms, most possess complex mechanisms to facilitate intercellular information exchange. Some of these, such as quorum sensing, operate at a distance and coordinate the production of diffusible commodities (84, 85). Recent work has revealed evolutionarily distinct pathways present in Gram-negative bacteria that

are predicted to function at much closer length scales (5, 86), including Tra-mediated lipoprotein exchange in *Myxococcus xanthus* (87), and the widely distributed contact-dependent inhibition and type VI secretion systems (T6SSs) (88, 89). These pathways can exert dramatic phenotypic changes in neighboring cells, thus they likely play important roles in the development, composition, and homeostasis of bacterial communities.

The T6SS is a complex secretory apparatus with the ability to translocate effector proteins between Gram-negative bacterial cells (68, 78). Our knowledge of T6S effector protein function derives primarily from studies of the *Pseudomonas aeruginosa* Hcp Secretion Island I-encoded T6SS (H1-T6SS). This pathway delivers at least three effector proteins, Tse1-3 (type VI secretion exported 1-3), to the periplasm of recipient Gram-negative bacteria. Two of these proteins, Tse1 and Tse3, act within this compartment by hydrolyzing peptidoglycan, whereas Tse2 accesses the cytoplasm where it induces stasis (67, 68, 90). In addition to targeting other bacteria, cells can deliver effectors to their own kind in a process termed intercellular self-intoxication. To avert the harmful consequences of this process, cells possess specific immunity proteins, Tsi1-3 (type VI secretion immunity 1-3), that bind to and inactivate cognate effectors.

The T6SS displays a broad target range; however, there are limits to its activity. As cell wall-degrading T6S effectors require compartmentalization in the periplasm in order to exert effects on recipient cells, their action is restricted to Gram-negative organisms (91). There is also evidence for disparate susceptibilities to T6S-dependent intoxication among Gram-negative species (92-94); however, the basis for this has remained unknown.

Quantitative time-lapse microscopy has revolutionized the way in which bacterial populations can be characterized (95, 96). By measuring phenomena at the single cell level, cell subpopulations not discernable in traditional population studies can be resolved. Here we

developed quantitative time-lapse fluorescence microscopy (TLFM) tools for the study of T6S-mediated interactions between *P. aeruginosa* and two Gram-negative species, *Burkholderia thailandensis* (*B. thai*) and *Salmonella enterica* serovar Typhimurium. Using this technique, we resolve key questions pertaining to spatiotemporal characteristics and potency of T6S-mediated intercellular lysis. We further show that coordinated T6S apparatus assembly between neighboring cells leads to a "double-edged sword" phenomenon – T6S activation within a cell leaves it more susceptible to T6S-based intoxication by its competitor.

2.3 Results

2.3.1 *Quantitative Single-Cell Analysis of Interbacterial Interactions*

We developed a customized Matlab-based software package for quantitative single cell analyses of interspecies bacterial interactions. Like related tools, this package identifies bacteria from phase images using a watershed algorithm, performs cell tracking, links cells between frames (allowing lineage analysis), and can identify and track fluorescent subcellular foci representing punctate protein localization patterns (96, 97). Figure 2.1 provides an overview of our analysis methods. We added to these capabilities a number of analysis modules tailored to the unique questions we sought to address in this study. Specifically, we endeavored to quantitatively describe T6S-dependent interactions between two species of bacteria in a spatially and temporally resolved manner.

Cell lysis is a known consequence of intoxication by the H1-T6SS (91); thus, we utilized this readily observable process as a means of tracking T6S activity. Given that cells undergoing lysis release their cytoplasmic contents, we defined a lytic event as a precipitous drop of cellular fluorescence between frames. Using an iterative approach, we defined the optimal fluorescence

decrease (minimizing false positive and negative observations) at 80% and required that this drop be maintained beyond a single frame (Figure 2.1A). We implement the lysis detection module post-segmentation so that information including the identity and cellular neighborhood of lysed cells can be analyzed. A second functionality we introduced to the software is the capacity to distinguish cells of a population based on fluorescence intensity (Figure 2.1*B*). Following segmentation, the average fluorescence intensity in each channel within each cell mask is calculated and background is subtracted. This feature allows for gating of donor and recipient cells based on expression of a unique fluorescent protein – green and monomeric cherry fluorescent proteins (GFP and mCherry, respectively) in this study. The combination of recorded cell-specific measurements with frame-to-frame cell linking, lysis detection, and donor/recipient identification provides the capability to measure T6S-dependent effects between mixed populations of bacteria in a spatially and temporally resolved manner (Figure 2.1*C*).

2.3.2 *Spatiotemporal Analysis of T6S-Dependent Interactions*

To our knowledge, there are no reports describing the direct visualization of T6S-dependent interactions between two species of bacteria. We initially chose to investigate the *P. aeruginosa–B. thai* donor–recipient pair, as both organisms are genetically tractable, thrive in similar temperature and nutrient conditions, and serve as models for understanding the T6SS in our laboratory. To increase the number of measureable T6S-dependent interactions occurring under the short timescale of our studies, we used the *P. aeruginosa* Δ*retS* parental background in all experiments (80, 98). In this background, which has been extensively used for the study of the H1-T6SS, Tse1-3 export is constitutive and the expression of genes associated with sessile *P. aeruginosa* is stimulated at the posttranscriptional level (67, 99, 100). Homogeneous mixtures of

P. aeruginosa attTn7::*mCherry* and *B. thai* attTn7:*gfp* were inoculated onto growth medium-infused agarose pads and observed using TLFM. Control experiments were performed with *P. aeruginosa* bearing a mutation known to inactivate the H1-T6SS (Δ*tssM1*) (101). Initial inspection of image sequences revealed apparent phenomenology attributable to T6SS activity. Most strikingly, we observed extensive lysis of *B. thai* grown with *P. aeruginosa*, but not with *P. aeruginosa* Δ*tssM1* (Figure 2.2*A* and Figure 2.3, Movies 2.1 and 2.2).

Next we quantitatively analyzed TLFM sequences of *P. aeruginosa–B. thai* co-cultures using our custom image analysis software. Consistent with our initial visual inspection, automated analyses indicated a significantly higher cellular lysis in co-cultures containing the parental *P. aeruginosa* strain than in those bearing the *tssM1* deletion (Figure 2.2*A,B*). To determine which of the two species was undergoing lysis, we gated cells using green and red fluorescence levels to identify the constituents of the lysed cell population. This analysis revealed that the *P. aeruginosa* parental and Δ*tssM1* strains experience a consistently low basal lysis rate, whereas *B. thai* undergoes lysis only in the presence of *P. aeruginosa* with a functional T6SS (Figure 2.2*C* and Movies 2.3 and 2.4). Importantly, switching the fluorescent proteins used to mark the two organisms did not significantly impact the number of detected lysis events (Figure 2.4).

The T6SS has been suggested to function as a cell contact-dependent puncturing device (102, 103). Data supporting this contention derives from studies wherein donor and recipient populations are separated by a synthetic membrane of many microns in thickness (92); thus, whether the T6SS includes an appendage that allows it to act at a distance between cells – as is often speculated and depicted – has not been addressed experimentally. To interrogate this question with higher resolution, we measured the lysis of individual *B. thai* cells as a function of

contact with *P. aeruginosa* in a TLFM sequence. Of the 116 *B. thai* lysis events recorded, 114 occurred within cells in immediate contact (≤200 nm) with *P. aeruginosa*. This observation strongly suggests that the T6S apparatus does not function via an extended extracellular appendage.

The efficiency of T6S intoxication has also not been measured directly. Population level studies provide a sensitive means to assess the contribution of T6S to fitness; however, without resolving cell contact and its duration, the potency of the system cannot be directly ascertained from these experiments. To probe the efficiency of H1-T6SS-mediated intoxication, we measured the occurrence of recipient cell lysis as a function of contact duration with *P. aeruginosa*. We calculated contact duration such that ten minutes of contact with a single *P. aeruginosa* donor cell would be equivalent to five minutes of contact with two cells. *B. thai* lysis displayed a linear ($R^2 = 0.96$) dose-dependence over a large range of *P. aeruginosa* contact (0-150 contact minutes), suggesting that successful delivery of effectors is a rare event, cells require multiple payloads in order to lyse, or both (Figure 2.2*D*). Based on our analysis, we determined that *P. aeruginosa* lyses *B. thai* cell populations at a rate of 5.2% per hour of contact. To understand how this rate compares with efficiency of H1-T6S-mediated lysis of other bacteria, we performed similar TLFM analyses of *P. aeruginosa–S.* Typhimurium co-cultures (Movies 2.5 and 2.6). *P. aeruginosa* stimulated lysis of *S.* Typhimurium in a contact-, H1-T6SS-, and dose-dependent manner ($R^2 = 0.97$), however the efficiency of lysis was significantly lower against this organism (0.44% per hour) (Figure 2.2*E*). This may in part be due to a prolonged spheroplast intermediate that precedes H1-T6SS catalyzed lysis of *S.* Typhimurium (Movie 2.5).

The H1-T6SS is thought to act on recipient cells through the combined actions of its known effectors, Tse1-3 (67). We measured the contribution of the individual H1-T6SS effectors

to the observed interspecies cell lysis phenotype. To circumvent the potential complications of synergy, we generated a panel of *P. aeruginosa* single effector strains. *B. thai* lysis incurred during growth with the single effector strains was compared with that promoted by the parental, a strain lacking all three known effectors, and the Δ*tssM1* strain using our TLFM analysis method. This revealed that Tse1 is responsible for the majority (80%) of H1-T6SS-dependent lysis of *B. thai* and *S.* Typhimurium (Figure 2.5*A* and Figure 2.6). Comparison of Tse1 levels in parental and Δ*tse2* Δ*tse3* culture supernatants indicated that the high lytic activity of the Δ*tse2* Δ*tse3* background is not the result of compensatory effector release (Figure 2.5*B*). Surprisingly, our results showed that neither Tse2 nor Tse3 contribute to Tse1-independent H1-T6SS-catalyzed *B. thai* lysis. Indeed, *P. aeruginosa* cells lacking all known H1-T6SS effectors caused lysis of *B. thai* with slightly greater efficiency than strains possessing only Tse2 or Tse3 (Figure 2.5*A*). Introduction of the *tssM1* deletion to the Δ*tse1-3* background abrogated recipient lysis, ruling out the possibility that this strain acquired H1-T6SS-independent lytic activity. The lysis rate of *B. thai* catalyzed by each strain was also examined. Tse1-dependent and -independent lysis mechanisms displayed temporal separation, with Tse1 inducing recipient cell lysis earlier (Figure 2.5*C,D*). Together, our data conclusively demonstrate the occurrence of interspecies antagonistic interactions mediated by the T6SS under conditions suitable for single cell study. Our analyses show that H1-T6SS-dependent lysis requires direct donor–recipient cell contact and that the efficiency of recipient cell intoxication varies significantly between two species of proteobacteria. Finally, we discovered a late-acting, Tse1-3-independent mechanism of the H1-T6SS that promotes lysis of recipient cells.

2.3.3 *Adjacent Cells Influence T6S Apparatus Assembly and Localization*

Our ability to quantitatively measure T6S-dependent cellular interactions under TLFM conditions motivated us to extend our analyses to include the localization properties of the T6S apparatus. To visualize the secretory apparatus, we examined a *P. aeruginosa* strain expressing *clpV1–gfp* from the native *clpV1* locus (101). As reported previously, we observed that localization of this conserved AAA+ family ATPase is highly dynamic – oscillating between a diffuse cytoplasmic pattern, and filamentous and punctate structures, representing active and inactive forms of the T6S apparatus, respectively (Movie 2.7) (99).

It has been proposed that non-diffuse ClpV1–GFP structures represent conformational states in the assembled phage tail-like T6S apparatus (82, 99). As a first step toward determining the functional significance of ClpV1 localization properties, we measured the occurrence and subcellular localization of ClpV1–GFP puncta within cells as a function of neighbor cell characteristics (Figure 2.7*A*). Since T6S-dependent self-intoxication is well documented and occurs efficiently, we performed this analysis in *P. aeruginosa* monocultures. Based on automated focus identification within 12,233 cells, we determined the probability of a given cell displaying a focus to be 15.3 ± 0.27% (Figure 2.7*B* and Materials and Methods). The probability of observing a focus in the subpopulation of cells with neighbors was similar (14.9 ± 0.37%, p-value = 0.38), suggesting that apparatus assembly is not activated by cell–cell contact under the conditions of our assay. However, when we examined the subpopulation of cells with observed foci, the probability of neighboring cells displaying foci increased dramatically to 46 ± 2.4% (p-value < 0.0001). We also searched for spatial correlations in T6S assembly within neighboring cells. Although the presence of a neighboring cell did not influence assembly of the apparatus, we detected a significant bias in the subcellular localization of the apparatus – favoring

localization to cell–cell interfaces (P_{calc}, 32 ± 7.1 x 10^{-2}%, P_{obs}, 49 ± 3.6%, p-value < 0.0001). In summary, our data indicate that H1-T6SS activation is correlated among neighboring cells and suggest that neighbor cells recruit the T6S apparatus to cell interfaces. Our results are in alignment with the recent observation that T6S assembly between adjacent cells is spatially and temporally linked (99).

2.3.4 *Efficient Intoxication by the T6SS Requires a Functional T6S Apparatus in Recipient Cells*

One explanation for the heightened probability of observing concurrent T6SS assembly in neighboring cells is that assembly proceeds more efficiently in neighbor A if neighbor B itself possesses an assembled apparatus. We term this the "sensing model." An alternative explanation is that T6SS activation is highly sensitive to undetermined micro-environmental fluctuations that cells A and B experience concomitantly. Given our earlier observations linking T6SS assembly to activity, a paradoxical prediction of the sensing model is that T6SS activity should contribute both to intoxication of neighbors and apparent susceptibility to intoxication – the lack of a functional T6SS in a recipient cell would lead to a failure to stimulate T6S activation in a donor, thereby decreasing the extent of recipient targeting.

To test this prediction of the sensing model, we measured the effect of an HSI-I gene cluster deletion on susceptibility to T6S-mediated intoxication using interbacterial competition assays. Interestingly, inactivation of the H1-T6SS dramatically improved the competitive fitness of a Tse2-susceptible background of *P. aeruginosa* (Δ*tse2* Δ*tsi2*) (Figure 2.8*A* and Figure 2.9) (67). According to the sensing model, the protection afforded by T6S inactivation should not be specific to a particular effector. Indeed, we found that the HSI-I deletion also granted increased

fitness to a strain susceptible to Tse3-dependent intoxication (Figure 2.8*B*) (68). Many mechanisms could explain the apparent T6S resistance accompanied by an HSI-I deletion. To determine whether it is specifically the activity of the T6S apparatus in the recipient that increases targeting efficiency, we next examined the effect of the *clpV1* deletion on recipient fitness. The ClpV1 protein stimulates T6S activity by promoting turnover of the apparatus (74, 103). As anticipated, *clpV1* deletion increased the fitness of the Tse2-susceptible strain and, furthermore, susceptibility of the strain was returned to parental levels by genetic complementation of the *clpV1* gene. Although the *clpV1* deletion provided a statistically significant increase in fitness to the Δ*tse2* Δ*tsi2* strain, our data indicate that it does so to a lesser extent than a deletion of the entirety of HSI-I, and neither of these deletions restores fitness to that of a fully immune strain. Notably, *clpV1* deletions are known to retain partial T6SS activity (68, 93, 94); thus, we find that cellular targeting efficiency correlates to T6S activity in recipient cells.

We also interrogated the sensing model in a less biased fashion by performing a genome-wide screen for transposon (Tn) insertions within *P. aeruginosa* that lead to resistance to T6S-based intoxication. Using a 96-well interbacterial competition assay format, we screened 2,748 random Tn insertions in the *P. aeruginosa* Δ*retS* Δ*tse2* Δ*tsi2* attB::*lacZ* background (recipient) for resistance to intoxication by *P. aeruginosa* Δ*retS* (donor). Positive clones were selected visually based on LacZ activity (Figure 2.8*C*). We identified and mapped 14 independent Tn insertions (hit rate, 0.5%) that conferred T6S resistance in our screen (Table S1). Remarkably, three of these were located within the HSI-I gene cluster (Figure 2.8*D*). Seven additional insertions mapped to the *gacA* and *gacS* genes, which encode known positive regulators of the H1-T6SS (98). The genes immediately disrupted by Tn insertions within HSI-I include *tagR*,

tssC1 and *tssK1*. Prior studies indicate each of these is essential to T6S function (81, 92, 104). Quantitative growth competition assays with the Tn insertion strains verified that they display significant increased fitness relative to the parental (Figure 2.8*E*).

Having demonstrated that efficient T6S-dependent intercellular self-intoxication requires an active T6SS within recipient cells, we next probed whether the requirement for T6S in recipient cells extended to interactions between bacterial species. Our laboratory previously found that T6SS-1 of *B. thai* targets bacterial cells (92). Furthermore, under standard laboratory conditions, T6SS-1 is the only one of five T6SSs in *B. thai* that exports effectors to levels detectable using a sensitive mass spectrometry assay employed by our laboratory. Given these data, we reasoned that T6SS-1 inactivation might provide *B. thai* resistance to intoxication by the H1-T6SS of *P. aeruginosa*. To test this, we compared the lysis rates of wild-type and T6SS-1-inactive (Δ*clpV*) *B. thai* strains grown with *P. aeruginosa* using our single cell TLFM analysis method. Similar to our findings in self-intoxication studies, T6S inactivation in *B. thai* provided significant resistance to T6S-dependent lysis by *P. aeruginosa* (Figure 2.8*F*). We also performed population level lysis and growth competition assays, which further confirmed T6SS-1 inactivation protects *B. thai* against the H1-T6SS of *P. aeruginosa* (Figure 2.8*G* and Figure 2.10). In total, our TLFM analyses and genetic data support the hypothesis that T6S activation is transmitted between neighboring bacterial cells. The consequence of this positive feedback loop is that T6S apparatus activation exposes a cell to heightened intoxication.

2.4 Discussion

Our data lead us to hypothesize that T6S is a double-edged sword. The activity of T6S within a bacterial cell exposes that cell to increased T6S-mediated intoxication by its neighbors.

This effect could be widespread, as we find inactivating mutations in the system confer apparent resistance to both intra- and inter-species H1-T6SS-mediated attack. Interestingly, a similar phenomenon has been observed with type IV secretion (T4S). Binns and colleagues showed that the transfer efficiency of an IncQ plasmid between *Agrobacterium tumefaciens* is increased dramatically when both donor and recipient possess the Ti plasmid (105), which encodes the T4S apparatus. As observed in our study, this effect required the function of many essential components of the secretion system within the recipient cell.

The molecular mechanisms underlying the double-edged sword effect of T6S remain incompletely understood, however our quantitative analysis of the effect of neighboring cells on T6S activation and localization, combined with the observation of "T6SS dueling" made recently by the Mekalanos laboratory, support the hypothesis that an activated T6SS within a cell triggers T6S activation in its neighbors (99). Further consistent with this hypothesis, we do not observe complete resistance by T6S inactivation, mutations impact resistance in a manner proportional to their effect on T6S apparatus function, and resistance is not effector specific. It is important to emphasize that our data do not predict that bacteria lacking a T6SS are immune to T6S-mediated attack. The potency of T6S is also likely determined by other factors such as the general suitability of the organism for T6S apparatus-mediated protein transfer and its inherent susceptibility to the particular cargo of effectors. For example, we have shown that the H1-T6SS promotes relatively efficient lysis of an *E. coli* K-12 derivative that lacks T6S (91).

What is the mechanism of coupled T6S activation? We observe that susceptibility to T6S intoxication of a strain lacking *tse1-3* remains T6S-dependent, suggesting that effector proteins, or at least those currently known, are not required for sensing. We speculate that coupling is achieved by homo- or heterotypic interactions between extracellular apparatus components of

adjacent cells. These may either induce a signaling cascade leading to T6S activation or they may simply act as a nucleation point for the further assembly of the apparatus.

Whether coupled T6S activation has an adaptive role, and whether this benefits the donor or recipient, remains to be determined. It is noteworthy that the net consequence of T6S inactivation in *B. thai* is unfavorable to the organism. This implies that the offensive capacity of *B. thai* T6SS-1, at least against *P. aeruginosa*, is greater in magnitude under the conditions of our assay than the detrimental consequences of additional exposure to the effectors of the *P. aeruginosa* H1-T6SS. Coupled T6S activation could provide a means for cells to avoid wasteful T6S activation. In this scenario, an exogenous T6SS may act as a cue to the donor that a susceptible cell is in its vicinity. This is conceivable given the broad distribution of T6S among Gram-negative bacteria.

The unexpected finding that Δ*tse1-3* promotes T6S-dependent *B. thai* lysis suggests that either there are lytic H1-T6S effector(s) in addition to Tse1-3 that act on *B. thai* or that the H1-T6S apparatus itself can induce lysis. If the apparatus were sufficient to cause lysis, we would predict extensive lysis – regardless of effector immunity – occurring among cells undergoing intercellular self-intoxication. However, we did not find evidence of T6S-mediated lysis between adjacent *P. aeruginosa* cells in our experiments. Furthermore, we do not observe an increase in *P. aeruginosa* lysis when neighboring *B. thai* cells, despite the latter also possessing a functional T6SS. Thus, our results suggest that Tse1-3 do not encompass the complete effector repertoire of the H1-T6SS. The delayed kinetics of Tse1-independent lysis may explain why previous studies failed to identify H1-T6SS effectors beyond Tse1-3 (67). The temporal regulation of such effector(s) may be distinct from that of Tse1-3 or these substrates may be present at reduced levels.

To our knowledge, a quantitative single cell analysis of interspecies bacterial interactions has not yet been reported. Here we used this method to characterize T6S-dependent processes; however, the technology could be applicable to many important questions in the field of microbiology. For example, it could be used to examine the spatiotemporal regulation of phenotypes modulated by the presence of other bacteria including motility, growth rate, and the production of virulence factors. With increased automation, the method could also be implemented as a discovery tool for identifying processes influenced by neighboring cells, including novel interbacterial interaction mechanisms. There is growing recognition of the health, agricultural and environmental consequences of emergent properties within bacterial communities. Single cell analyses of mixed populations offer a means to decipher the complex interactions that underlie these traits.

2.5 Materials and Methods

DNA Manipulation and Growth Conditions. *P. aeruginosa*, *B. thai*, and *S.* Typhimurium strains were generated using PAO1 (106), E264, and LT2 backgrounds, respectively. For *P. aeruginosa*, media was supplemented with 300 μg/mL carbenicillin, 25 μg/mL irgasan, 30 μg/mL gentamycin, 5% w/v sucrose, 25 μg/mL tetracycline, 40 μg/mL X-gal (5-bromo-4-chloro-3-indolyl β-D-galactopyranoside), or 0.2% arabinose as necessary. For *B. thailandensis*, media was supplemented with 200 μg/mL trimethoprim as necessary. *Escherichia coli* SM10 λpir was propagated in LB medium containing 15 μg/mL gentamycin (for *P. aeruginosa* conjugation) or 200 μg/mL trimethoprim (for *B. thailandensis* conjugation). *S.* Typhimurium was propagated in LB containing 150 μg/mL carbenicillin.

Gene deletions within *P. aeruginosa* were generated in-frame using allelic exchange

using the *sacB* gene for counter-selection as described previously (107). The mini-Tn7 system was used to create strains with constitutive stable expression of GFP or mCherry in *P. aeruginosa* (108) and *B. thailandensis* (92). The pDW5 GFP expression plasmid and its mCherry derivative, pPtctA::*mCherry* (109), were used for fluorescence expression in *S.* Typhimurium. To generate pPtctA::mCherry, the mCherry coding sequence from Clontech's pmCherry Vector (Catalog No. 632522) was amplified with primers TCTAGATGGTGAGCAAGGGCGAGGAG (upstream) and GTCGACCTACTTGTACAGCTCGTCCA (downstream). The product was cloned into pCR2.1, sequence confirmed, excised with XbaI and SalI and ligated into pDW5 that was previously digested with XbaI and SalI. For lacZ expression, the plac-*lacZ* cassette was inserted at the neutral phage attachment site (110). Construction of deletion, chromosomal fusion, and complementation constructs for *P. aeruginosa* have been described: ΔPA4856 (Δ*retS*), ΔPA0090 (Δ*clpV*), ΔPA0077 (Δ*tssM1*), and PA0090-gfp (101) (*clpV1-gfp*), effector and/or immunity (PA1844-5, PA2702-3, PA3484-5, *tse/i1-3*) deletions and the *clpV1* complementation construct (67, 68, 90). The *B. thailandensis* BTH_I2958 (*clpV*) deletion construct was described in ref (111).

Microscopy. Microscopy images were acquired using a Nikon Ti-E inverted microscope fitted with a 60x oil objective, automated focusing (Perfect Focus System, Nikon), a Xenon light source (Sutter Instruments), a CCD camera (Clara series, Andor), a custom environmental chamber, and image acquisition software (NIS Elements, Nikon). For TLFM experiments, overnight-cultivated *P. aeruginosa* were washed in a Luria Broth (LB) formulation low in NaCl (68) and mixed with either *B. thai* or *S.* Typhimurium at a ratio of 1:1 or 1:2, respectively. The bacterial suspension (1 mL) was spotted onto growth pads prepared from Vogel Bonner minimal media containing 2.5% agarose w/v, 0.2% w/v sodium nitrate, and a 19 amino acid cocktail

defined in ref (112). For snapshot images, log phase bacteria were spotted. Inoculated growth pads were hermetically sealed using rubber gaskets coated with VALP (1:1:1 vaseline, paraffin, and lanolin). For time-lapse series, automated image acquisition was performed at 5-minute intervals for 4-8 hours.

TLFM Analysis. Cells were identified using a watershed segmentation algorithm and linked between frames using custom Matlab software (2012a, The Mathworks, Natick, MA). Distinct populations within an experiment were identified using empirically-defined fluorescence intensity gates. Debris (non-cells) was size-excluded and fluorescence-excluded. Automated lysis detection flagged cells in which a decrease in mean cellular fluorescence of >80% occurred between consecutive frames. Contact duration was calculated by summing the number of donor cells in contact with a recipient in each frame over the lifetime of that cell. Unless otherwise indicated, results represent a single experiment typically utilizing two fields of view (10,000-20,000 cells). Each experiment was repeated at least 3 times independently.

For the neighbor analysis, cell concentration was chosen so that the majority of cells had zero or one neighbor. A mixture of *P. aeruginosa* Δ*retS clpV-gfp* and *P. aeruginosa* Δ*retS clpV-gfp* attTn7::*mCherry* were imaged in bright field/mCherry/GFP channels. Following image segmentation, cell populations were identified using gates based on fluorescence intensity. Punctate foci of GFP fluorescence fusions were identified automatically and scored based on fluorescence localization and intensity. Each focus was mapped to a location on the cell boundary corresponding to the closest pixel to the focus in the cell boundary. Two cells were called neighbors if the smallest distance between cell boundaries was one pixel or less. All pixels on the boundary of a cell within one pixel of the boundary of a differentially labeled neighboring cell are defined as the Neighbor Boundary Region. Foci in this Neighbor Boundary Region are

defined as Neighbor Touching. If the boundary mapped position of foci in neighboring cell are within two pixels of each other, they were defined to be in contact. The conditional probability that A, B and C are observed given d and e is

$$P(A \cap B \cap C|\ d\ ,\ e) = N(A \cap B \cap C \cap d \cap e)/\ N(d \cap e),$$

where $N(x \cap y)$ is the number of observations with x and y. For example, to calculate the probability of cells with foci (A) and neighbors (B) whose foci are in contact with the neighbor (C), given the presence of a focus (d) and a neighbor (e), we measure the number of cells with characteristics A, B, and C (i.e. number of cells with foci and neighbor whose foci are in neighbor contact) and divide that by the number of all cells with foci and neighbors. Statistical significance was determined using Welch's t-test.

Screen for T6SS Susceptibility Determinants. *P. aeruginosa* Δ*retS* Δ*tse2* Δ*tsi2* attB::*lacZ* was mutagenized using Tn5 as described in ref (113). Mutants (recipients) were inoculated into 96-well plates containing 200 µL LB and propagated overnight at 37°C. An equal volume of *P. aeruginosa* Δ*retS* (donor) overnight culture was added to each well and the mixture was spotted onto LB 3% w/v indicator (40 mg/mL 5-bromo-4-chloro-indolyl-β-D-galactopyranoside) plates. Each plate contained a positive control (recipient, Δ*retS* attB::*lacZ*). Strains containing transposon insertions that conferred resistance to the donor generated a blue spot. These were isolated from the competition spot and arbitrary PCR was performed as described previously (114) to determine transposon insertion sites.

Growth competition assays. For *P. aeruginosa*-*P. aeruginosa* growth competitions, overnight cultures of donor and recipient strains were mixed at a 1:1 ratio to a total density of approximately 3 OD_{600}. In each experiment, either the donor or recipient strain expressed

constitutive lacZ. Ten µl of bacterial suspension was spotted onto a nitrocellulose filter on 3% LB-low salt agar plates. Following a 6-hour incubation at 37°C, bacteria were harvested and plated on LB-agar containing X-gal for enumeration of colony forming units. *B. thailandensis*-*P. aeruginosa* assays were performed identically except with a starting OD_{600} of 2, a *P. aeruginosa:B. thailandensis* ratio of 1:5, and an 8-hour incubation. Interspecies competitions were also plated on LB supplemented with 60 µg/mL gentamycin to select for *B. thailandensis*. Statistical analyses were performed using a two-tailed Student's t-test.

Competitive Lysis Assays. Overnight cultures of *B. thailandensis* strains labeled chromosomally with *lacZ* using a mini-CTX integration vector. Donor *P. aeruginosa* strains were diluted 1:2 and mixed 1:1. This mixture was then spotted on nitrocellulose on LB-LS 3% agar. Following a 3 hour 45 minute incubation at 37°C cells were resuspended in PBS pH 7. Whole cell and supernatant fractions were prepared as described previously, and the LacZ activity of each fraction was determined using the Tropix Galacto-Light kit from Applied Biosystems following manufacturer's instructions (91). Relative lysis was then calculated as the percentage of total LacZ activity partitioning to the supernatant fraction. Two-tailed student's t-test was used to analyze data.

Protein Preparation and Western Blotting. Protein samples (cell and supernatant fractions) were prepared and western blotting was performed as previously described (101).

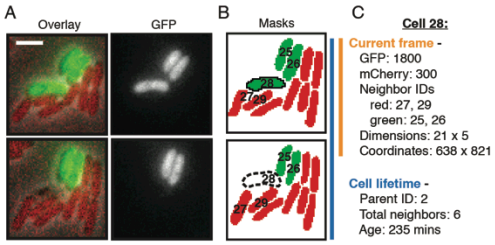

Figure 2.1: Overview of TLFM-based intercellular interaction analyses.
(*A*) Consecutive cropped frames from a typical TLFM experiment in which two populations of differentially labeled cells (*B. thai* attTn7::*gfp* and *P. aeruginosa* attTn7::*mCherry*) were co-cultured and imaged. The overlay includes phase, GFP and mCherry channels. Scale bar, 2 μm. (*B*) Cell masks generated by image segmentation. Red and green coloring corresponds to distinct subpopulations identified by gating on fluorescence intensity. Dashed outline in the lower mask image depicts a software-identified lysis event. Hypothetical cell identification numbers are shown. (*C*) Example of cell-specific values measured during automated analysis. Certain data are recorded once and pertain to the cell lifetime as a whole (blue); other parameters vary between frames (orange).

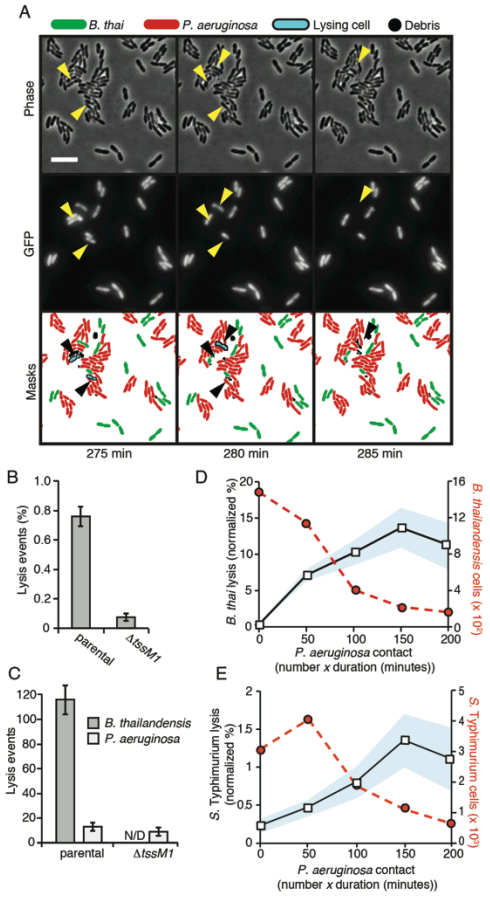

Figure 2.2: The *P. aeruginosa* H1-T6SS causes dose- and contact-dependent lysis of recipient cells.
(*A*) TLFM image sequence of a *P. aeruginosa–B. thai* co-culture. *B. thai* and *P. aeruginosa* are GFP and mCherry labeled, respectively. Outlined blue cells on masks lyse in subsequent frame. Arrows point to *B. thai* cells that lyse following *P. aeruginosa* contact. Figure 2.3 shows the corresponding Δ*tssM1* control. Scale bar, 6 mM. (*B*-*C*) Lysis quantification from TLFM experiment depicted in (*A*). Either percent lysis of total cellular population (*B*) or distinct lysis counts for indicated bacterial populations (*C*). Error bars depict standard counting error (C.E.). N/D, none detected. (*D*-*E*) *B. thai* (*D*) or *S.* Typhimurium (*E*) lysis increases linearly with increased contact to *P. aeruginosa.* Red dashed and solid black lines depict total cells and percent lysis, respectively. Results represent data pooled from two independent experiments.

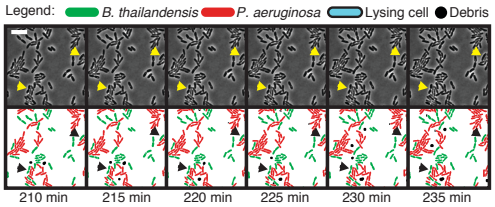

Figure 2.3: Co-culture of *B. thai* with a *P. aeruginosa* strain lacking a functional T6SS does not undergo lysis.
TLFM image sequence of a *P. aeruginosa–B. thai* co-culture. *B. thai* and *P. aeruginosa* are GFP and mCherry labeled, respectively. Scale bar, 3 μm. Arrows point to *B. thai* cells with heavy *P. aeruginosa* contact.

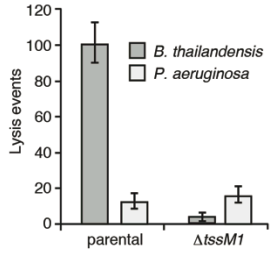

Figure 2.4: Reversing fluorophore combination in donor and recipient strains does not affect lysis detection.
TLFM experiment wherein *B. thai* attTn7::*mCherry* was co-cultured with indicated *P. aeruginosa* attTn7::*gfp* strain and lysis quantification of *B. thai* was performed.

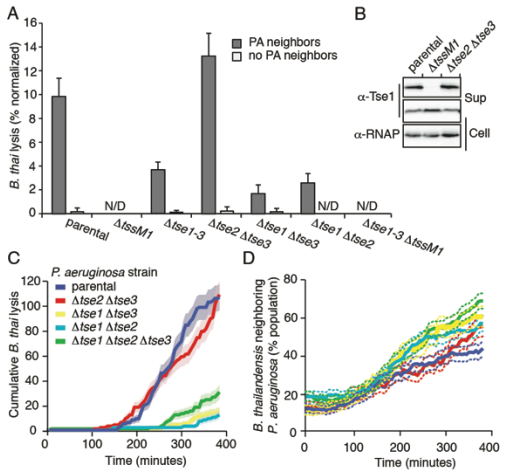

Figure 2.5: Tse1 acts early to promote the majority of H1-T6SS-catalyzed *B. thai* lysis. (*A*) Lysis quantification from TLFM sequences of *B. thai* co-culture with the indicated *P. aeruginosa* strains. Error bars, ± C.E. (*B)* Western blot analysis of Tse1 expression in supernatant (Sup) and cell-associated (Cell) fractions of the indicated *P. aeruginosa* strains. RNA polymerase (RNAP) was used as a loading control. (*C*) Running total of frame-by-frame *B. thai* lysis events observed in co-culture experiments with the indicated *P. aeruginosa* strains. Shading corresponds to C.E. (*D*) Neighbor-cell analysis of co-cultures in (*C*) indicating similar neighbor density for each experiment. Dotted lines of corresponding color depict C.E.

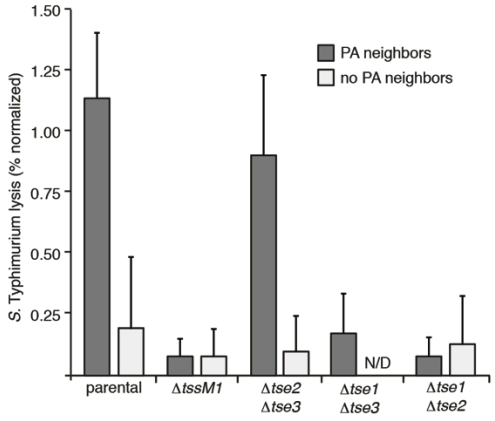

Figure 2.6: Tse1 promotes the majority of H1-T6SS-catalyzed *S.* Typhimurium lysis. Lysis quantification from TLFM sequences of *S.* Typhimurium co-culture with the indicated *P. aeruginosa* strains. Image acquisition occurred every 7 minutes. Error bars, counting error.

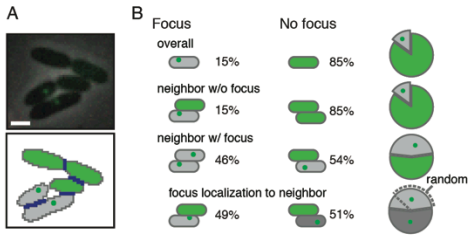

Figure 2.7: Assembly and localization of the T6S apparatus is influenced by neighboring cells.
(*A*) Overlay of phase and GFP channels of *P. aeruginosa* cells expressing *clpV1-gfp* (top image) with corresponding cell masks (lower image). Scale bar, 1μm. Cell–cell interfaces (blue lines) and foci (green dots) were identified and quantified to determine observed and predicted conditional probabilities (see *Materials and Methods*). (*B*) Schematic depicting conditions for which probabilities of T6S apparatus localization were determined with paired results. Grey cells with green dots and filled green cells represent observations of localized or diffuse ClpV1-GFP, respectively.

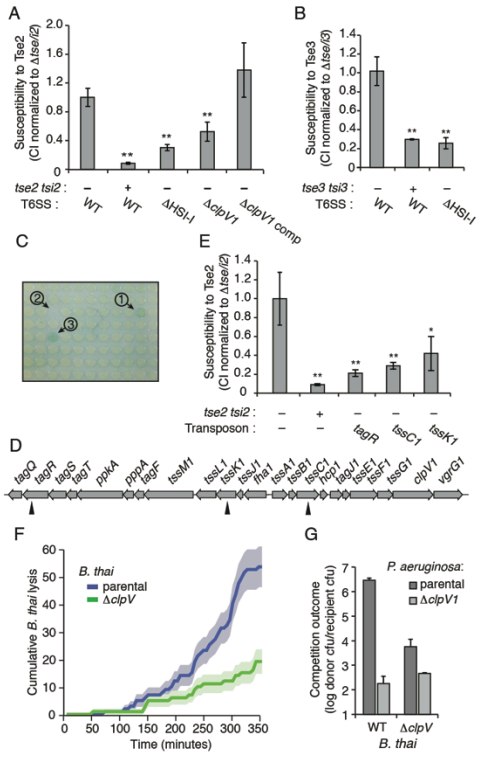

Figure 2.8: Efficient intoxication by the T6SS requires a functional T6S apparatus in recipient cells.

(*A-B*) Outcome of growth competition experiments between the parental and *P. aeruginosa* recipient strains. The presence (+) or absence (–) of *tse2 tsi2* (*A*) and *tse3 tsi3* (*B*) in the recipient strain and the genetic status of the H1-T6SS cluster (WT, wild-type) are indicated. Fitness differences were not observed in control experiments performed under T6S non-conducive conditions (see Figure 2.9). Competitive index (CI) is defined as the change (final/initial) in ratio of donor and recipient colony forming units (cfu) normalized to the susceptible control (*A*, Δ*tse/i2*; *B*, Δ*tse/i3*). (*C*) Representative 96-well plate used in screen for H1-T6SS resistance. Each plate contained a positive control (1) and a no-growth control (2). This plate also includes a positive hit (3). (*D*) Schematic of the H1-T6SS gene cluster with identified Tn insertion sites indicated (arrowheads). A complete list of mutants is provided in Table 2.1. (*E*) Outcome of growth competition experiments between the parental and indicated *P. aeruginosa* strains normalized as described for *A*. (*F*) Frame-by-frame running total of lysis events from a TLFM sequence in which the indicated *B. thai* strain was co-cultured with parental *P. aeruginosa.* Shading indicates counting error. (*G*) Outcome of growth competition experiments between the indicated strains. Asterisks mark competition outcomes significantly different than the corresponding effector immunity deficient strain (*, $p < 0.05$; **, $p < 0.01$). Error bars, ± standard deviation. n = 3.

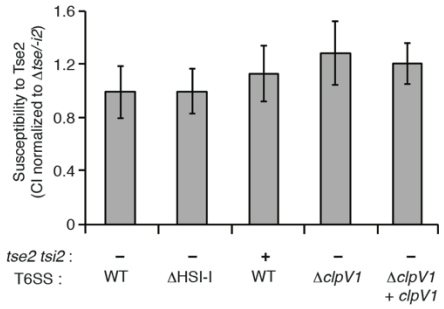

Figure 2.9: T6SS-dependent fitness differences observed in Figure 2.8*A* are contact-dependent.
Outcome of growth competition experiments between the indicated strains performed in liquid media. No significant differences detected. Error bars, ± standard deviation (S.D.). n = 3.

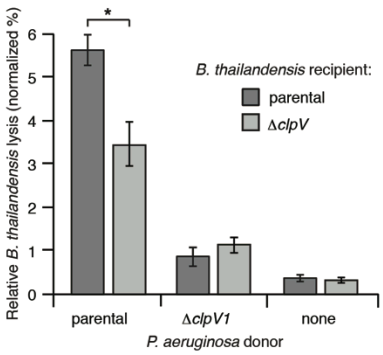

Figure 2.10: Less efficient lysis is observed when the recipient organism lacks a functional T6SS.
Relative lysis of indicated co-cultures under T6S-conducive conditions determined by measuring lacZ activity in culture supernatant. **, $p < 0.01$. Error bars, ± SD; n = 3.

Movie 2.1. *P. aeruginosa* attTn7::mCherry parental strain co-cultured with *B. thai* attTn7::gfp results in *B. thai* lysis. Overlaid images of phase, mCherry, and GFP images acquired at 5-minute intervals. *P. aeruginosa* (donor strain) appears in the red channel; *B. thai* (recipient strain) in the green channel.

Movie 2.2. *P. aeruginosa* attTn7::mCherry Δ*tssM1* strain co-cultured with *B. thai* attTn7::gfp without any observable lysis of *B. thai*. Overlaid images of phase, mCherry, and GFP images acquired at 5-minute intervals. *P. aeruginosa* (donor strain) appears in the red channel; *B. thai* (recipient strain) in the green channel.

Movie 2.3. *P. aeruginosa* attTn7::mCherry parental strain co-cultured with *B. thai* attTn7::gfp. Overlaid images of phase, mCherry, and GFP images acquired at 5-minute intervals. *P. aeruginosa* (donor strain) appears in the red channel; *B. thai* (recipient strain) in the green channel. Automated lysis detection depicted by outlines around lysing cells (blue and white outlines for cells in the mCherry and GFP channels respectively).

Movie 2.4. *P. aeruginosa* Δ*tssM1* attTn7::mCherry strain co-cultured with *B. thai* attTn7::gfp. Overlaid images of phase, mCherry, and GFP images acquired at 5-minute intervals. *P. aeruginosa* (donor strain) appears in the red channel; *B. thai* (recipient strain) in the green channel. Automated lysis detection depicted by outlines around lysing cells (blue and white outlines for cells in the mCherry and GFP channels respectively).

Movie 2.5. *P. aeruginosa* attTn7::mCherry parental strain co-cultured with *S.* Typhimurium pDW5 with observable spheroplasting and lysis of *S.* Typhimurium. *P. aeruginosa* (donor strain) appears in the red channel; *S. Typhimurium* (recipient strain) in the green channel.

Movie 2.6. *P. aeruginosa* Δ*tssM1* attTn7::mCherry parental strain co-cultured with *S.* Typhimurium pDW5 with a notable lack of *S.* Typhimurium lysis or spheroplasting. Overlaid images of phase, mCherry, and GFP images acquired at 5-minute intervals. *P. aeruginosa* (donor strain) appears in the red channel; *S. Typhimurium* (recipient strain) in the green channel.

Movie 2.7. *P. aeruginosa clpV1-gfp* mono-culture displays coordinated apparatus assembly between neighboring cells. Bacteria were imaged in the GFP channel every 2.5 seconds.

Table 2: Transposon insertions providing resistance to T6S-dependent intoxication

Locus tag	Name	Position on chromosome	Orientation (F/R)	Position within ORF (% from 5' end)
T6SS locus insertions				
PA0071	tagR1	84929-84930	R	1464-1465 (85.5)
PA0084	tssC1	102628-102629	R	851-852 (56.8)
PA0079	tssK1	96952-96953	R	783-784 (58.7)
Gac Pathway				
PA2586	gacA	2926374-2926375	R	529-530 (82.0)
PA0928	gacS	1013816-1013817	F	841-842 (30.3)
PA2586	gacA	2626314-2626315	R	548-549 (85.0)
PA0928	gacS	2925885-2925886	F	978-979 (35.2)
PA0928	gacS	1014793-1014794	F	1818-1819 (65.1)
PA0928	gacS	1014790-1014791	F	962-963 (34.6)
PA0928	gacS	1013195-1013196	F	220-221 (8.0)
Other				
Inter PA0652-PA0653	n/a	706812-706813	F	n/a
PA2585	uvrC	2923981-2923982	F	20-21 (10.9)
PA3345	hypothetical	3757250-3757251	R	342-343 (97.1)
PA5184	hypothetical	5837787-5837788	R	106-107 (19.0)

Chapter 3. Kin cell lysis is a danger signal that activates antibacterial pathways of *Pseudomonas aeruginosa*

Published as: LeRoux M., Kirkpatrick R. L., Montauti E. I., Tran B. Q., Peterson S. B., Harding B. N., Whitney J.C., Russell A.B., Traxler B., Goo Y.A., Goodlett D.R., and Mougous J.D. (2015). *eLife*, 4. doi:10.7554/eLife.05701

3.1 Abstract

The perception and response to cellular death is an important aspect of multicellular eukaryotic life. For example, damage-associated molecular patterns activate an inflammatory cascade that leads to the removal of cellular debris and the promotion of healing. Here we demonstrate that lysis of *Pseudomonas aeruginosa* cells triggers a program in the remaining population that confers fitness in interspecies co-culture. We find that this program, termed *P. aeruginosa* response to antagonism (PARA), involves rapid deployment of antibacterial factors and is mediated by the Gac/Rsm posttranscriptional global regulatory pathway. Type VI secretion, and, unexpectedly, conjugative type IV secretion within competing bacteria, induce *P. aeruginosa* lysis and activate PARA, thus providing a mechanism for the enhanced capacity of *P. aeruginosa* to target bacteria that elaborate these factors. Our finding that bacteria sense damaged kin and respond via a widely distributed pathway to mount a complex response raises the possibility that danger sensing is an evolutionarily conserved process.

3.2 Introduction

Bacteria can occupy highly dynamic environments, where survival is linked to the ability to sense and respond to an assortment of threats (10). It is increasingly clear that in addition to well-understood environmental and nutritive stresses, antagonistic factors elaborated by other bacteria are a common threat that bacteria must cope with (42, 115). A number of antagonistic strategies have been identified, including the production of diffusible factors such as small molecule antibiotics. It has been suggested that sub-inhibitory concentrations of these molecules induce specific changes in bacteria, including the production and distribution of resistance mechanisms (24, 116, 117). Other antagonistic pathways, such as contact-dependent inhibition

(CDI) and the type VI secretion system (T6SS), require cell contact (5, 118). Kin are protected from the toxic proteins delivered by these pathways by specific cognate immunity proteins; however, escape from or defense against these pathways by non-kin is not well understood (67, 68).

The T6SS is a versatile export machinery that can deliver a wide range of proteinaceous effector molecules from donor to recipient Gram-negative bacterial cells (66, 67, 119). One of the best characterized bacterial targeting T6SSs is the Hcp Secretion Island I-encoded T6SS (H1-T6SS) of *Pseudomonas aeruginosa* (67). The H1-T6SS transports a cargo of at least seven effectors, termed type VI secretion exported 1-7 (Tse1-7) (69, 71). The outcome of intoxication by these proteins can be lysis or cessation of growth (90, 120). Like other species with interbacterial T6SSs, *P. aeruginosa* has the capacity to target cells of its own genotype with the H1 pathway. To inhibit self-intoxication, cognate type VI secretion immunity proteins (Tsi) are produced and localized to the cellular compartment that contains the target of the corresponding effector (66, 77, 121, 122). T6SSs are found in at least three genetically distinct configurations present among multiple bacterial phyla, making it one of the most widespread pathways mediating interbacterial antagonism known (123).

Expression and activity of the H1-T6SS is tightly regulated at multiple levels (78). Stringent post-transcriptional regulation of the H1-T6SS is achieved through the global activation of antibiotic and cyanide synthesis/regulator of secondary metabolism (Gac/Rsm) pathway (80, 124). This global regulatory system impacts protein production via RsmA, a CsrA-type protein that binds to target mRNA molecules and generally acts to represses their translation (125). RsmA is modulated by levels of the small RNA (sRNA) molecules *rsmY* and *rsmZ*, which bind to and sequester it from its targets. Transcription of the sRNAs is promoted by

phosphorylated GacA, the cognate response regulator of the sensor kinase GacS. Finally, two hybrid sensor kinases, RetS and LadS, acting through GacS, repress or stimulate GacA phosphorylation, respectively (126, 127). Consistent with regulation of T6S by the Gac/Rsm pathway, many of its targets in *P. aeruginosa* and related g-proteobacteria are involved in the production of social or antagonist factors (125). This theme of Gac/Rsm-dependent modulation of antibiotic activity is exemplified by the defect of *P. fluorescens gac* mutants in bacterial and fungal growth inhibition on plants (128). Though the precise cues that activate the Gac/Rsm pathway are unknown, Haas and colleagues have found that one or more signals accumulate in spent bacterial culture supernatants deriving from both self and non-self organisms (129).

Posttranslational regulation by the threonine phosphorylation pathway (TPP) constitutes a second level of control over H1-T6SS activity. In this pathway, phosphorylation of a fork head-associated domain-containing protein, Fha1, triggers apparatus assembly and effector secretion (82). PppA, a phosphatase, opposes the activity of PpkA on Fha1, returning the system to the inactive state. Additional components of the TPP, encoded by type VI secretion associated genes Q-T (*tagQ-T*), act upstream of these proteins and are thought to be involved in signal transduction (81, 83). Two signals of the TPP have been proposed: surface-associated growth and membrane perturbation (130, 131). The latter signal is thought to underlie the observation that organisms with active T6S or type IV secretion (T4S) are more efficiently targeted by the H1-T6SS than those without (132). It was proposed that the activity of these apparatuses induces local membrane perturbations in *P. aeruginosa* that are sensed by the TPP, leading to posttranslational activation of the H1-T6SS and enhanced recipient cell death (131). A caveat of these studies is that the *P. aeruginosa* strain used bears an inactivating mutation in *retS*, which constitutively activates the Gac/Rsm pathway, potentially masking the contribution of this major

regulatory mechanism to the defense mounted by *P. aeruginosa* against the antagonistic pathways of competing bacteria.

Here we show that lysed kin cells act as a danger signal that is sensed by the Gac/Rsm pathway of wild-type *P. aeruginosa*. Our experiments provide a mechanism for T6S-dependent killing of competitor bacteria possessing either the T6 or T4 secretion pathways, as both induce *P. aeruginosa* lysis, stimulate the Gac/Rsm pathway, and lead to posttranscriptional de-repression of the H1-T6SS. These findings provide a rationale for the regulation of promiscuous antibiotic mechanisms by a pathway that can respond to self-derived signals.

3.3 Results

3.3.1 *P. aeruginosa T6 activity is stimulated by the presence of a non-self organism*

Prior work suggests that efficient T6S-dependent effector delivery between *P. aeruginosa* cells (self-targeting) requires deletion of *retS*, whereas this activating mutation is not required for robust T6S-dependent intoxication of other bacteria by *P. aeruginosa* (non-self targeting) (67, 68, 132). To quantify these observations, we performed bacterial growth competition experiments with wild-type (PAO1) and Δ*retS* with both self- and non-self recipients under comparable conditions. *Burkholderia thailandensis* (*B. thai*) was used as the non-self competitor for these studies, while a *P. aeruginosa* background lacking four H1-T6SS effector–immunity pairs (Δ*tse1-4* Δ*tsi1-4*) was employed as the self recipient. T6S-dependent fitness was determined by comparing the competitive index of a wild-type donor to that of a donor strain lacking *tssM*, which encodes a core structural component of the T6S apparatus (133). We found that both *P. aeruginosa* wild-type and Δ*retS* strains reduced populations of *B. thai* in a T6S-dependent manner by several orders of magnitude; however, only *P. aeruginosa* Δ*retS* displayed

T6S-dependent fitness in co-culture with self recipients (Figure 3.1). This direct comparison of H1-T6SS-dependent antibiosis by *P. aeruginosa* wild-type and Δ*retS* demonstrates that unlike self-intoxication, non-self targeting by the pathway does not require activation of the system by relief of negative regulation. A parsimonious explanation for these data is that the presence of a non-self competitor stimulates H1-T6SS activity.

3.3.2 *Expression and activity of the H1-T6SS is enhanced by T6S of competitor organisms*

To test the hypothesis that H1-T6SS activity is affected by the presence of a non-self organism, we used time-lapse fluorescence microscopy (TLFM) in conjunction with customized cell and protein tracking software to monitor the expression and subcellular localization of the conserved T6S ATPase ClpV1 (120, 134). Previous studies have established that translational fusion of *gfp* to the 3' end of *P. aeruginosa clpV1*, encoded within the H1-T6SS gene cluster, yields a stable and functional chimera (101). The fluorescence intensity of ClpV1–GFP provides readout of H1-T6SS expression and the assembly of ClpV1–GFP into punctate foci correlates with activity of the system (75, 82). Surprisingly, we observed significantly elevated ClpV1–GFP levels in *P. aeruginosa–B. thai* co-cultures relative to *P. aeruginosa* monocultures, suggesting that *B. thai* stimulates H1-T6SS expression (Figure 3.2A, B, Movie 3.1). We obtained similar results from a strain bearing a chromosomal, functional translational fusion of *gfp* to *fha1* (*fha1-gfp*), a locus found on the second major H1-T6SS transcript (Figure 3.2A, C, Movie 3.2) (82, 101). To determine whether elevated H1-T6SS arises from increased expression throughout the population or from high expression within a subset of *P. aeruginosa*, we examined ClpV1-GFP at the level of individual cells. Consistent with a population-wide, graded response, we found that ClpV1-GFP exhibits a normal distribution both in monoculture and when *P.*

aeruginosa is co-cultivated with *B. thai* (Figure 3.3). Mirroring the observed trends in expression, after an initial increase in foci frequency – a correlate of T6S activity – associated with growth on a surface (130), a larger percentage of *P. aeruginosa* cells grown in the presence of *B. thai* contained ClpV1–GFP and Fha1–GFP foci compared to those grown in mono-culture (Figure 3.2D, E). To investigate the generality of these effects on the H1-T6SS, we repeated our experiments using the g-proteobacterium *Enterobacter cloacae* as the competing organism. *P. aeruginosa* co-cultivated with *E. cloacae* also displayed increased ClpV1–GFP levels and higher foci frequency in comparison to *P. aeruginosa* in monoculture, indicating that this response is not specific to *B. thai* (Figure 3.4; Movie 3.3).

Previous studies demonstrated that the H1-T6SS of *P. aeruginosa* targets recipient cells that possess an active T6SS with greater efficiency than those that do not (120, 131). Though this behavior was shown for *P. aeruginosa* Δ*retS*, and not wild-type cells, the apparent capacity of the organism to sense the T6SS of a recipient cell prompted us to test whether T6S in non-self competitors is involved in stimulation of the H1 pathway. Indeed, we found that *B. thai* and *E. cloacae* strains bearing in-frame deletions of the *tssM* genes associated with their known antibacterial T6S pathways, are unable to stimulate T6S in *P. aeruginosa* (Figure 3.2, Figure 3.4, Movies 3.1-3.3) (71, 92, 135). Changes in *P. aeruginosa* growth rate dependent upon recipient T6S could influence gene expression and protein accumulation, potentially accounting for altered expression and activity of H1-T6SS proteins. However, this possibility was excluded by our observation that the doubling time of *P. aeruginosa* is insensitive to the activity of the bacterial cell-targeting T6SS of *B. thai* ($T6S^{BT}$) (Figure 3.5). Taken together, these data demonstrate that co-cultivation of *P. aeruginosa* with a non-self organism possessing an active T6S apparatus

leads to elevated expression and activity of the H1-T6SS. Henceforth, we refer to this response of *P. aeruginosa* as PARA (*P. aeruginosa* response to antagonism).

3.3.3 *PARA does not require the TPP*

A recent report implicated the TPP in the capacity of *P. aeruginosa* to sense and respond to T6S in target cells (131). To determine if PARA requires the TPP, we monitored the T6S-dependent response of *P. aeruginosa* bearing a deletion in *pppA*, which encodes a TPP-associated phosphatase (82). Interestingly, though this deletion was previously shown to abrogate the ability of *P. aeruginosa* Δ*retS* to respond differentially to bacteria containing or lacking a functional T6SS, we found that in the wild-type background, Δ*pppA* retains the capacity to respond to $T6S^{BT}$ (Figure 3.6A, B). PppA is a negative regulator of the TPP; therefore, we sought to rule out the possibility that the remaining TPP components, TagQ-T and PpkA, are sufficient to mediate PARA. Inactivation of all known components of the TPP results in a failure to assemble an active T6S apparatus, which would confound our analyses. However, activity can be restored to TPP deficient strains by the deletion of a gene encoding an independent post-translational repressor of the H1-T6SS, TagF (130). As observed with Δ*pppA*, the H1-T6SS of a *P. aeruginosa* strain lacking *tagF* and all known TPP components (ΔTPP Δ*tagF*) was activated by *B. thai* in a $T6S^{BT}$-dependent manner (Figure 3.6C, D). Consistent with measurements of expression and activation, growth competition experiments revealed that wild-type, Δ*pppA*, and Δ*tagF* ΔTPP strains of *P. aeruginosa* intoxicate *B. thai* and *E. cloacae* with active interbacterial T6SSs more efficiently than those without (Figure 3.6E, F). These data indicate that the TPP is not required for PARA.

It is worth noting that several lines of evidence suggest PARA is a process distinct from the previously characterized intercellular T6-based response referred to as "T6SS dueling" (99). First, PARA is accompanied by changes to T6S gene expression, whereas dueling is a posttranslational behavior thought to involve rapid changes in protein localization. Second, the TPP was found to be essential for T6SS dueling (131); however, this pathway is dispensable for PARA. Finally, spatiotemporal coordination of ClpV1-GFP-containing foci forms the basis for T6SS dueling, while such paired focus events are not correlated with PARA (data not shown). Motivated by the finding of PARA as a distinct pathway of clear functional relevance to interbacterial interactions, we proceeded to investigate its mechanistic underpinnings.

3.3.4 *PARA is a multifaceted response that requires the Gac/Rsm pathway*

The H1-T6SS is regulated at the transcriptional level by the quorum sensing regulator LasR, and at the posttranscriptional level by RsmA and RsmF, RNA binding proteins that directly mediate the effects of Gac/Rsm signaling (Figure 3.7A) (79, 98, 136). As a first step toward defining the pathway through which PARA operates, we measured H1-T6SS transcription and translation in response to co-culture with *B. thai* using previously characterized chromosomal b-galactosidase reporters (98). In contrast to minor effects on transcription, we found that co-culture of *P. aeruginosa* with *B. thai* markedly stimulates H1-T6SS translation (Figure 3.7B). In control experiments with *B. thai* Δ*tssM-1* as the competitor, we observed no enhancement of H1-T6SS expression. Based on these data, we hypothesized that PARA is driven by the Gac/Rsm pathway.

If the Gac/Rsm pathway were involved in PARA-mediated H1-T6SS activation, we would expect transcription of its associated sRNA molecules to be elevated in cells co-cultivated

with *B. thai* (Figure 3.7A). Indeed, using a chromosomal fluorescent reporter of *rsmZ* transcription, we found *B. thai* stimulates expression of this sRNA on a time scale consistent with other effects associated with PARA (Figure 3.7C, D, Movie 3.4). Cells exposed to *B. thai* Δ*tssM-1* did not exhibit changes in *rsmZ* expression. To further explore the link between Gac/Rsm and PARA, we measured the expression of a validated direct target of RsmA that is unrelated to the H1-T6SS, *magA* (98, 137). As observed for H1-T6SS reporters, a translational chromosomal fusion of the *magA* promoter to *gfp* (p-*magA-gfp*) displayed increased expression in response specifically to co-cultivation with *B. thai* bearing an active interbacterial T6SS (Figure 3.7E). Taken together with our β-galactosidase reporter results, these data show that PARA is a Gac/Rsm-mediated posttranscriptional response of *P. aeruginosa* to T6S in other bacteria.

Next we examined upstream components of the Gac/Rsm pathway that might mediate PARA. In *P. aeruginosa*, the output of the Gac/Rsm pathway is modulated by three sensor kinases (Figure 3.7A) (138). We began by investigating GacS, which directly phosphorylates GacA, the response regulator that activates *rsmY* and *rsmZ* expression (Figure 3.7A). Consistent with our hypothesis that PARA requires Gac/Rsm mediated signaling, we found that a strain bearing an in-frame deletion of *gacS* fails to elevate H1-T6SS expression in response to $T6S^{BT}$ (Figure 3.7F). The remaining Gac/Rsm-associated sensor kinases, RetS and LadS, play accessory roles in the Gac/Rsm pathway by positively or negatively regulating GacS phosphorylation of GacA, respectively (Figure 3.7A). Our experiments showed that strains lacking *ladS* respond to $T6S^{BT}$ similarly to the wild-type (Figure 3.7G, 3.8A); however, we found that PARA is abrogated in strains lacking *retS* (Figure 3.7H, Figure 3.8B). This finding suggests that the relief of RetS repression of GacS-catalyzed phosphorylation of GacA is important in PARA induction.

This might occur through direct binding of RetS to a signal produced by the presence of the competitor organism, or, alternatively, RetS could transduce a signal from an upstream sensor. To investigate these possibilities, we generated a *P. aeruginosa* strain bearing a chromosomally-encoded RetS variant containing an amino acid substitution of a highly conserved residue in the predicted periplasmic signal binding pocket (W90A) (139, 140). Consistent with RetS acting as the direct sensor for PARA, in the *retS*^{W90A} background, neither ClpV1 expression levels nor activity were affected by co-cultivation with *B. thai* (Figure 3.7H, Figure 3.8C). A general disruption of RetS function cannot be excluded; however, the finding that H1-T6SS expression levels in *retS*^{W90A} do not approach those detected in a Δ*retS* mutant demonstrates that this allele retains partial function. Altogether, our findings suggest that RetS functions upstream in the Gac/Rsm pathway to mediate PARA.

Gac/Rsm is a pathway generally noted as a regulator of antibiosis; its stimulation in pseudomonads can increase the expression of a variety of antibiotic factors in addition to T6S, including hydrogen cyanide, secreted hydrolytic enzymes, and phenazines (125). We reasoned that the fitness of cells undergoing PARA is derived not only from an increase in expression and activity of the H1-T6SS, but also from increased levels of these co-regulated factors. To test this, we used growth competition assays and TLFM co-cultures to compare the fitness of Δ*gacS* to a strain lacking only the function of the H1-T6S pathway (Δ*tssM1*). Consistent with our hypothesis, the fitness of Δ*gacS* was reduced beyond that of Δ*tssM1* only when in competition with either *B. thai* (34-fold reduction) or *E. cloacae* (15-fold reduction) bearing an active interbacterial T6S pathway (Figure 3.9A, B). TLFM experiments further indicated a substantial increase in lysis of *P. aeruginosa* Δ*gacS* relative to wild-type or Δ*tssM1* (Figure 3.9C, Movie 3.5). These phenotypes are not due to a general growth defect, as neither *P. aeruginosa* Δ*gacS*

nor Δ*tssM1* exhibit a competitive defect when grown in co-culture with the parental strain (Figure 3.9D). In total, these data indicate that PARA is a complex bacterial defense mechanism comprising the H1-T6SS and other Gac/Rsm-regulated factors of *P. aeruginosa*.

3.3.5 *T6S-dependent interactions result in release of a diffusible signal*

T6S-dependent interactions require direct cell–cell contact; therefore, we asked whether PARA is also contact-dependent. To examine this, we computationally sorted *P. aeruginosa* into populations contacting or not contacting *B. thai* during the course of TLFM experiments (Figure 3.10A). Surprisingly, we found no significant difference in ClpV1-GFP levels between these populations of cells (Figure 3.10B), suggesting that either PARA does not require immediate cell contact between *P. aeruginosa* and a competitor, or *P. aeruginosa*–competitor contacts can be sensed by non-contacting cells. To differentiate between these possibilities, we employed a population-level approach in which we measured PARA-associated phenotypes in *P. aeruginosa* cells following cultivation on an agar plate (Figure 3.10C). Consistent with our microscopy experiments, PARA was detected in *P. aeruginosa* cultivated in the presence of *B. thai,* but not in monoculture or with *B. thai* Δ*tssM-1* (Figure 3.10D, E; Condition 1). We next measured PARA in *P. aeruginosa* cells separated by a membrane from either a *B. thai* monoculture or a *P. aeruginosa–B. thai* co-culture. Strikingly, PARA was detected when *P. aeruginosa* was adjacent to contacting *P. aeruginosa–B. thai* mixtures, but not when adjacent to *B. thai* alone (Figure 3.10D, E; Conditions 2 and 3). Combined with our microscopy results, these data strongly suggest that during co-culture with *P. aeruginosa*, the activity of $T6S^{BT}$, or $T6S^{BT}$ itself, generates a diffusible molecule that triggers PARA in surrounding cells.

3.3.6 *Self-derived lysate is sufficient to trigger PARA*

One outcome of T6S-dependent interactions is cell lysis. Thus, we posited that lysed *P. aeruginosa* – a consequence of $T6S^{BT}$ activity – could be the source of the diffusible factor mediating PARA. In agreement with this hypothesis, when *P. aeruginosa* is cultivated with *B. thai*, but not *B. thai* Δ*tssM-1*, there is a significant increase in the number of *P. aeruginosa* cells that undergo lysis (Figure 3.11A). Furthermore, concurrent temporal analysis of H1-T6SS expression and cell lysis in TLFM sequences indicated that *P. aeruginosa* lysis precedes elevation of ClpV1-GFP expression and the initiation of *B. thai* cell death (Figure 3.11B, Movie 3.6). To determine if lysed *P. aeruginosa* cells are sufficient to induce PARA, we incubated reporter strains with lysate derived from wild-type *P. aeruginosa*. Lysate derived from *P. aeruginosa*, but not from *B. thai*, stimulated the Gac/Rsm pathway and recapitulated downstream PARA-associated phenotypes (Figure 3.11C, D).

Due to its complex nature, lysate has the potential to lead to non-specific changes in cellular physiology that could confound interpretation of a small set of individual reporters. To gain a more comprehensive view of the effects of self-derived lysate on *P. aeruginosa* physiology, we used quantitative mass spectrometry to measure changes in protein abundance at the proteome level. To our knowledge, the global impact of Gac/Rsm activation on the *P. aeruginosa* proteome has not been reported. In lieu of this, we utilized a microarray study published by Lory and colleagues (Δ*retS* versus wild-type) in order to generate a list of proteins under Gac/Rsm control. Given the short time scale of our experiment and the relatively slow rate by which many proteins are recycled, we focused on factors positively regulated by Gac/Rsm. Remarkably, despite constituting only 4.5 percent of the proteins detected in our proteome, known Gac/Rsm targets accounted for 49 percent of proteins induced greater than two-fold by

the addition of lysate (Figure 3.11E). We performed a gene set enrichment analysis and found that both Gac/Rsm regulated proteins and H1-T6SS proteins are significantly enriched in cells treated with lysate (Gac/Rsm: NES, 2.1, FDR ≤ 0.2%, $P > 0.01$; H1-T6SS: NES, 1.6, FDR ≤ 5.1%, $P < 0.01$) (141, 142). The remaining 51 percent of induced proteins could include novel Gac/Rsm targets and lysate-responsive factors outside of the Gac/Rsm regulon. Together, these data show that self-derived lysate activates the Gac/Rsm pathway and is sufficient to induce PARA.

A predicted consequence of PARA is a diminished capacity of *P. aeruginosa* to kill competitor organisms that lack an active lytic pathway. Our finding that lysate is sufficient to induce PARA provided an opportunity to test this directly. Specifically, we asked whether artificial induction of PARA by lysate could stimulate *P. aeruginosa* killing of *B. thai* lacking an active interbacterial T6SS. To this end, we measured the effect of lysate-induced PARA on *P. aeruginosa* fitness in growth competition experiments with *B. thai* Δ*tssM-1*. In agreement with our prediction, the fitness of *P. aeruginosa* increased approximately 2.5-fold in the presence of lysate (Figure 3.11F, Appendix A). In summary, our data suggest that *P. aeruginosa* cells that undergo lysis as a result of interspecies antagonism serve as a signal for Gac/Rsm-mediated stimulation of antibiosis in the remainder of the population.

3.3.7 *Type IV secretion triggers PARA*

Ho et al. recently demonstrated that *E. coli* cells possessing an active IncP-type conjugative type IV secretion (T4S) apparatus are targeted more efficiently by the H1-T6SS of wild-type *P. aeruginosa* than *E. coli* lacking this system (132). The authors of this study proposed that – like T6SS dueling – this effect is a result of enhanced T6S activity against *E. coli*

deriving from local membrane perturbations made by the incoming conjugative apparatus. We hypothesized that the effect observed could also be a result of PARA. To test this, we performed interbacterial growth competition experiments between *P. aeruginosa* and *E. coli, E. coli* containing the IncP-type RP4 conjugative plasmid used by Ho *et al.*, or *E. coli* bearing a mutant form of this plasmid lacking a functional T4S apparatus (Δ*traG*) (143, 144). Similar to earlier findings, we found that the H1-T6SS of *P. aeruginosa* reduces populations of $T4S^+$ *E. coli* to a greater extent than $T4S^-$ *E. coli* (Figure 3.12A, Figure 3.13). However, contrary to observations made by Ho *et al.* using the *P. aeruginosa* Δ*retS* background, we found that removal of the TPP did not abrogate the ability of *P. aeruginosa* to differentially target $T4S^+$ and $T4S^-$ *E. coli* with the H1-T6SS (Figure 3.12A).

Having ruled out a requirement for the TPP in T4S sensing by wild-type *P. aeruginosa*, we next measured PARA-associated phenotypes in *P. aeruginosa–E. coli* co-cultures. These experiments showed that *P. aeruginosa* cultivated with $T4S^+$ *E. coli* exhibit increased *rsmZ* expression and elevated ClpV1–GFP levels in a manner dependent upon *retS* (Figure 3.12B-F). Moreover, these phenomena were observed at a time point similar to $T6S^{BT}$-induced PARA.

Our data suggest that the mechanism underlying PARA is lysis of *P. aeruginosa* cells by a competitor; however, to our knowledge, T4S has not been noted to cause lysis of recipient cells. To determine whether *E. coli* lyse *P. aeruginosa* in a T4S-dependent manner, we quantified extracellular b-galactosidase activity from co-cultures of $T4S^+$ and $T4S^-$ *E. coli* with *P. aeruginosa attB*::*lacZ*. Consistent with PARA induction by *E. coli* involving cell lysis, we observed a strong enhancement of *P. aeruginosa* lysis by $T4S^+$ *E. coli* (Figure 3.12G). Together, these data demonstrate that the T4SS encoded on the RP4 plasmid induces lysis within a subset

of *P. aeruginosa* cells, which in turn induces PARA, leading to H1-T6SS-dependent *E. coli* cell death.

3.4 Discussion

We have shown that self-derived signal(s) generated as a consequence of cell lysis activate the Gac/Rsm pathway of *P. aeruginosa*, and thus stimulate the production of antibiotic factors under its control. In growth competition experiments, the capacity to mount this multifaceted response grants *P. aeruginosa* a significant fitness benefit. Our results suggest that similar to multicellular organisms, injury to a bacterial colony can trigger the release of danger signals that lead to a coordinated response against the threat (145, 146). In this study, we focused on offensive factors under control of the Gac/Rsm pathway; however, defensive factors are also likely to be elaborated. For example, a consequence of Gac/Rsm activation in *P. aeruginosa* is the production of c-di-GMP, which activates exopolysaccharide production of *P. aeruginosa* (147, 148). This increases cellular adhesiveness, which facilitates multicellular aggregates that are more resistant than planktonic cells to an assortment of antibacterial molecules and environmental stresses (149, 150). In the context of an infection such as the chronic lung infections that occur in cystic fibrosis patients, host-induced cellular lysis could activate Gac/Rsm and inadvertently convert cells to a state that is more resistant to killing by antibiotics and the immune system.

If PARA were the sole mechanism contributing to enhanced T6S-dependent killing of bacteria with T6 or T4 systems, it would follow that *P. aeruginosa* cells lacking the sensor kinase RetS should target bacteria irrespective of these pathways. However, previous studies have shown that *P. aeruginosa* Δ*retS* retains some ability to differentially target T6S- and T4S-

positive versus -negative cells (120, 131). Thus, the response of *P. aeruginosa* to antagonism is comprised of a global response mediated by the Gac/Rsm pathway and a secondary T6S-specific element that is not fully understood. We speculate that this ability of a Δ*retS* strain is related to coordinated spatiotemporal localization of the apparatus among adjacent cells, and that these two mechanisms operate in concert to hone the offensive response of *P. aeruginosa*. PARA may constitute an initial adaptation in which cells perceive a threat in their proximity and increase expression of the H1-T6SS, followed by the orientation of effector translocation specifically toward aggressor cells.

We find that RP4-containing *E. coli* cells induce lysis in *P. aeruginosa*, trigger PARA, and in turn are subject to increased antagonism by the H1-T6SS. This mechanism differs from the model put forth by the Mekalanos laboratory, which suggested that the TPP is required for the response of wild-type *P. aeruginosa* to an incoming conjugative apparatus (132). A key finding in the prior study was that polymyxin B, an outer membrane-disrupting antibiotic, induces *clpV1* foci formation in wild-type *P. aeruginosa*, but not in a strain lacking *tagT.* This finding, among other data involving strains in the Δ*retS* background of *P. aeruginosa*, led the authors to propose that membrane perturbations caused by an incoming T4 apparatus are sensed by the TPP. A *tagT* deletion strain intrinsically lacks H1-T6SS activity; therefore, interpreting its inability to respond to the antibiotic as evidence of TPP involvement is problematic (83, 131, 132). We found that H1-T6SS-active strains that lack the TPP (ΔTPP Δ*tagF*) display a generalized targeting defect, but retain the ability to discriminate $T4S^+$ and $T4S^-$ *E. coli*. An alternative explanation for the findings of Ho *et al.* is that the application of polymyxin B promotes cell lysis, leading to PARA induction (132, 151). Attempts to test the validity of this explanation were confounded by pervasive cell death at the antibiotic concentration reported by

the authors (20 mg/mL, ~40-fold the minimum inhibitory concentration against *P. aeruginosa* PAO1) (151).

The adaptive significance of RP4-induced lysis and its mechanistic basis remain to be resolved. This process could be an altruistic behavior of *P. aeruginosa* that both aborts the T4S-dependent transfer event and alerts surrounding kin, thus decreasing the probability of foreign DNA acquisition by the colony. However, a second possibility is that plasmids such as RP4 carry interbacterial antagonistic factors that provide fitness to their hosts under certain conditions. It is interesting to note that Ho *et al.* identified an RP4 transposon mutant that was not targeted by *P. aeruginosa* but retained a functional T4SS (132). This insertion resides in *trbN*, a gene encoding a periplasmic transglycosylase. It is plausible given the requirement for both T4 structural genes and this peptidoglycan-degrading accessory factor, that the T4S apparatus facilitates the transfer of this protein to recipient cells, where it induces lysis. Alternatively, upon plasmid transfer, the product of *trbN* may stochastically trigger lysis in a small portion of recipient cells.

Efforts to characterize Gac/Rsm-stimulating signal(s) have been performed primarily in *P. fluorescens* (125). This organism is a close relative of *P. aeruginosa*, and the Gac/Rsm pathways of the two species share a number of characteristics including regulation of hydrogen cyanide production and an H1-T6SS-like pathway. Haas and colleagues have made a number of intriguing observations pertaining to the production and sensing of Gac/Rsm-stimulating signals in *P. fluorescens* that are consistent with our findings in *P. aeruginosa*. Most notably, they found that conditioned media extracts derived from dense cultures of *P. fluorescens*, and, to a lesser extent, *P. aeruginosa* and *Vibrio cholerae*, are sufficient to activate the Gac/Rsm pathway (129). In agreement with our results, this indicates that the signal can be self-produced; however, it also raises the intriguing possibility that the lysis of non-self bacteria may activate PARA. While we

found that neither *B. thai*- nor *E. coli*-derived lysates were sufficient to stimulate PARA, it is possible that other organisms produce the signal. This could lead to a positive feedback loop by which killed competitor cells further stimulate *P. aeruginosa* to produce antibacterial factors.

Despite decades of research, the chemical structure of the molecule(s) that stimulate the Gac/Rsm pathway of *P. aeruginosa*, presumably via interaction with the periplasmic ligand binding domains of its associated sensor kinases, remain unknown. Our own efforts to identify the signaling molecule(s) contained within *P. aeruginosa* lysate, which included assorted enzymatic treatments, have so far been unsuccessful. Structural studies of RetS revealed its periplasmic region bears a fold resembling known carbohydrate interaction domains. A similar domain is predicted in the ecto domain of LadS (140). Given that RetS is required for PARA transduction, it is tempting to speculate that cell-associated carbohydrate(s) are released upon lysis and serve as a signal that activates Gac/Rsm in *P. aeruginosa* (139). The additional observation that extracts derived from multiple bacterial species can stimulate Gac/Rsm in *P. fluorescens* suggests two non-mutually exclusive hypotheses: that the molecule is broadly conserved or that the pathway has evolved to respond to a number of inputs (129). The existence of three sensor kinases that operate upstream in the Gac/Rsm pathway of *P. aeruginosa* supports the latter hypothesis.

In what they referred to as "competition sensing," Cornforth and Foster recently proposed that bacterial stress responses include antagonistic components, and that these pathways have evolved to respond to threats posed by other bacteria (10). For example, in response to DNA damage, the SOS pathway stimulates colicin production in *E. coli*, and in *P. aeruginosa*, exogenous peptidoglycan fragments have been shown to stimulate quorum-regulated toxins (152, 153). Our study demonstrates that "competition sensing" includes an antibacterial response to

cellular damage in kin cells. While we found that T6S-dependent killing by *P. aeruginosa* is part of an antagonistic response to lytic threats, Borgeaud *et. al.* reported that in *V. cholerae*, T6S is co-regulated with competence machinery and utilized for obtaining access to exogenous DNA (154). Together, these studies demonstrate how functionally conserved machinery can be incorporated into diverse cellular programs exhibited by bacteria.

The "danger theory" of eukaryotic immunity proposes that in addition to the foreign substances that they introduce, threats can be sensed by virtue of cellular damage and ensuing mislocalization of host factors (2, 146). For instance, uric acid microcrystals, which form upon release of the molecule to the sodium-rich extracellular milieu, stimulate dendritic cell maturation (3). Our study shows that bacteria can also recognize threats by sensing self-derived signals associated with cell damage (Figure 3.14). Moreover, we find that the response to such signals includes the activation of factors that combat the threat – akin to the stimulation of inflammation in eukaryotes. It remains to be determined whether danger sensing is common among bacteria. The Gac/Rsm pathway is conserved widely among Gram-negative g-proteobacteria; however, the variability of genes under its control confounds a prediction of its general involvement in danger sensing (125). An intriguing possibility is that bacteria can utilize a diversity of signaling systems to sense and respond to kin cell damage.

3.5 Materials and Methods

Bacterial strains and culture conditions. All strains used in this study were derived from *P. aeruginosa* PAO1 (106), *B. thai* E264 (155), *E. cloacae* ATCC 13047 (156), and *E. coli* XK1502 (157). Routine cultivation of bacteria was performed using Luria broth (LB) medium. A low salt formulation of LB in which no additional sodium chloride was added (LS-LB), was used for plate-based co-culture and competition assays. For *P. aeruginosa*, media were supplemented with 25 μg/mL irgasan, 30 μg/ mL gentamycin, 75 μg/mL tetracycline, or 40 μg/ mL X-gal (5-bromo-4-chloro-3-indolyl β-D-galactopyranoside) as necessary, and counter selection for allelic exchange was performed on low-salt LB supplemented with 5% w/v sucrose. For *B. thai*, media were supplemented with 25 μg/mL irgasan and 200 μg/mL trimethoprim as necessary, and counter-selection for allelic exchange was performed on M9 minimal medium agar plates containing 0.4% glucose and 0.2% (w/v) *p*-chlorophenylalanine (158). For *E. coli*, media was supplemented with 15 μg/mL gentamycin, 200 μg/mL trimethoprim, 25 μg/mL chloramphenicol, and 150 μg/mL carbenicillin as necessary.

Construction of genetically modified strains. Markerless deletions of genes in *P. aeruginosa* and *B. thai* were generated in frame by allelic exchange with the suicide vectors pEXG2 and pEX18gm (*P. aeruginosa*), or pJRC115 (*B. thai*) (107, 158). *SacB* and *pheS*-A304G were used for counterselection in *P. aeruginosa* and *B. thai*, respectively. Deletion alleles were constructed by splicing together 500-600 bp regions flanking the gene to be deleted by overlap extension PCR, and cloning them into the appropriate vector. The open reading frame, except the first and last 4-8 codons of the gene, was replaced by the sequence 5'-TTCAGCATGCTTGCGGCTCGAGTT -3'. A detailed list of strains and vectors used this study are provided in Tables 1 and 2, respectively.

Functional translational fluorescent fusions to ClpV1 and Fha1 at their native promoters were achieved by allelic exchange. Constructs were generated by amplification of 500-600 bps regions flanking the C-terminus of the gene. These regions were spliced together, with a BamHI site replacing the stop codon, and cloned into pEXG2. *Gfp* and *superfolder-gfp (sfgfp*) containing a stop codon was cloned into the BamHI site for *clpV1* and *fha1* constructs, respectively. The translational fusion to MagA was generated using a similar strategy, except that only the first 12 codons of *magA* were retained. A resulting clone was introduced to *P. aeruginosa* by allelic exchange. To generate *P. aeruginosa attB*::p-*rsmZ-gfp,* the *rsmZ* promoter was amplified, spliced to an unstable *gfp* variant, and cloned into mini-CTX2 (159). The resulting clone was introduced to *P. aeruginosa* by conjugation. The retS^{W90A} strain was generated by amplification of 500-600 bps flanking the W90 residue of RetS. The W90A substitution was encoded on the overlap primers and the two regions were spliced together by overlap extension PCR and cloned into pEXG2. The mutation was introduced to PAO1 by allelic exchange. Transcriptional and translational *lacZ* fusions to *tssA1*, original described by Brencic et al. (98), were introduced to *P. aeruginosa* by conjugation and transformation, respectively. Integration of constitutive fluorescent reporters at the attTn7 site of *B. thai* and *P. aeruginosa* was achieved by four-parental mating or transformation, respectively (160).

TraG on RP4 was replaced with a chloramphenicol resistance cassette by λ Red recombination (161) in *E. coli* CC1254, resulting in RP4 Δ*traG*::chlmR (RP4 Δ*traG*). Following PCR confirmation, RP4 Δ*traG* was transferred to XK1502 by P1 phage transduction.

Time-lapse fluorescence microscopy. Overnight cultures were diluted 1:50 or 1:100 in LB and incubated with aeration at 37°C until an OD_{600} of 0.5-0.7 was reached. Cultures were concentrated 5-fold and mixed 1:1 by volume with the indicated competitor. 1-2 µL of the

bacterial suspension was spotted onto a 1.5% w/v agarose growth pads (prepared using Vogel Bonner minimal media containing 0.2% w/v sodium nitrate and 0.01% w/v casamino acids) and sealed.

Microscopy data was acquired using NIS Elements (Nikon) acquisition software on a Nikon Ti-E inverted microscope with a 60× oil objective, automated focusing (Perfect Focus System, Nikon), a Xenon light source (Sutter Instruments), and a CCD camera (Clara series, Andor). Lysis and growth rate were measured from TLFM sequences acquired at 5-minute intervals; expression was measured from 15-minute interval TLFM sequences. At least three fields were acquired and analyzed for each experimental group, and experiments were performed independently multiple times.

Image analysis. TLFM sequences were analyzed using previously described methods (120). Briefly, cells were identified from phase images using a watershed algorithm. *P. aeruginosa* and competitor cell populations were distinguished by the constitutive expression of cytoplasmic mCherry in either *P. aeruginosa* or the competitor organism. Non-cell debris was excluded based on a size threshold and/or fluorescence gating. For display in figures only, the GFP channel was g-transformed (ClpV1-GFP, exponent = 1.2; Fha1-GFP, exponent = 1.3), thresholded, and the Matlab colormap (jet) was applied.

To calculate average cellular fluorescence, GFP intensity of non-cell regions was subtracted from GFP intensity of cell regions as defined by cell masks. To identify foci within cells, the cytoplasmic fluorescence of each cell was fit to an empirical model for cytoplasmic fluorescence. A cell template image was generated by applying a 74 Gaussian blur (radius 2 pixels) to the square root of the distance transform applied to the cell mask. A least-squares fit of a constant times the cell template was then performed to the observed cell image. The noise was

computed as the standard deviation of the cell intensity after subtracting the fits of the cytoplasmic fluorescence and the fits of all potential foci. The signal to noise of a potential focus was computed as the intensity of the brightest pixel divided by the noise of that cell, and was defined as a focus if the value exceeded an empirically determined threshold. Candidate foci were identified globally using a watershed algorithm, then assigned to cells whose masks overlapped the focus position. The average and standard deviation of the percentage of *P. aeruginosa* cells with foci calculated for three fields is plotted.

For contact-dependence analyses, cell neighbors were defined as cells with a boundary within a 2-pixel radius of the current cell (120). Growth rate and cellular lysis was determined from datasets in which cells were linked over time based on frame-to-frame overlap of bright-field images. Doubling times – defined as minutes between birth and death – were calculated for cells that arose from a division after the start of the experiment and divided prior to the end of the experiment. A lysis event was defined as an 80% decrease in fluorescence intensity of a single cell between consecutive frames and was measured for in strains expressing a constitutive fluorophore (mCherry, GFP, or CFP). For figures in which end-point *P. aeruginosa* lysis was presented, the number of *P. aeruginosa* cells that lysed was normalized to the initial number of *P. aeruginosa–B. thai* contacts to control for small fluctuations in cell density and *P. aeruginosa*–competitor ratio.

Growth-competition assays. For all end-point growth competition assays, except when noted, overnight cultures were used. Cultures were washed and mixed at the indicated volumetric ratios, five microliters of the resulting mixture was spotted on a nitrocellulose membrane placed on a LS-LB 3% w/v agar plate, and incubated at 37°C. For intraspecies growth competition experiments, *P. aeruginosa attB::lacZ* was used as the donor strain background, experiments

were initiated at a 1:1 donor:recipient ratio, and were plated on LB containing X-gal for enumeration. Growth competition experiments with *B. thai* competitors were initiated with overnight cultures at a donor:recipient ratio of 5:1 (interspecies wild-type and T6S-dependent fitness, Figure 3.1; TPP strain experiments, Figure 3.6) or 1:1 (Δ*tssM1* and Δ*gacS* fitness, Figure 3.9A) and plated on LB containing gentamycin (30 μg/mL) for *B. thai* selection and trimethoprim (200 μg/mL) for *P. aeruginosa* selection. For *E. cloacae* competitors, which encode *lacZ*, log-phase cultures were mixed at a ratio of 8:1 (TPP strain experiments, Figure 3.6) or 1:1 (Δ*tssM-1* and Δ*gacS* fitness, Figure 3.9B) and plated on media containing X-gal for *P. aeruginosa–E. cloacae* enumeration. For growth competition experiments with *E. coli* competitors, a *P. aeruginosa attB::lacZ* background was used, experiments were initiated at a donor:recipient ratio of 1:2, incubated for 3 hours, and plated on LB containing X-gal.

H1-T6SS transcriptional and translational assays. *P. aeruginosa* strains bearing previously validated chromosomally encoded transcriptional or translation fusions to *tssA1* (PA0082) were utilized to quantify transcription and translation (see also Table 3.1 and 3.2) (98). Overnight cultures were washed, mixed at a 1:2 ratio with media (monoculture), *B. thai*, or *B. thai* Δ*tssM-1,* then spotted on a nitrocellulose membrane placed on a LS-LB 3% w/v agar plate. Following a 3-hour incubation at 37°C, cells were harvested in PBS, washed, and assayed for relative levels of β-galactosidase activity using the Galacto-Light™ Plus Reporter Gene Assay System (Life Technologies).

Diffusion experiments. Bacterial suspensions composed of overnight cultures, washed once and mixed at a 2:1 *P. aeruginosa*:*B. thai* ratio were spotted as depicted in Figure 3.10C on LS-LB 3% w/v agar. Following 3 hours of incubation at 37°C, bacteria growing on top of the filter (Figure 3.10C, black dashed lines) were resuspended in LB and imaged by microscopy to

determine PARA induction. To exclude dead *P. aeruginosa* cells from our analysis, which were prevalent in Condition 1, a *P. aeruginosa* strain constitutively expressing mCherry was used and only mCherry-positive cells were considered.

Lysate experiments. Stationary phase *P. aeruginosa* or *B. thai* cultures were pelleted and resuspended in growth media or PBS before sonication. Colony forming units (c.f.u.) of cultures and lysates were enumerated to verify that >95% of cells were lysed. For TLFM experiments, an agarose pad prepared as described above was infused with either lysate or PBS (control). The concentration of lysate in the agarose pad was approximately $5x10^4$ lysed cells/μL. Reporter strains were cultivated to OD_{600} of 0.5-0.7, spotted on the lysate-containing agarose pad, and imaged. For the growth competition assays, lysate or PBS (control) was spotted on a LS-LB 3% w/v agar growth plate, a nitrocellulose filter was placed on top, and indicated mixtures of cells were spotted directly over the lysate.

Sample preparation for proteomic analysis. LB plates were prepared by applying either lysate (25-fold concentrated *P. aeruginosa* at an OD_{600} of 0.5-0.7 resuspended in PBS and lysed by sonication) or PBS (control) at 2% (v/v). A concentrated *P. aeruginosa clpV1-gfp* culture (at OD_{600} 0.5- 0.7) was spotted on the nitrocellulose membrane placed on each plate then incubated for 2.5 hrs at 37°C. Cells were harvested in PBS, washed, then stored at -80°C. Duplicate biological samples were prepared for mass spectrometry analysis as described previously (71).

The semi-quantitative technique of spectral counting was used to determine the relative abundance of identified proteins in each sample as described in Whitney *et al.* (71, 162). Only proteins present in both biological replicates and with a sum of 20 spectral counts or greater across all replicates were considered in our analysis.

T4S-dependent lysis of *P. aeruginosa.* Overnight cultures of *P. aeruginosa attB::lacZ* were washed, mixed 1:2 with *E. coli* strains, and spotted on a nitrocellulose membrane placed on a NS-LB 3% w/v agar plate. Following 3 hours of incubation at 37°C, levels of extracellular and total β-galactosidase activity were determined as previously described (91). The percentage of lysed *P. aeruginosa* lysis was determined by normalizing extracellular to total β-galactosidase activity.

Statistical tests. All TLFM datasets were analyzed by 2-way ANOVA using a Bonferroni correction for testing multiple hypotheses. End-point assays were analyzed using a two-tailed Student's *t* test. Asterisks indicate significance at $P < 0.05$. Proteomic data was analyzed using Gene Set Enrichment Analysis (GSEA) (141, 142). Genes positively regulated by the Gac/Rsm pathway were defined as those found differentially regulated in a prior study comparing mRNA levels of Δ*retS* and wild-type *P. aeruginosa* (80). 1000 permutations of the analysis were performe d across both phenotype and gene set, and the ratio of classes metric was used for ranking genes.

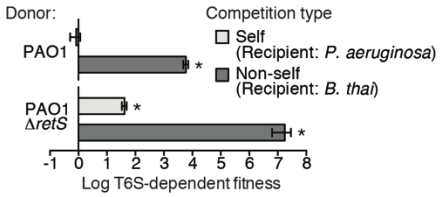

Figure 3.1: Wild-type *P. aeruginosa* cells display a strong T6S-dependent fitness advantage in co-culture with non-self but not self competitors
Outcome of growth competition experiments measuring fitness of *P. aeruginosa* PAO1 parental or Δ*retS* strains in co-cultures with self or non-self recipients under T6SS-promoting conditions. The self recipient was *P. aeruginosa* Δ*tse1-4* Δ*tsi1-4* in the strain background corresponding to the donor genotype (PAO1 or PAO1 Δ*retS*). T6S-dependent fitness was parental donor competitive index (change (final/initial) in ratio of donor and recipient colony forming units (c.f.u.)) normalized to Δ*tssM1* competitive index. Error bars represent ± standard deviation (SD); n = 3 co-cultures. Asterisks denote a fitness advantage significantly > 1 ($P < 0.01$).

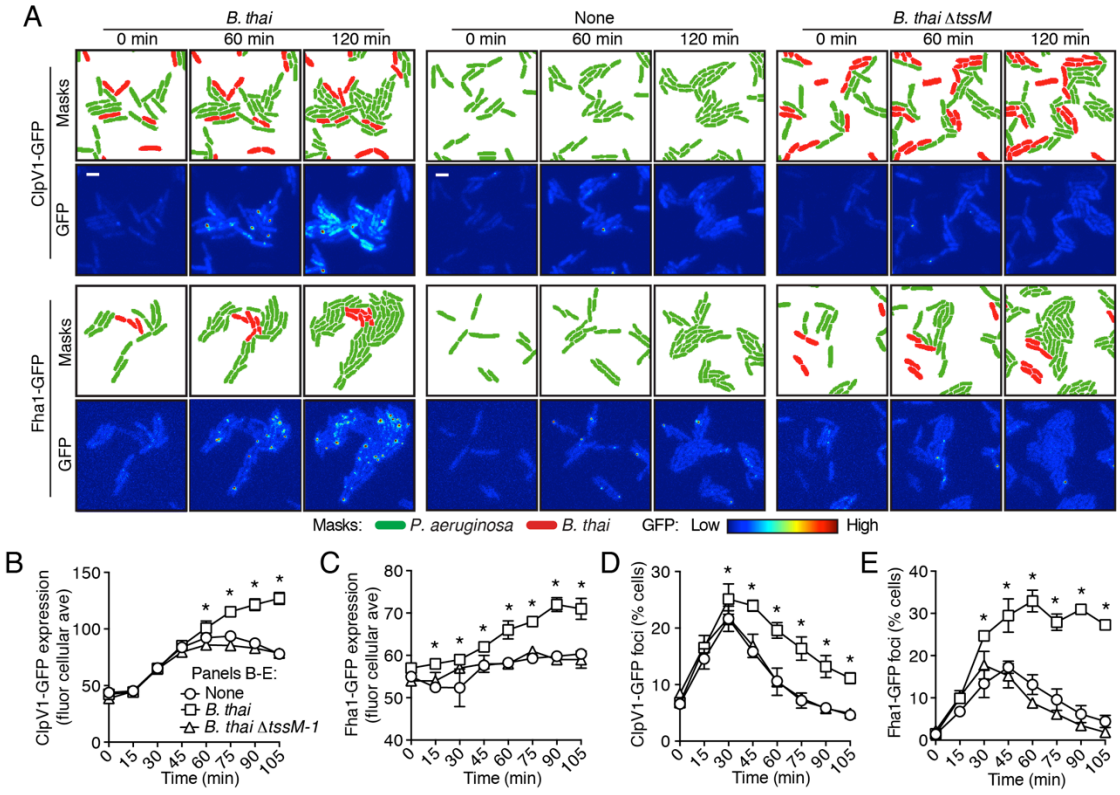

Figure 3.2: Non-self competitor bacteria stimulate expression and activity of the H1-T6SS. (**A**) H1-T6SS expression is increased in *P. aeruginosa* co-cultured with *B. thai* expressing an active T6SS. Time-lapse fluorescence microscopy (TLFM) sequences of *P. aeruginosa clpV1-gfp* (upper) or *fha1-gfp* (lower) in monoculture or in co-culture with the indicated competitor. Cropped regions from representative time-points are displayed. See also Movies 3.1 and 3.2. Masks colored by cell identity depict automated cell identification generated from the phase image. Scale bar, 6 μm. (**B-C**) Quantification of H1-T6SS expression from the *P. aeruginosa clpV1-gfp* (**B**) and *fha1-gfp* (**C**) mono and co-culture TLFM experiments described in (**A**). Average cellular GFP intensity for *P. aeruginosa* cells was calculated from background-subtracted images. (**D-E**) H1-T6SS activity is increased in the presence of *B. thai* with an active T6SS. Percentage of *P. aeruginosa clpV1-gfp* (**D**) or *fha1-gfp* (**E**) cells with GFP foci for experiments described in (**A**). Error bars represent ± SD; n = 3 fields. Asterisks indicate significant differences when *B. thai* was present ($P < 0.05$).

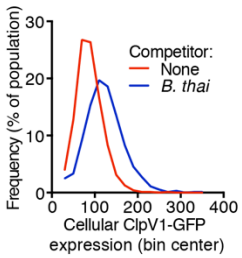

Figure 3.3: Increased H1-T6SS expression occurs throughout the population.
Histograms of cellular ClpV1-GFP intensity of *P. aeruginosa clpV1-gfp* following 90 minutes of growth in monoculture or in co-culture with *B. thai.* Histograms bin size is 20 intensity units and is normalized to total cells.

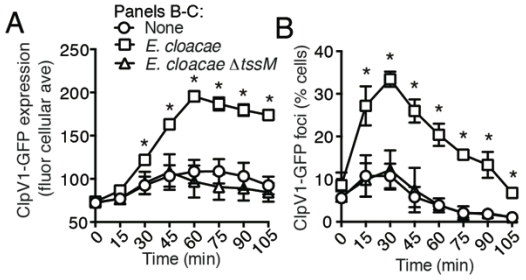

Figure 3.4 *E. cloacae* stimulates the H1-T6SS of *P. aeruginosa* in a T6S-dependent manner. Average cellular ClpV1-GFP expression (**A**) and the percentage of cells with ClpV1-GFP foci (**B**) of *P. aeruginosa clpV1-gfp* in monoculture or in co-culture with the indicated *E. cloacae* competitor. Data was collected and analyzed as described in Figure 3.2. Error bars represent ± SD; n = 3 fields. Asterisks indicate significant differences when *B. thai* was present ($P < 0.05$). See also Movie 3.3.

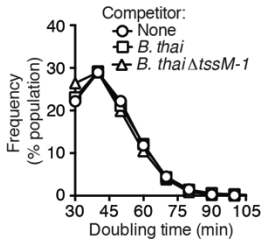

Figure 3.5: *P. aeruginosa* doubling time is not affected by the presence of *B. thai.*
Histograms depicting *P. aeruginosa* doubling times during growth in monoculture or co-culture with *B. thai* under TLFM conditions. Error bars represent ± SD; n = 3 fields.

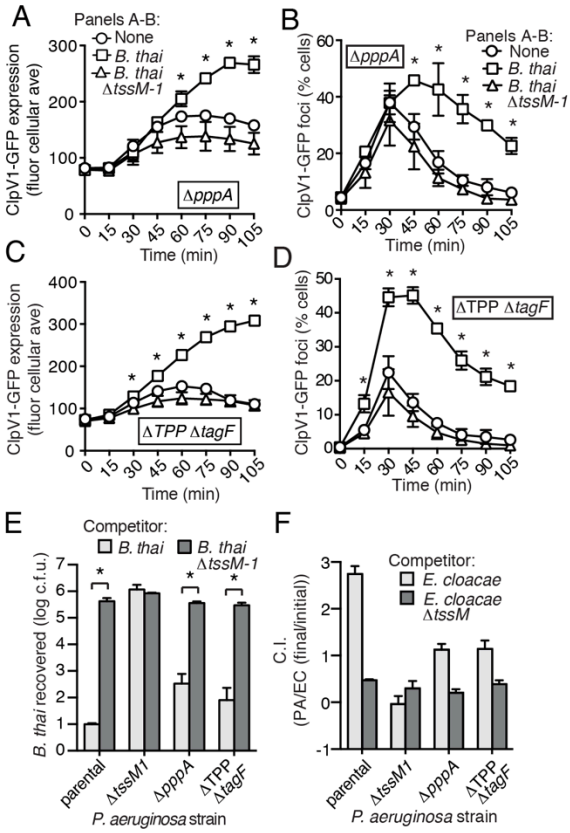

Figure 3.6: PARA does not require the TPP.
(**A-D**) Increased H1-T6SS expression and activity in the presence of *B. thai* does not require a functional TPP. Average ClpV1-GFP cellular fluorescence intensity in *P. aeruginosa clpV1-gfp* Δ*pppA* (**A-B**) and ΔTPP Δ*tagF* (**C-D**) backgrounds during monoculture or co-culture with the indicated competitors. Error bars represent ± SD; n = 3 fields. Asterisks indicate significant differences when *B. thai* was present ($P < 0.05$.). (**E-F**) The TPP is not required for preferential targeting of a competitor with an active T6SS. Outcome of growth competition experiments measuring survival of *B. thai* (**E**) or *E. cloacae* (**F**) following co-culture with the indicated *P. aeruginosa* strain under T6SS-promoting conditions. Error bars represent ± SD; n = 3 co-cultures.

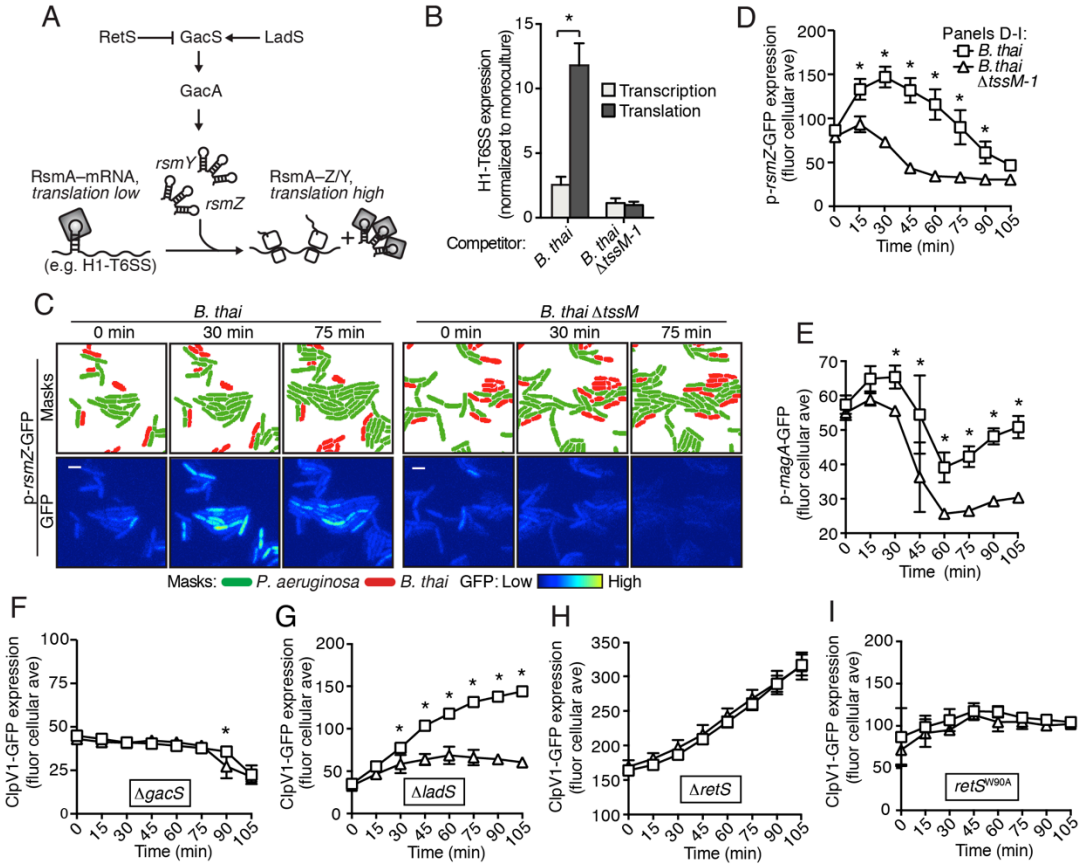

Figure 3.7: The Gac/Rsm pathway is required for PARA.
(**A**) Schematic depicting the Gac/Rsm pathway of *P. aeruginosa*. The orphan sensor kinases RetS and LadS exert opposing activity on a third sensor kinase, GacS, which activates its cognate response regulator, GacA. Active GacA promotes transcription of the sRNAs *rsmY* and *rsmZ*., which sequester RsmA and therefore prevent RsmA binding and destabilization of target mRNAs. (**B**) Elevated H1-T6SS expression in the presence of *B. thai* occurs post-transcriptionally. *P. aeruginosa* strains bearing chromosomally encoded transcriptional or translational fusions to *tssA1* (Brencic and Lory, 2009) were incubated with the indicated competitor. Fold H1-T6SS increase in expression was determined by normalizing *P. aeruginosa* co-cultures to the monoculture. n = 3 co-cultures; asterisk, significant differences between translational and transcriptional activity (P<0.05). (**C**) *RsmZ* expression is elevated in the presence of *B. thai* containing a T6SS. Cells masks and GFP channel from representative TLFM sequences of the indicated co-cultures. See also Movie 3.4. (**D**) Average cellular fluorescence intensity from *P. aeruginosa* of p-*rsmZ-gfp* corresponding to (**C**). (**E**) MagA expression is elevated in the presence of $T6S^{BT}$. Average cellular GFP intensity for *P. aeruginosa* p-*magA-gfp* in co-culture with competitor. (**F-H**) GacS and RetS, but not LadS are required for H1-T6SS activation in response to $T6S^{BT}$. ClpV1-GFP expression was quantified for co-cultures of *P. aeruginosa clpV1-gfp* in the Δ*gacS* (**F**), Δ*ladS* (**G**), and Δ*retS* (**H**) or $retS^{W90A}$ (**I**) backgrounds with indicated competitor. n = 3 fields; asterisks indicate significant differences when *B. thai* was present (P < 0.05).

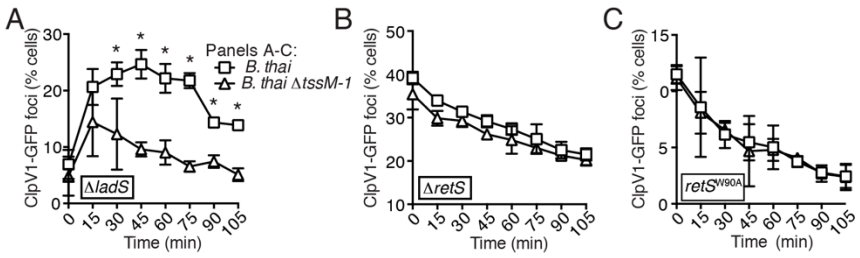

Figure 3.8: PARA-associated increases in H1-T6SS activity depend on RetS but not LadS. (**A**) LadS is not required for increased activity of the H1-T6SS in the presence of *B. thai*. Percentage of *P. aeruginosa clpV1-gfp* Δ*ladS* cells with fluorescent foci during co-culture with the indicated *B. thai* strain. (**B**) Stimulation of H1-T6SS activity by *B. thai* requires RetS. Percentage of *P. aeruginosa clpV1-gfp* Δ*retS* cells with fluorescent foci during co-culture with the indicated *B. thai* strain. (**C**) A putative signal-binding RetS mutant does not respond to the presence of *B. thai.* Percentage of *P. aeruginosa clpV1-gfp retS*^{W90A} cells with fluorescent foci during co-culture with the indicated *B. thai* strain. Error bars represent ± SD; n = 3 co-cultures. Asterisks indicate significant differences when *B. thai* was present ($P < 0.05$).

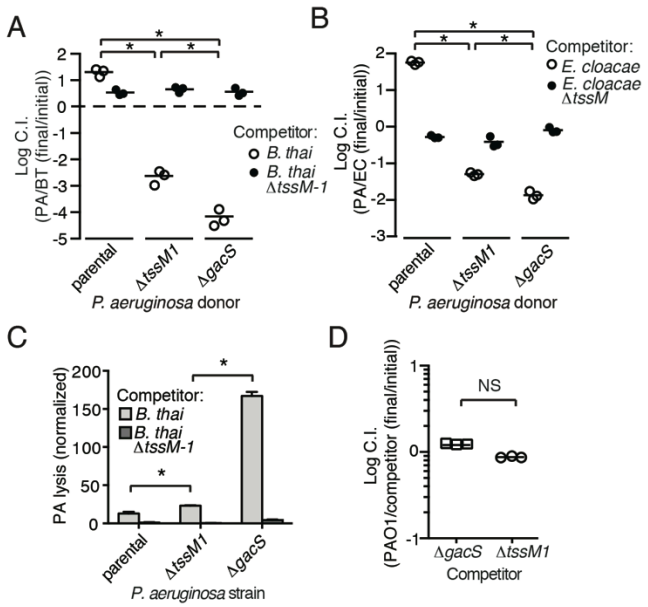

Figure 3.9: Disruption of the Gac/Rsm pathway results in a profound fitness defect in interspecies co-culture.
(**A-B**) A *P. aeruginosa* strain with an inactivated Gac/Rsm pathway displays fitness defects beyond a strain lacking H1-T6S. Outcome of interspecies growth competition experiments between the indicated *P. aeruginosa* and *B. thai* (**A**) or *E. cloacae* (**B**) strains. n = 3 co-cultures. C.I., competitive index. PA, *P. aeruginosa*. BT, *B. thai*. EC, *E. cloacae.* (**C**) *P. aeruginosa* lysis promoted by $T6S^{BT}$ is increased in a strain lacking a functional Gac/Rsm pathway. *P. aeruginosa* lysis events from TLFM sequences were normalized to initial number of contacts with *B. thai*. See also Movie 3.5. n = 3 fields. (**D**) A *gacS* deletion strain does not alter growth rate. Outcome of intraspecies growth competition experiments between PAO1 and the indicated competitor strains under conditions identical to those used in (**A-B**). n = 3 co-cultures. (**A-D**) Error bars represent ± SD; asterisks indicate significant differences between indicated groups ($P < 0.05$). NS, not significant.

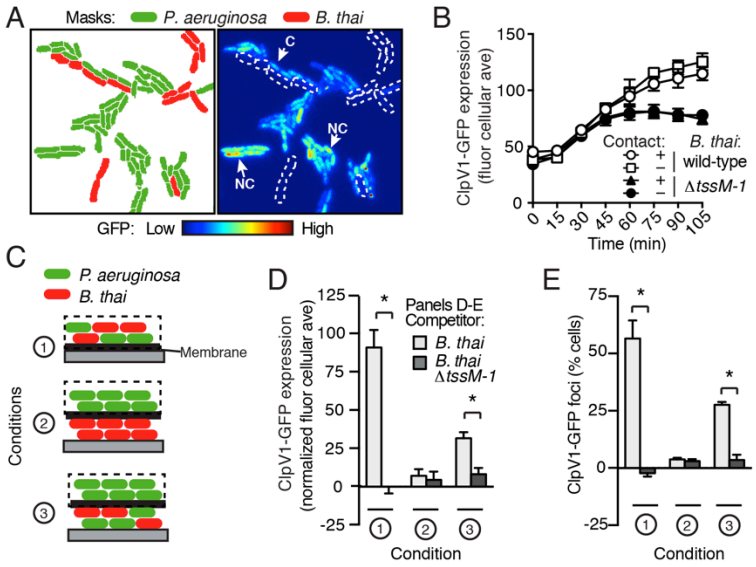

Figure 3.10: PARA is induced by a diffusible signal.
(**A**) The PARA-associated increase in H1-T6SS expression is not contact-dependent. A representative region from a *P. aeruginosa clpV1-gfp–B. thai* co-culture following 120 minutes of growth is depicted. Cells masks are colored by cell identity (left panel); GFP intensity with *B. thai* cell positions outlined in white dashed lines (right panel). Arrows indicate *P. aeruginosa* cells contacting (C) or not contacting (NC) *B. thai.* (**B**) Average cellular ClpV1-GFP expression for contacting and non-contacting subpopulations described in (**A**). (**C**) Schematic depicting the experimental setup for (**D**). (**D**-**E**) PARA induction requires proximity to contacting *P. aeruginosa–B. thai* cells. Bacterial growth was initiated as pictured in (**C**). ClpV1-GFP was measured in populations on the membrane (black dashed lines). Average cellular ClpV1-GFP expression (**D**) and percentage of cells with foci (**E**) was determined. ClpV1-GFP expression measured in co-cultures was normalized by subtracting *P. aeruginosa* monoculture measurements. Error bars represent ± SD; n = 3 fields. Asterisks indicate significant differences between indicated groups ($P < 0.05$).

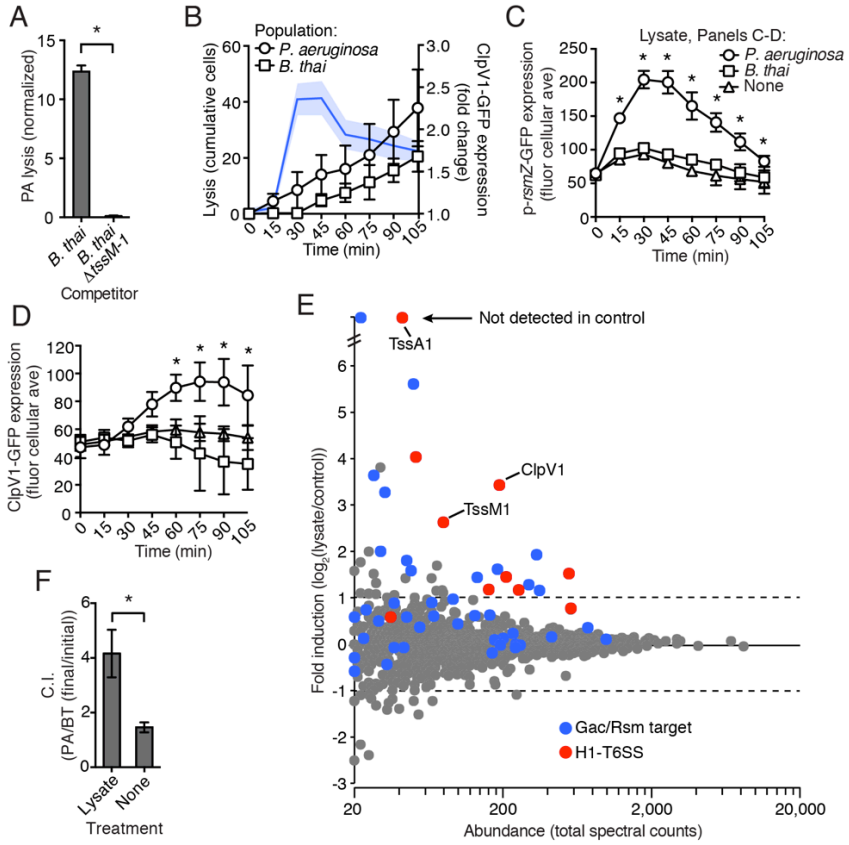

Figure 3.11: *P. aeruginosa* lysis is sufficient to induce PARA.
(**A**) T6S^{BT} promotes *P. aeruginosa* lysis. Lysis of *P. aeruginosa* was measured under TLFM conditions and data were normalized to contacts with *B. thai*. n = 3 fields. Asterisk indicates significant difference between *B. thai* and *B. thai* Δ*tssM-1* ($P < 0.05$). (**B**) *P. aeruginosa* lysis precedes induction of H1-T6SS expression and *B. thai* lysis. Lysis (left axis) and fold increase in ClpV1-GFP (blue line, right axis) measured concurrently under TLFM conditions. ClpV1-GFP levels from *P. aeruginosa*–*B. thai* co-culture were normalized to *P. aeruginosa* monoculture. Error bars and light blue shading, ± SD. n = 4 fields. See also Movie 3.6. (**C**) *P. aeruginosa* lysate stimulates the Gac/Rsm pathway. Average cellular p-*rsmZ*-GFP expression in *P. aeruginosa* cultivated on lysate-infused growth pads. Cellular GFP expression was calculated as described in Figure 3.2. (**D**) H1-T6SS expression is stimulated by *P. aeruginosa* lysate. Average cellular ClpV1-GFP expression of *P. aeruginosa* cultivated on lysate-infused growth pads. (**C**-**D**) n = 3 fields; asterisks indicated significant differences between *P. aeruginosa* lysate and no lysate ($P < 0.05$). (**E**) Expression of Gac/Rsm-regulated proteins is increased in lysate-treated *P. aeruginosa* cells. Quantitative mass spectrometry was used to compare the proteome of PBS (control) and lysate treated *P. aeruginosa*. Previously identified Gac/Rsm targets are indicated and H1-T6SS proteins discussed in this study are labeled. Data derive from two biological replicates. (**F**) Lysate stimulates H1-T6SS-mediated killing of *B. thai* Δ*tssM-1*. Outcome of interspecies growth competition experiments between the indicated *P. aeruginosa* and *B. thai* in the presence or absence of *P. aeruginosa*-derived lysate. Error bars represent ± SD; n = 3 co-cultures. Asterisk indicates significant difference between lysate and no lysate treatments ($P < 0.05$).

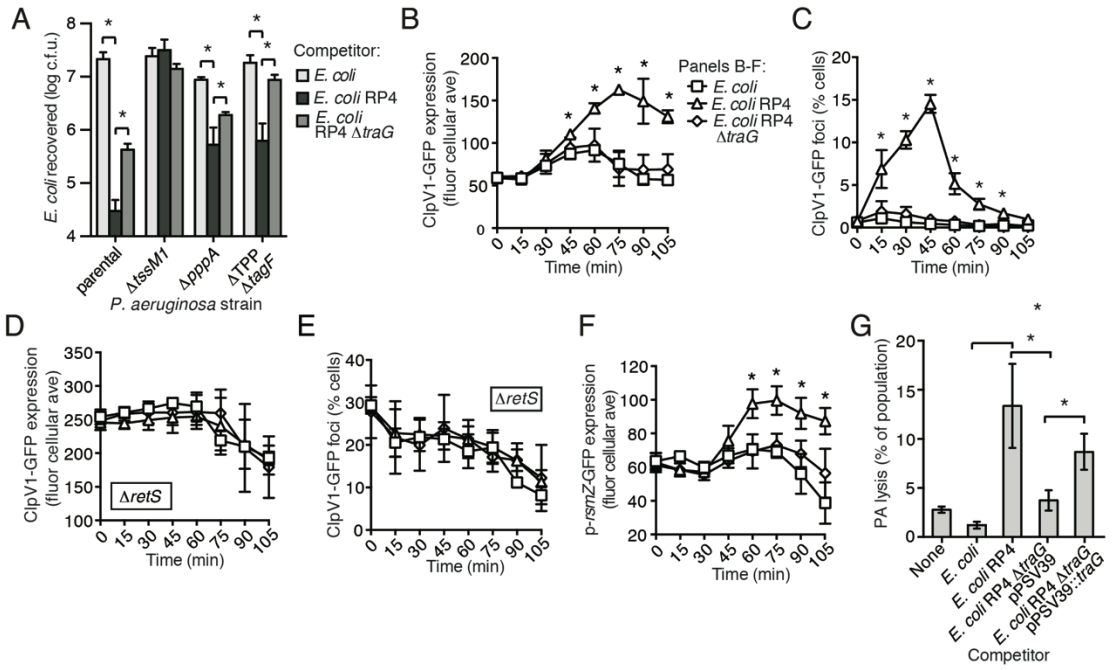

Figure 3.12: The RP4-encoded IncP-type T4SS induces PARA through lysis of *P. aeruginosa.*

(**A**) The TPP is not required to differentially target *E. coli* with a T4SS. Outcome of growth competition experiments demonstrating increased susceptibility of T4S^{+} *E. coli* to the H1-T6SS of *P. aeruginosa*. See also Figure 3.13 for genetic complementation data of the *traG* deletion. n = 4 co-cultures. (**B-C**) H1-T6SS expression and activity is elevated in the presence of *E. coli* containing a T4SS. Average cellular ClpV1-GFP expression (**B**) or foci (**C**) of the *P. aeruginosa clpV1-gfp* throughout co-culture with the indicated *E. coli strains*. (**D-E)** RetS is required for increased H1-T6SS expression and activity. Average cellular ClpV1-GFP expression (**D**) and percent cells with foci (**E**) of *P. aeruginosa clpV1-gfp* Δ*retS* throughout co-culture with the indicated *E. coli strains*. (**F**) *E. coli* bearing a T4SS stimulates *rsmZ* expression. Average cellular GFP levels of *P. aeruginosa* p-*rsmZ-gfp* in TLFM co-culture experiments with the indicated *E. coli* strains. (**B-F**) n = 3 fields; asterisks indicate significant differences between *E. coli* and *E. coli* RP4 co-cultures ($P < 0.05$). (**G**) The T4SS encoded on RP4 promotes *P. aeruginosa* lysis. Relative *P. aeruginosa attB::lacZ* lysis was measured following co-cultivation with the indicated *E. coli* strain by comparing extracellular to total β-galactosidase activity. Error bars represent ± SD; (**A**) and (**G**) n = 3 co-cultures; asterisks indicate significant differences between indicated groups ($P < 0.05$).

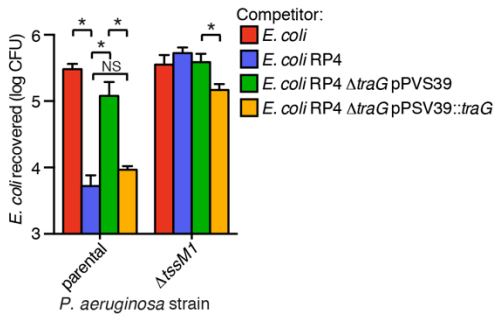

Figure 3.13: Genetic complementation of *traG* restores H1-T6SS-dependent targeting of *E. coli* RP4.
Outcome of growth competition experiment in which *P. aeruginosa* and *E. coli* were co-cultivated under T6SS-promoting conditions. n = 4 co-cultures. Asterisks indicates significant differences between groups ($P < 0.05$); NS, not significant.

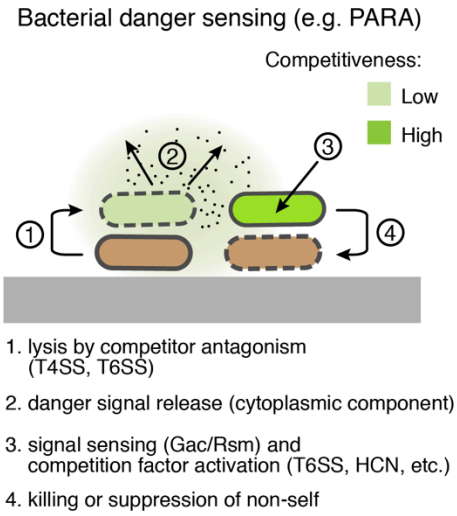

Figure 3.14: Bacterial danger sensing.
The model depicts antagonism between two species of bacteria, represented in green and brown. The green cells possess a danger sensing pathway; specifics of PARA are provided in parentheses

Movie 3.1: ClpV1 expression increases in the presence of *B. thai* bearing an active T6SS.
TLFM sequences of ClpV1-GFP in *P. aeruginosa* during mono-culture or interspecies co-culture. *P. aeruginosa clpV1-gfp* cells without competitor (left sequence), with *B. thai mCherry* (middle sequence), or with *B. thai* Δ*tssM-1 mCherry* (right sequence) were imaged at 15 minute intervals. Overlays of GFP and mCherry channels are displayed. The same thresholds were applied to all background-subtracted GFP channels. See Figure 3.2B, D for quantification.

Movie 3.2: Fha1 expression increases in the presence of *B. thai* bearing an active T6SS.
TLFM sequences depicting expression of Fha1-GFP in *P. aeruginosa* during mono-culture or interspecies co-cultures. *P. aeruginosa fha1-gfp* cells without competitor (left sequence), with *B. thai mCherry* (middle sequence), or with *B. thai* Δ*tssM-1 mCherry* (right sequence) were imaged at 15 minute intervals. Overlays of GFP and mCherry channels are displayed. The same thresholds were applied to all background-subtracted GFP channels. Quantification is provided in Figure 3.2C, E.

Movie 3.3: ClpV1 expression increases in the presence of *E. cloacae* bearing an active T6SS.
TLFM sequences depicting expression of ClpV1-GFP in *P. aeruginosa* during mono-culture or interspecies co-cultures. *P. aeruginosa clpV1-gfp mCherry* cells without competitor (left sequence), with *E. cloacae* (middle sequence), or with *E. cloacae* Δ*tssM* (right sequence) were imaged at 15 minute intervals. Overlays of GFP and mCherry channels are displayed. *P. aeruginosa* cells were labeled with constitutive mCherry and therefore the overlay of GFP and mCherry appears yellow. The unlabeled *E. cloacae* cells are visible (light green) due to autofluorescence in the GFP channel. The same thresholds were applied to all background-subtracted GFP channels. Quantification is provided in Figure 3.4.

Movie 3.4: *RsmZ* expression is elevated in the presence of *B. thai* bearing an active T6SS.
TLFM sequences depicting expression of *rsmZ* in *P. aeruginosa* during interspecies co-cultures. *P. aeruginosa* p-*rsmZ-gfp mCherry* cells with *B. thai* (left sequence) and *B. thai* Δ*tssM* (right sequence) were imaged at 15 minute intervals. Overlays of GFP and mCherry channels are displayed. *P. aeruginosa* cells were labeled with constitutive mCherry, thus cells appear yellow. The unlabeled *B. thai* cells are visible (light green) due to autofluorescence in the GFP channel. The same thresholds were applied to all background-subtracted GFP channels. See Figure 3.7D for quantification.

Movie 3.5: Inactivation of the Gac/Rsm pathway results in a loss of interbacterial fitness
TLFM sequences of the indicated *P. aeruginosa mCherry* strains cultivated with *B. thai GFP*. Overlays of GFP and mCherry channels are displayed. Lysing *P. aeruginosa* cells are outlined in white. Quantification is provided in Figure 3.9C.

Movie 3.6: Lysis of *P. aeruginosa* precedes an increase in H1-T6SS expression and *B. thai* lysis.
TLFM sequences depicting lysis (left) and ClpV1-GFP expression (right) in a *P. aeruginosa–B. thai* co-culture. A mixture of *P. aeruginosa clpV1-GFP mCherry* and *B. thai CFP* were imaged

at 5-minute intervals. Right panel displays the background-subtracted GFP channel with *P. aeruginosa* cells outlined in red and *B. thai* outlined in blue. Left panel displays an overlay of mCherry (*P. aeruginosa*) and CFP (*B. thai*) channels; lysing *P. aeruginosa* (white outlines) and lysing *B. thai* (magenta) are indicated. See Figure 3.11B for quantification.

Table 3.1: Strains used in Chapter 3.

Organism	Genotype	Reference
P. aeruginosa PAO1	Type strain	(106)
	attB::*lacZ*	(101)
	Δ*tssM1 attB::lacZ*	This study
	Δ*retS* attB::*lacZ*	(101)
	Δ*retS* Δ*tssM1* attB::*lacZ*	This study
	Δ*tse1* Δ*tsi1* Δ*tse2* Δ*tsi2* Δ*tse3* Δ*tsi3* Δ*tse4* Δ*tsi4*	This study
	Δ*retS* Δ*tse1* Δ*tsi1* Δ*tse2* Δ*tsi2* Δ*tse3* Δ*tsi3* Δ*tse4* Δ*tsi4*	This study
	clpV1-gfp	(101)
	fha1-sfgfp	This study
	clpV1-gfp attTn7::mCherry	This study
	Δ*pppA clpV1-gfp*	(130)
	ΔTPP Δ*tagF clpV1-gfp*	This study
	Δ*pppA*	(82)
	ΔTPP Δ*tagF*	(130)
	Δ*tssM1*	(130)
	attTn7::PA0082-lacZ10-Gm	(98)
	attB::PA0082-lacZ-tet	(98)
	p-*rsmZ-gfp attTn7::Gm-mCherry*	This study
	Δ*retS clpV1-gfp*	(120)
	Δ*ladS clpV1-gfp*	This study
	Δ*gacS clpV1-gfp attTn7::Gm-mCherry*	This study
	p-*magA-sfgfp*	This study
	$retS^{W90A}$	This study
	Δ*gacS*	This study
	attTn7::*Gm-gfp*	(120)
	attTn7:: *Gm-mCherry*	(120)
	Δ*tssM1 attTn7::Gm-mCherry*	This study
	Δ*gacS attTn7:: Gm-mCherry*	This study
B. thailandensis E264	Type strain	(155)
	Δ*tssM-1*	This study
	attTn7::Tp-P_{S12}*-mCherry*	(120)
	Δ*tssM-1 attTn7::Tp-*P_{S12}*-mCherry*	This study
	attTn7::Tp-P_{S12}*-GFP*	(120)
	Δ*tssM-1 attTn7::Tp-*P_{S12}*-GFP*	This study
	attTn7::Tp-CFP	This study
E. cloacae	Type strain	(156)
	Δ*tssM*	(71)
E. coli	Type strain	(157)

XK1502	RP4	(143)
	RP4 Δ*traG*	This study
	RP4 Δ*traG* pPSV39	This study
	RP4 Δ*traG* pPSV39::*traG*	This study

Table 3.2: Plasmids used in Chapter 3.

Plasmid	Utility	Reference
***P. aeruginosa* PAO1**		
miniCtx::lacZ	constitutive LacZ expression	(110)
pUC18T-miniTn7T-Gm-gfp	constitutive GFP expression	(160)
pUC18T-miniTn7T-Gm-mCherry	constitutive mCherry expression	(120)
pEXG2_ΔPA4856	*retS* deletion allele	(101)
pEXG2_ΔPA0077	*tssM1* deletion allele	(101)
pEXG2_ΔPA1844-5	*tse1 tsi1* deletion allele	(68)
pEXG2_ΔPA2702-3	*tse2 tsi2* deletion allele	(67)
pEXG2_ΔPA3484-5	*tse3 tsi3* deletion allele	(68)
pEXG2_ΔPA2774-5	*tse4 tsi4* deletion allele	(71)
pEXG2_PA0090-gfp	*clpV1* functional translational GFP fusion allele	(101)
pEXG2_PA0081-sfgfp	*fha1* functional translational GFP fusion allele	This study
pEXG2_ΔPA0075	*pppA* deletion allele	(82)
pEXG2_ΔPA0070-0076	TPP *tagF* deletion allele	(130)
attTn7::PA0082-lacZ10-Gm	*tssA1* translational *lacZ* reporter	(98)
attB::PA0082-lacZ-tet	*tssA1* transcriptional *lacZ* reporter	(98)
miniCtx_p-PA3621.1-gfp	*rsmZ* transcriptional GFP reporter	This study
pEXG2_ΔPA0928	*gacS* deletion allele	This study
pEXG2_ΔPA3974	*ladS* deletion allele	This study
pEXG2_p-PA4492-gfp	*magA* translational GFP fusion allele	This study
pEXG2_PA4856^{W90A}	*retS*^{W90A} allele	This study
***B. thailandensis* E264**		
pJRC115_ΔBTH_I2954	*tssM-1* deletion allele	This study
pUC18T-miniTn7T-Tp-PS12-gfp	constitutive GFP expression	(Schwarz et al., 2010)
pUC18T-miniTn7T-Tp-PS12-mCherry	constitutive mCherry expression	(120)
pUC18T-miniTn7T-Tp-ecfp	Constitutive CFP expression	(160)
E. coli		
RP4	Naturally occurring plasmid	(143)

	encoding IncP-type T4SS	
E. coli RP4 Δ*traG*	RP4 bearing *traG* deletion	This study
pPSV39	Expression vector	(70)
pPSV39-*traG*	IPTG-inducible TraG expression for complementation	This study

Chapter 4. Self-lysis pathway that enhances the virulence of a pathogenic bacterium

Published as: McFarland, K. A., Dolben, E. L.*, LeRoux, M.*, Kambara, T. K., Ramsey, K. M., Kirkpatrick, R. L., et al. (2015). *Proceedings of the National Academy of Sciences.*
*These authors contributed equally to this work

M.L. performed all time-lapse fluorescence microscopy experiments and analyses. These are presented in Figures 4.2D-E, 4.11, and 4.12 and Movies 4.1-4.11

4.1 Abstract

In mammalian cells, programmed cell death (PCD) plays important roles in development, in the removal of damaged cells, and in fighting bacterial infections. Although widespread among multicellular organisms, there are relatively few documented instances of PCD in bacteria. Here we describe a potential PCD pathway in *Pseudomonas aeruginosa* that enhances the ability of the bacterium to cause disease in a lung infection model. Activation of the system can occur in a subset of cells in response to DNA damage through cleavage of an essential transcription regulator we call AlpR. Cleavage of AlpR triggers a cell lysis program through derepression of the *alpA* gene, which encodes a positive regulator that activates expression of the *alpBCDE* lysis cassette. While this is lethal to the individual cell in which it occurs, we find it benefits the population as a whole during infection of a mammalian host. Thus host and pathogen each may employ PCD as a survival-promoting strategy. We suggest that activation of the Alp cell lysis pathway is a disease-enhancing response to bacterial DNA damage inflicted by the host immune system.

4.2 Introduction

Programmed cell death (PCD) refers to cell suicide that results from a genetically-encoded program (163). It is well recognized that PCD occurs in mammalian cells, where it plays important roles in development, in the removal of damaged cells, and in fighting bacterial infections (163-166). In contrast to the situation in multicellular organisms, the proposal that PCD occurs in bacteria has been controversial, largely because the evolutionary advantage of PCD to a single-celled organism is unclear (167, 168). In bacteria, PCD appears to have roles in

limiting the spread of bacteriophage (169), in the formation of biofilms (170, 171), and has been suggested to prevent the proliferation of compromised cells (172, 173). Whether PCD of pathogenic bacteria influences the ability of these organisms to cause disease has remained unclear.

Pseudomonas aeruginosa is a Gram-negative bacterium and an important opportunistic pathogen of humans (174). The organism is one of the most common causes of ventilator-associated and hospital-acquired pneumonia (175) and it is notorious as the principal cause of morbidity and mortality in cystic fibrosis (CF) patients (174). Chronic colonization of the CF lung by *P. aeruginosa* typically leads to progressive lung damage and, eventually, respiratory failure and death (174). A distinctive feature of *P. aeruginosa* is that it encodes a large number of putative transcription regulators (176). These are speculated to facilitate adaptation of the organism to varied environments, including those within the human host.

Here we discover an essential transcription regulator in *P. aeruginosa* that we call AlpR. We show that AlpR is essential because it represses a previously undocumented PCD pathway. We present evidence that the AlpR-regulated PCD pathway can be activated in a subset of cells in response to DNA damage and promotes colonization of the murine lung. Our findings suggest that bacterial PCD can enhance the virulence of *P. aeruginosa* and that PCD functions altruistically during the course of an infection. In addition, these findings have implications for the role of PCD pathways in other pathogens. PCD may represent a survival strategy common to both host and pathogen that each mounts during the course of an infection.

4.3 Results

4.3.1 *Loss of AlpR results in cell lysis*

Analysis of the *P. aeruginosa* strain PAO1 genome revealed a putative transcription regulator encoded by the *PA0906* gene that is highly conserved amongst different strains of *P. aeruginosa* and exhibits homology to the CI repressor protein from bacteriophage λ (λCI), and the LexA protein from *Escherichia coli* (Figure 4.1) (177). Although no transcription regulator has been definitively shown to be essential for growth of *P. aeruginosa* under standard laboratory conditions, *PA0906* is amongst the set of candidate essential genes in *P. aeruginosa* strains PAO1 and PA14 (178, 179). We therefore reasoned PA0906, which we refer to here as AlpR, might be essential in *P. aeruginosa* because it represses the expression of genes whose products can be lethal. We first used a ClpXP-based protein depletion system to explicitly test whether or not AlpR is essential in *P. aeruginosa* strain PAO1 (180). Depletion of AlpR resulted in at least a 10^5-fold decrease in colony-forming units (Figure 4.2*A*). Thus, loss of AlpR results in a loss of viability or inhibition of cell growth in PAO1. AlpR therefore appears to be essential in this strain of *P. aeruginosa*.

Proteins related to AlpR, such as λCI and LexA, must be dimeric in order to bind the DNA and contain dimerization determinants in their C-terminal domains (CTDs) (177, 181). We found that the predicted CTD of AlpR could (i) interact with itself in a bacterial two-hybrid assay (Figure 4.3*A*), and (ii) functionally substitute for the CTD of λCI (Figure 4.3*B*), suggesting that the AlpR-CTD contains a dimerization determinant. We thought we might be able to interfere with the activity of AlpR in wild-type cells of *P. aeruginosa* by synthesizing the AlpR-CTD; our expectation was that the AlpR-CTD would sequester an AlpR monomer into an inactive heterodimer and function as a dominant-negative mutant (Figure 4.2*B*). Indeed, synthesis of the

AlpR-CTD in *E. coli* interfered with the binding of a hybrid repressor, in which the CTD of λCI had been replaced with the CTD of AlpR, to a λ operator (Figure 4.3*C*). Consistent with the idea that AlpR is essential, ectopic synthesis of the AlpR-CTD appeared to be lethal to wild-type cells of PAO1 (Figure 4.2*C*); similar results were observed when the AlpR-CTD was ectopically synthesized in *P. aeruginosa* strains CF18, PA14 and in the CF epidemic strain LESB58 (Figure 4.3*A* and *B*). Furthermore, ectopic synthesis of the AlpR-CTD did not result in lethality or impair growth in cells that contained a second copy of *alpR* (Figure 4.2*C*), suggesting that the deleterious effect of the AlpR-CTD observed in wild-type cells is mediated by sequestration of AlpR.

We next sought to determine whether ectopic synthesis of the AlpR-CTD results in lethality or prevents cell growth. In wild-type PAO1 cells grown in liquid culture, induction of the AlpR-CTD resulted in a decrease in the OD_{600} of the culture and an increase in the abundance of DNA in the culture supernatant (Figure 4.4*C*). To directly observe the phenotypic consequences of AlpR sequestration, we employed time-lapse fluorescence microscopy (TLFM) (120). The growth of cells that synthesized mCherry and the AlpR-CTD was visualized alongside control cells that synthesized GFP alone. Following induction of the AlpR-CTD, most red fluorescent cells lysed, with some noticeably losing structural integrity or forming spheroplasts before lysis (Figure 4.2*D*, Movie 4.1). Prior to cell lysis, green fluorescent foci appeared despite the absence of GFP in these cells (Figure 4.2*D*, Movie 4.1). These fluorescent foci that appeared as a prelude to cell lysis might represent a marker for cell death, or may form in a manner that is mechanistically unrelated to the onset of cell death. Cell lysis did not occur in control cells that synthesized GFP (Figure 4.2*D* and *E*, Movie 4.1). Time-lapse microscopy revealed that the ClpXP-based depletion of AlpR also resulted in cell lysis (Movie 4.2, Movie

4.3). These findings indicate that the loss of AlpR function, either through ectopic synthesis of the AlpR-CTD or through depletion of AlpR, results in cell death through cell lysis. The name AlpR stands for *P. aeruginosa* lysis phenotype repressor.

4.3.2 *AlpR undergoes autocleavage in response to DNA damage and functions as a repressor*

Like the related λCI and LexA proteins, AlpR contains a so-called Ser-Lys dyad that in LexA and in λCI mediates autocleavage (181). The autocleavage of LexA and λCI occurs in response to DNA damage, leading to inactivation of these regulators and the de-repression of target genes. We therefore asked whether AlpR undergoes autocleavage in response to DNA damage. Exposure of *P. aeruginosa* cells to the antibiotic ciprofloxacin, which leads to DNA damage, resulted in cleavage of wild-type AlpR but not the AlpR mutant AlpR(S153A) that contained amino acid substitution S153A that is predicted to prevent autocleavage (181) (Figure 4.5*B*). Exposure of cells to hydrogen peroxide, which also damages DNA, resulted in cleavage of AlpR but did not result in cleavage of AlpR(S153A) (Figure 4.6). These findings suggest that AlpR undergoes cleavage in response to DNA damage and establish that substitution S153A results in a mutant version of AlpR that cannot undergo autocleavage.

Exposure of PAO1 cells to ciprofloxacin was shown previously to result in an increase in expression of *alpR* and the *PA0907-PA0911* genes (named here *alpABCDE*) (21), which are in a putative operon that is located adjacent to and transcribed divergently from *alpR* (Figure 4.5*A*). Exposure to ciprofloxacin induced expression of the *alpR*, *alpA*, *alpB*, *alpC* and *alpE* genes in wild-type cells but not in cells that synthesized AlpR(S153A) (Figure 4.5*C*). These findings suggest that AlpR, either directly or indirectly, represses expression of the *alpR* and *alpABCDE* genes.

4.3.3 *ChIP-Seq reveals that AlpR regulates the alp genes directly*

To determine whether the effect of AlpR on expression of the *alp* genes might be direct or indirect we used chromatin immunoprecipitation coupled with high-throughput DNA-sequencing (ChIP-Seq) to identify those regions of the PAO1 chromosome that AlpR associates with. ChIP-Seq with an epitope-tagged version of AlpR revealed that AlpR associates with only two regions of the PAO1 chromosome—the *alpR-alpA* and *alpA-alpB* intergenic regions (Figure 4.5*D*). Global transcription start-site mapping experiments in PAO1 (182) reveal the existence of promoters in each of these regions, and the expression of *alpR* promoter-, *alpA* promoter-, and *alpB* promoter-*lacZ* fusions was repressed by ectopic synthesis of AlpR (Figure 4.7*A* and *B*). AlpR therefore exerts its effect on expression of these target genes directly.

4.3.4 *The essential function of AlpR is to repress expression of alpA*

Having established that AlpR represses expression of the *alpABCDE* genes we wondered whether this might be the essential function of AlpR. That is, we wondered whether de-repression of *alpABCDE* results in cell lysis. Although the *alp* genes have not previously been shown to influence cell lysis, AlpB is annotated as a holin (176), which are small pore-forming proteins typically produced by bacteriophage that facilitate cell wall degradation and cell lysis at the end of a phage lytic cycle (183). Consistent with this idea, we found that AlpB could functionally substitute for the holin from bacteriophage λ in *E. coli* (Figure 4.8) (184).

AlpC may be an anti-holin, a protein that counters the activity of a holin. In keeping with this notion, genes that encode anti-holins can be found immediately downstream of those

encoding the cognate holin, and AlpC is predicted to contain transmembrane domains, which are a feature common to anti-holins (183). AlpD and AlpE are hypothetical proteins of unknown function and AlpB, AlpC, and AlpD homologs are encoded by *P. aeruginosa* phage DE3 (185). De-repression of *alpABCDE* might therefore influence cell lysis through a holin-dependent mechanism and the *alp* genes, which are highly conserved in strains of *P. aeruginosa*, may have originated from a phage.

If the essential function of AlpR is to repress expression of the *alpABCDE* genes then a strain that lacked these genes would be expected to tolerate ectopic synthesis of the AlpR-CTD. Synthesis of the AlpR-CTD did not result in lethality in cells that lacked the *alpABCDE* cluster (Figure 4.9*A*), suggesting that AlpR is essential because it represses expression of one or more of the *alpABCDE* genes. To assess the individual contribution of each of the genes in this operon to the lethality that results upon ectopic synthesis of the AlpR-CTD we constructed strains in which each of these genes (except *alpB* alone) was deleted. The results depicted in Figure 4.9*A* suggest that *alpA* is essential for the cell lysis that occurs upon ectopic synthesis of the AlpR-CTD and that genes *alpB*, *alpD* and *alpE* also contribute. Consistent with the possibility that AlpC might serve to limit the holin-like activity of AlpB, cells that lack *alpC* were found to be more sensitive to the lethal effects of the AlpR-CTD than wild-type cells (Figure 4.9*A*).

4.3.5 *AlpA is a positive regulator of the alpBCDE genes*

Structural prediction algorithms suggest that AlpA may contain a winged-helix DNA-binding domain. We therefore asked whether AlpA might be a positive regulator that in turn is required for expression of the *alpBCDE* genes. Ectopic expression of *alpA* strongly activated expression of an *alpB* promoter-*lacZ* fusion in PAO1 cells, demonstrating that AlpA is a positive

regulator of the *alpB* promoter (Figure 4.9*B*), and in cells of *E. coli*, suggesting that AlpA regulates the *alpB* promoter directly (Figure 4.7*C*). Furthermore, comparing the effects of ciprofloxacin on the abundance of transcripts in cells of the PAO1 AlpR(S153A) mutant strain, to those in wild-type cells and to those in cells that contain a premature stop codon early on in the *alpA* ORF, indicates that genes in the putative *alpBCDE* operon are positively regulated by AlpA (Figure 4.9*C*). Consistent with the hypothesis that the principal role of AlpA in promoting cell lysis is to positively regulate expression of the *alpBCDE* genes, we found that cells lacking either *alpBCDE* or *alpA* did not lyse following ectopic synthesis of the AlpR-CTD (Figure 4.2*E*, Figure 4.10*A*). In addition, we found that ectopic expression of the *alpBCDE* cassette resulted in lethality (Figure 4.10*B*). Inactivation of AlpR therefore initiates a regulatory cascade that de-represses *alpA* expression resulting in the production of a positive regulator that then goes on to drive expression of the *alpBCDE* genes.

4.3.6 *DNA damage induces the Alp system in a subset of cells and results in cell lysis*

We next asked whether treatment of PAO1 cells with ciprofloxacin resulted in a homogeneous or heterogeneous response. The analysis of cells containing an *alpB* promoter-*yfp* fusion by TLFM revealed that the addition of ciprofloxacin to cells for 1 hour resulted in induction of *alpB* promoter activity in a subset of cells (Figure 4.11, Movies 4.4-4.11). *P. aeruginosa* possesses a pyocin-associated cell death mechanism that can respond to DNA damage (186). Because we sought to define the causal link between *alpBCDE* induction and cell death upon DNA damage, we inactivated this potentially confounding pathway by deletion of *prtN*, a gene required for its activity (187). Importantly, essentially all of the Δ*prtN* mutant cells in which the *alpB* promoter-*yfp* reporter was induced lysed (Figure 4.11, Movie 4.8), whereas few of the Δ*prtN* Δ*alpBCDE*

mutant cells in which the *yfp* reporter was induced lysed (Figure 4.10, Movie 4.11). These findings indicate that DNA damage-dependent induction of the Alp system results in cell lysis. Moreover, the strong association of *alp* induction and cell death indicates that triggering the Alp system commits a cell to death. Indeed, even in the presence of the pyocin system, we see that following DNA damage a significantly greater fraction of Alp-induced cells survive when *alpBCDE* are absent, implying that the Alp system contributes to the lysis of wild-type cells (Figure 4.12, Movie 4.6, Movie 4.4). In total, our findings suggest that the Alp system represents a PCD pathway that can be activated in a subset of cells in response to DNA damage.

4.3.7 *The AlpR-regulated PCD pathway enhances colonization of the host lung*

P. aeruginosa is a notorious lung pathogen and is the principal cause of chronic and intractable pulmonary infections in individuals with CF, as well as a major cause of acute pneumonias in compromised individuals such as those on mechanical ventilation (174, 175). *P. aeruginosa* elicits a strong neutrophil response, which includes the generation of reactive oxygen species including H_2O_2 as an antimicrobial defense (188, 189). We posited that *P. aeruginosa* present in the lung would experience DNA damage resulting in cleavage of AlpR and induction of the Alp PCD pathway in a subset of cells. We therefore asked whether the *alp* system influences the ability of *P. aeruginosa* to colonize the murine lung in a model of acute infection. Figure 4.13*A* indicates that cells of the Δ*alpA* mutant strain, cells of the Δ*alpBCDE* mutant strain, and cells of the AlpR(S153A) mutant strain were unable to colonize the murine lung as well as wild-type cells. Furthermore, cells of a derivative of the Δ*alpA* mutant strain in which the *alpA* gene was restored (PAO1 *alpA*-IN), colonized the murine lung similarly to wild-type cells, demonstrating that the effect of the Δ*alpA* deletion on lung colonization was not the result of a

secondary mutation introduced during construction of the Δ*alpA* mutant strain (Figure 4.13*A*). Note that cells containing deletions of *alpA* or *alpBCDE*, or that synthesized AlpR(S153A), grew similarly to wild-type cells when grown *in vitro* (Figure 4.14), ruling out the possibility that the colonization defects observed *in vivo* could be attributed to any differences in growth rate observed *in vitro*. These findings suggest that *alpA*, the *alpBCDE* genes, and the ability of AlpR to undergo autocleavage are all important for lung colonization.

We hypothesized that the virulence defect in the Δ*alpA* strain was due to the fact that PCD-mediated lysis of a subset of the *P. aeruginosa* cells in the lung benefitted the remaining cell population rather than due to intrinsic defects in the virulence of individual cells upon the loss of this regulator. To test this, we compared lung colonization by tagged wild-type and tagged Δ*alpA* mutant cells in an excess of wild-type cells. When wild-type PAO1 with an intact PCD pathway dominated the population, colonization by cells of the tagged wild-type and tagged Δ*alpA* strains was indistinguishable (Figure 4.13*B*). Together, these findings strongly suggest that in the acute lung infection model used here, PCD that occurs in a subset of cells through the de-repression of AlpR-controlled genes promotes colonization by *P. aeruginosa*. Although both the Alp and pyocin systems can contribute to the lysis of cells that occurs in response to DNA damage *in vitro*, we do not know their relative contributions to the lysis of *P. aeruginosa* that appears to occur in the host lung. Nonetheless, our findings demonstrate that the Alp system is functionally relevant in this context.

4.4 Discussion

The findings we have described reveal a possible PCD pathway in *P. aeruginosa* that can be activated in response to DNA damage in a subset of cells. DNA damage results in de-

repression of *alpA* expression. In turn, AlpA positively regulates expression of the *alpBCDE* lysis genes. The cell lysis that ensues could provide nutrients or liberate toxins or other bacterial factors that might facilitate lung colonization by the remaining *P. aeruginosa* cells in the population (190, 191). PCD pathways in other pathogenic bacteria could enhance virulence in the same fashion.

The PCD of mammalian cells is thought to control bacterial infections through a variety of mechanisms. In particular, neutrophil extracellular traps that promote the killing of pathogenic bacteria are generated through apoptosis (165). In addition, eradication of infected cells through death-receptor-induced apoptosis is thought to limit disease caused by attaching and effacing pathogens such as enteropathogenic *E. coli* (166). Our findings with the Alp system suggest that the PCD of a subpopulation of *P. aeruginosa* cells can enhance colonization of the host by the remainder of the cell population. PCD may therefore represent a survival-promoting strategy common to both pathogen and host during infection.

The Alp pathway has distinct similarities to as well as distinct differences from other PCD pathways that have been defined in both eukaryotes and prokaryotes. In *S. aureus*, a holin encoded by *cidA* is thought to be responsible for mediating cell lysis in a PCD pathway that contributes to biofilm formation and might play a role in virulence (170, 192). We have found that AlpB can functionally substitute for the λ holin, suggesting that in *P. aeruginosa* AlpB might contribute to PCD in a manner related to CidA or holin-like pro-apoptotic factors of the BCL-2 family in eukaryotes (184). In *E. coli*, LexA has been shown to not only mediate the classic SOS response, but also to mediate a PCD pathway referred to as apoptosis-like death (ALD) in response to extensive DNA damage (172, 173). The Alp system is analogous to the ALD system in *E. coli* in that both are under the control of a repressor that becomes inactivated

in response to DNA damage through autocleavage. However, in *P. aeruginosa*, LexA does not appear to control expression of the *alp* genes (193). Furthermore, in *E. coli*, ALD is not mediated by genes analogous to *alpABCDE*, and LexA does not exclusively control the expression of a dedicated death cassette like AlpR does in *P. aeruginosa*. The Alp system is therefore distinct from the ALD response with respect to both the genes that directly mediate PCD and the specific DNA damage-responsive regulator used to control PCD.

We cannot exclude the possibility that in the host lung, expression of the *alpABCDE* genes becomes induced, but to a degree that is insufficient to promote cell lysis. In this case, induction of the *alp* genes in a subset of cells would facilitate colonization of the lung by a lysis-independent mechanism. In relation to this, it is noteworthy that in *Serratia marcescens*, a protein with features similar to that of a holin has been implicated in promoting the secretion of chitinases (194). It is therefore conceivable that expression of the *alp* genes might promote colonization of the host lung through an effect on protein secretion. However, because we find that the vast majority of cells in which the *alp* system is induced in response to DNA damage undergo lysis, we favor the hypothesis that the lysis of Alp-induced cells plays a key role in facilitating infection of the host lung by the remainder of the cells in the population.

Pathogens present in the host can experience DNA damage as a result of the host immune response (188) Although host processes that generate DNA-damaging agents are principally thought to limit infections, our findings suggest that they can also act to promote the virulence of *P. aeruginosa* by activating the *alp* genes. Conceivably, treatment of *P. aeruginosa* infections with antibiotics such as ciprofloxacin that damage the DNA may also inadvertently promote the virulence of any surviving cells through the activation of the Alp system. Control of the *alp* genes by a DNA damage-responsive transcription regulator may provide a facile way for *P.*

aeruginosa to respond to these insults. In addition, the Alp system may facilitate the survival of *P. aeruginosa* in environments other than those of the host. Damage of *P. aeruginosa* DNA resulting from phage infection or from the actions of competing microbes could result in Alp-mediated lysis in a subset of cells, thereby limiting the spread of phage or promoting biofilm formation, and in turn enhancing the survival of the population as a whole (167-169)•(170, 171).

4.5 Materials and Methods

Bacterial strains and growth conditions. *P. aeruginosa* strains PAO1 and PA14 were provided by Arne Rietsch (Case Western Reserve University). PAO1 Δ*sspB,* LESB58, and CF18 have been described (176, 180, 195). *Escherichia coli* DH5 F′IQ (Invitrogen) was used for plasmid construction and maintenance, CSH100 and FW102 were used for *lacZ* reporter analyses (196), SM10 (λ*pir*) was used for conjugal transfer of plasmids into *P. aeruginosa,* FW123 was used for the λCI-CTD functional substitution assays (37), KDZif1ΔZ was used for the bacterial two-hybrid assays (197), and MC4100 λΔ(*SR*) was used for the λ holin functional replacement assay (184). For introducing in-frame deletions by conjugal transfer, *P. aeruginosa* was selected for on *Pseudomonas* Isolation Agar (PIA), and grown on low-salt LB agar supplemented with 5% (w/v) sucrose at 37 °C for *sacB* counter selection. *E. coli* strains were supplemented with 15 μg ml^{-1} gentamicin, 10 μg ml^{-1} tetracycline, 100 μg ml^{-1} carbenicillin, 30 μg ml^{-1} kanamycin and 25 μg ml^{-1} chloramphenicol as needed. *E. coli* strains that contained plasmids with IPTG-inducible promoters were supplemented with the indicated IPTG concentration. For *P. aeruginosa*, gentamicin (LB: 30 μg ml^{-1}; PIA: 60 μg ml^{-1}) and tetracycline (LB: 35 μg ml^{-1}; PIA: 200 μg ml^{-1}) were added as needed. Liquid *P. aeruginosa* cultures were inoculated at a starting OD_{600} of 0.01 and grown with aeration at 37 °C in LB broth. For

induction of IPTG-inducible promoters in liquid-grown *P. aeruginosa* cultures, IPTG was added at a concentration of 5 mM. Growth was monitored by measurement of optical density at 600 nm.

DNA manipulations. Standard molecular cloning procedures were followed. Primers used in this study were obtained from MWG and Sigma Life Sciences. DNA amplification was carried out using KOD polymerase (Novagen). DNA sequencing was performed by Genewiz Incorporated. Restriction enzymes were obtained from New England Biolabs.

Mutant strain construction. The suicide vector pEXG2 (107) was used to make the in-frame deletion constructs pEXG2-Δ*alpR,* pEXG2-Δ*alpA*, pEXG2-Δ*alpBC*, pEXG2-Δ*alpC,* pEXG2-Δ*alpD*, pEXG2-Δ*alpE*, pEXG2-Δ*alpABCDE*, pEXG2-Δ*alpBCDE* and pEXG2-Δ*prtN*. In-frame deletion constructs were synthesized by amplification of regions of approximately 400-base-pair (bp) flanking the deletion, ligation and subsequent cloning into pEXG2. Allelic replacement in PAO1 with pEXG2-Δ*alpR,* pEXG2-Δ*alpA,* pEXG2-Δ*alpC,* pEXG2-Δ*alpD*, pEXG2-Δ*alpE* and pEXG2-Δ*prtN* resulted in replacement of the ORF in question with ATGGCGGCCGCN-stop codon (where N is any base). As the genes of *alpB* and *alpC* overlap, the *alpC* ORF was replaced in PAO1 with ATGGTTGATCCGGCGGCCGCTTGA by allelic exchange using plasmid pEXG2-Δ*alpC*, thereby leaving intact the *alpB* ORF (stop codon of *alpB* underlined). Allelic replacement in PAO1 using both pEXG2-Δ*alpABCDE* resulted in replacement of *alpABCDE,* from the start codon of *alpA* to the stop codon of *alpE,* while pEXG2-Δ*alpBCDE* resulted in replacement of the *alpBCDE,* from the start codon of *alpB* to the stop codon of *alpE,* with ATGGCGGCCGCCTAA. Deletions were confirmed by the PCR.

Plasmid pEXG2 was also used to make mutant genes by allelic replacement (107). Plasmid pEXG2-*alpA*-STOP was generated by amplification of regions that flank and overlap

base pairs 181–186 of *alpA* by the PCR, using oligonucleotides that integrate an in-frame *Bsp*HI restriction site (TCATGA; coding for Ser followed by a stop codon) in place of base pairs 181–186. The resulting products were ligated together and cloned into pEXG2. Allelic replacement in PAO1 with pEXG2-*alpA*-STOP resulted in replacement of the *alpA* gene with one that contains a premature stop codon early in the *alpA* ORF. Mutations were confirmed by the PCR, followed by digestion of the PCR product with *Bsp*HI.

Plasmid pEXG2-V-AlpR was generated by amplification of regions flanking *alpR* by the PCR, using oligos that also contained an in-frame VSV-G tag that was codon optimized for use in *P. aeruginosa* (ATGTATACCGATATCGAAATGAATCGCCTGGGCAAA). The resulting products were spliced together by overlap extension PCR and cloned into pEXG2. Allelic replacement in PAO1 with pEXG2-V-AlpR resulted in replacement of the *alpR* gene with one that contains an in-frame N-terminal VSV-G tag. Mutations were confirmed by the PCR, followed by digestion of the PCR product with *Eco*RV (restriction site underlined above).

Plasmid pEXG2-AlpR(S153A) was generated by amplification of regions that flank and overlap base pairs 457–458 of *alpR* by the PCR, using oligonucleotides that introduce a mutation that results in both the Ser153Ala substitution and the introduction of an *Nco*I restriction site. The resulting products were spliced together by overlap extension PCR and cloned into pEXG2. Allelic replacement in PAO1 with pEXG2-AlpR(S153A) resulted in replacement of the *alpR* gene with one that encodes the substitution Ser153Ala. Mutations were confirmed by the PCR, followed by digestion of the PCR product with *Nco*I.

Plasmid pEXG2-*alpA*-IN was generated by amplification of a 1.2 kb region centered on the *alpA* gene, and subsequent ligation into pEXG2. Allelic replacement in PAO1 Δ*alpA* with

pEXG2-*alpA*-IN resulted in restoration of the Δ*alpA* lesion with the wild-type *alpA* lesion. Mutations were confirmed by the PCR.

The AlpR-CTD expression plasmids were made as follows: oligonucleotides that contained a restriction site, a Shine-Dalgarno sequence, spacer region, and an in-frame start codon fused to the final 327 bp of *alpR* were used to generate a DNA fragment, which was ligated into pPSV38 (182) to generate plasmid pL-AlpR-CTD. DNA was subcloned from pL-AlpR-CTD into pPSPK (180) to generate pAlpR-CTD. Expression of the 110-amino-acid CTD peptide was under the control of an IPTG-inducible promoter.

The expression plasmid pAlpA, used in Figure 4.5*B*, was constructed by amplification by the PCR of the *alpA* gene using an oligonucleotide that added a Shine-Dalgarno motif and spacer to the *alpA* ORF, followed by ligation into pPSV38. The expression plasmid pAlpR, was constructed by amplification by the PCR of the *alpR* gene using an oligonucleotide that added a Shine-Dalgarno motif and spacer to the *alpR* ORF, followed by ligation into pPSV38. The expression plasmid pAlpBCDE was constructed by amplification by the PCR of the *alpBCDE* genes using an oligonucleotide that added a Shine-Dalgarno motif and spacer to the *alpB* ORF, followed by ligation into pPSV38.

Plasmid pUC18-mini-Tn7T-P_{lpp}-*alpR* was generated by amplification of the *lpp* promoter from pBRα1 and ligation with pUC18-mini-Tn7T-LAC (108) to replace the *lac* promoter. A Shine-Dalgarno sequence, spacer region, and the *alpR* gene were placed downstream of the *lpp* promoter. The *alpB* fluorescent reporter plasmid pUC18-mini-Tn7T-*alpB*-*yfp* was derived as follows: the *lac* promoter and *lacI* gene of pUC18-mini-Tn7T-LAC was replaced with the *yfp* gene, which was amplified from pEYFP creating the resulting plasmid, pKHT190. The *alpB* regulatory region was amplified by PCR and ligated into pKHT190, upstream of the *yfp* gene and

controlling its expression. The plasmids pUC18T-mini-Tn*7*T-Gm-GFP and pUC18T-mini-Tn*7*T-Gm-mCherry, which were used to generate *P. aeruginosa att*Tn*7*::GFP and *att*Tn*7*::mCherry strains, were described previously (108, 120).

The DAS4-tag integration vector pDIVT was generated by cloning a DNA fragment containing a sequence that specifies the peptide AANDENYSENYADAS followed by a stop codon, into the plasmid pP30ΔFRT (197). The peptide consists of the DAS4 SspB-dependent degradation tag (180). The *aac1* gene that confers gentamicin resistance was replaced with the *tet* gene from plasmid mini-CTX-*lacZ* (159) which confers resistance to tetracycline. Plasmid pDIVT carries the mobilization region from RP4 (*mob*), the ColE1 origin of replication, the *tet* gene, FRT sites for efficient Flp recombinase-mediated excision, and DNA specifying the DAS4 tag. Plasmid pDIVT-*alpR* was generated by ligation of approximately 300 bp of the 3′ portion of *alpR* into pDIVT in-frame with the DNA specifying the DAS4 tag.

Plasmids P_{alpA}-*lacZ,* P_{alpB}-*lacZ,* and P_{alpR}-*lacZ* the F′ episome *lacZ* reporter plasmids, were produced by amplification and ligation of the *alpA*, *alpB* and *alpR* promoter regions into pFW11 (196) respectively. Plasmid pLX-AlpR was generated by amplification of the *alpR* gene followed by ligation into pLX10 (196), and it directs the synthesis of AlpR under the control of the *lac* promoter. Plasmid pCI was derived from plasmid pLX10 and directs the synthesis of the CI protein from bacteriophage λ under the control of the *lac* promoter (196).

The plasmid mini-CTX-*lacZ* (159) was used to make *lacZ* reporter fusions to the promoter regions of *alpB* and the control promoter, *orn,* by amplification of promoter regions by the PCR and ligation into mini-CTX-*lacZ*.

Induction of DNA damage. Cultures were grown to an OD_{600} of 0.5 and ciprofloxacin (Sigma-Aldrich) was added at a final concentration of 1 μg ml^{-1} for the specified times before harvesting. Hydrogen peroxide (Sigma-Aldrich) was added at a final concentration of 1 mM for the indicated times. For ciprofloxacin pulse experiments, growth was continued for an hour after addition of ciprofloxacin. Cells were then washed and resuspended in LB. Slides were prepared and imaged in the phase and YFP channels as described below. To quantify the surviving, *alp*-induced cells in the wild-type PAO1 background, YFP pixels with intensity exceeding an empirically determined threshold in the final frame (485 min) were divided by the cell-associated pixels from the phase image in the initial frame using ImageJ. The mean values for three fields of view are displayed.

AlpR sequestration assays on LB agar plates. The pAlpR-CTD plasmid, synthesizing the AlpR-CTD, was introduced into the indicated strains by electroporation. Colonies of plasmid-containing cells were selected on LB agar containing gentamicin and resuspended in PBS to an OD_{600} of 0.01 (considered the 10^{-2} dilution). Tenfold serial dilutions of cells (10 μl) were spotted onto LB agar plates containing gentamicin with or without 10 mM IPTG. Plates were incubated overnight at 37 °C before being photographed.

Depletion strain construction and depletion assay. The *alpR* depletion strain used in Figure 1*A* was generated as follows: plasmid pUC18-mini-Tn7T-P_{lpp}-*alpR* was used to integrate an *lpp* promoter-controlled *alpR* into the Tn7 attachment site in PAO1 Δ*sspB* as described (108). Plasmid pEXG2-Δ*alpR* was used to generate a deletion of the native *alpR* gene in the resulting strain by allelic exchange. Deletions were confirmed by the PCR. Plasmid pDIVT-*alpR*, together with recipient strain PAO1 *ΔalpR ΔsspB* P_{lpp}-*alpR*, was used to create strain PAO1 *ΔalpR ΔsspB* P_{lpp}-*alpR*-DAS4 by integration of the plasmid into the chromosome. Plasmid pSspB directs the

IPTG-inducible synthesis of SspB and confers resistance to gentamicin (180). The pSspB plasmid, synthesizing SspB, or the empty vector, were introduced into the strains described above by electroporation. Colonies of plasmid-containing cells were selected on LB agar containing gentamicin and resuspended in PBS to an OD_{600} of 0.01 (considered the 10^{-2} dilution). Tenfold serial dilutions of cells (10 µl) were spotted onto LB agar plates containing gentamicin with or without 10 mM IPTG. Plates were incubated overnight at 37 °C before being photographed. For microscopy, cells were prepared in an identical manner, but were spotted on agarose pads containing 10 mM IPTG and imaged in the phase channel as described below.

Time-lapse microscopy. Time-lapse microscopy sequences were acquired on a Nikon Ti-E inverted microscope with a 60x oil objective, automated focusing (Perfect Focus System, Nikon), a Xenon light source (Sutter Instruments), a CCD camera (Clara series, Andor), and image acquisition software (NIS Elements, Nikon), essentially as described previously (20). For all microscopy experiments, mid-log (OD_{600} = 0.5-0.8) *P. aeruginosa* cultures were concentrated 5x in LB. 1 µL of each bacterial suspension was spotted onto a 1.5% (w/v) agarose growth pad (prepared using Vogel Bonner minimal media containing 0.2% (w/v) sodium nitrate, and 0.01% (w/v) casamino acids). For the lysis analysis in Figure 1*E*, *P. aeruginosa att*Tn*7*::mCherry bearing pAlpR-CTD was compared with the same strain carrying pPSPK for the indicated genotypes (parental, Δ*alpBCDE*, and Δ*alpA*). Experiments were performed on agarose pads containing 5 mM IPTG and 30 µg ml^{-1} gentamicin, and data were acquired for phase and mCherry channels. For Movie 4.1, *P. aeruginosa att*Tn*7*::mCherry (pAlpR-CTD) and *P. aeruginosa att*Tn*7*::GFP (pPSPK) were mixed at a 1:1 ratio), spotted onto agarose pads containing 5 mM IPTG and 30 µg ml^{-1} gentamicin, and images were acquired in the phase, GFP, and mCherry channels. Data analysis was performed using custom Matlab based software as

previously described (120). Briefly, cells were identified using a watershed algorithm and linked between frames. A rapid, sustained drop in cellular mCherry intensity was defined as a lysis event. Mean lysis events from four frames were determined; experiments were repeated independently at least three times.

Western blot analyses. Equal numbers of cells were lysed by sonication and separated by SDS-PAGE on 12% Bis-Tris NuPAGE gels (Invitrogen). Western blotting was performed as described previously (180).

Quantitative PCR. Triplicate cultures were grown from separate single colonies. Ciprofloxacin was added to cultures at OD_{600} 0.5, and samples were harvested 120 min later. TriReagent was used for RNA isolation (Molecular Research Center) and cDNA synthesis was conducted as described previously for *P. aeruginosa* (182). Transcript abundances were determined relative to the 23S rRNA transcript by qRT-PCR with the i*Taq* SYBR Green Supermix (Bio-Rad) and an Applied Biosystems StepOnePlus detection system. The specificity of the PCR primers was verified by melting curve analyses. Relative transcript abundances are the average of three biological replicates. Error bars represent SD.

ChIP-Seq. Strains PAO1 V-AlpR and PAO1 (the mock control) were grown in LB to an OD_{600} of 0.5. ChIP was performed with 80 ml of culture by using anti-VSV-G agarose beads (Bethyl laboratories) for VSV-G-tagged proteins as previously described (180), except that cells were lysed and chromatin fragmented using a Bioruptor (Diagenode). Library preparation for ChIP-Seq was performed according to the TruSeq DNA Sample Preparation Guide (Illumina) with the following modification: adapters were diluted 10-fold prior to ligation and adapter-ligated DNA fragments were amplified by 15-cycle PCR using KOD polymerase (Novagen). ChIP libraries were sequenced by Elim Biopharmaceuticals, Inc. using an Illumina Genome

Analyzer Ilx generating 36 bp reads. Read mapping and peak calling was essentially as described previously (198) except that reads were mapped to the *P. aeruginosa* PAO1 genome allowing up to one mismatch per seed. All the mock IP data were merged and used as background for each biological replicate. Regions in each biological replicate were considered peaks if they were two-fold enriched for reads over background, had a positive peak shift and strand correlation, and had a q-value of less than 0.01. Peaks were defined as the minimal region identified in all biological replicates.

β-galactosidase assays. Cells were permeabilized with sodium dodecyl sulphate and $CHCl_3$ and assayed for β-galactosidase activity as described previously (197). Assays were performed in triplicate. Values are averages based on three independent measurements from one experiment. Error bars represent the standard deviation from the mean.

λCI dimerization and bacterial two-hybrid assays. For the bacterial two-hybrid assays, the AlpR-CTD was amplified by the PCR and ligated in frame into the vectors pACTR-ω-GP and pBR-V-Zif-AP (200), resulting in pACTR-ω-AlpR-CTD and pBR-V-Zif-AlpR-CTD, respectively. Plasmids were introduced into the *E. coli* strain KDZif1ΔZ and the assays were performed as described (197).

For the λCI-CTD dimerization-determinant assays, the AlpR-CTD was subcloned from pAC-ω-AlpR-CTD into pACλCILN (42), to make pAC-λCI_{NTD}-AlpR-CTD. Plasmid pACλCILN encodes the N-terminal domain and linker (residues 1–132) of λCI followed by three alanine residues (λCI_{NTD}) under the control of the *lac*UV5 promoter Castang, 2010 #219}. Plasmid pACλCI encodes full-length λCI, and pACΔCI is a version of pACλCI where a portion of the *cI* gene has been deleted. The indicated plasmids were introduced into the *E. coli* strain FW123 (196) and the assays were performed as described previously (197).

λ holin functional replacement assay. Plasmids pS105, pS105R– and pSam7 were provided by Ry Young (Texas A&M University). Plasmid pS105 contains the λSRRzRz1 lysis cassette placed downstream from the pR′ promoter. Expression of genes in the lysis cassette can be induced by thermal induction. The plasmid pS105R– contains two stop codons in the R gene resulting in a truncated, non-functional endolysin, and the pSam7 plasmid contains a stop codon in the S105 gene, resulting in the production of a truncated, non-functional holin (184). The λ S105 gene (except the portion that overlaps with the R gene) in the plasmids pS105 and pS105R– was replaced with the alpB gene using overlap extension PCR, to create pAlpB and pAlpBR–. Cultures of MC4100 λΔ(SR) carrying the pS105-derived plasmids were grown at 30°C to A550 of 0.3, then thermally induced for 15 min at 42°C, and aerated at 37°C thereafter. Lysis curves were obtained by measuring A550 after thermal induction (184).

***P. aeruginosa in vivo* infection**. Male C57BL/6 mice (Jackson Labs) 8 to 10 weeks of age were inoculated with $2x10^7$ CFU of *P. aeruginosa* suspended in sterile PBS via oropharyngeal aspiration following brief anesthesia with isofluorane (199). Animals were sacrificed and lung tissue harvested 24 hours post infection. Whole lungs were homogenized in 1 mL of cold sterile PBS using a Tissue-Tearor (BioSpec Products, MODEL 398) at medium speed for 15 seconds. Lung homogenate was then diluted and plated on PIA. In the strain mixing experiment, the input comprised of unmarked wild type and either wild type or *alpA* mutant carrying a gentamicin resistance marker (50 unmarked: 1 marked). After 24 h, the lungs were harvested, homogenized, and the ratios of gentamicin resistant bacteria to total bacteria were determined. The experiment was performed twice with no apparent or statistically significant differences in relative abundance detected between wild type or *alpA* mutant in ability to

colonize in the presence of a larger population of wild-type cells. Means were compared using Student's t-test with GraphPad Prism.

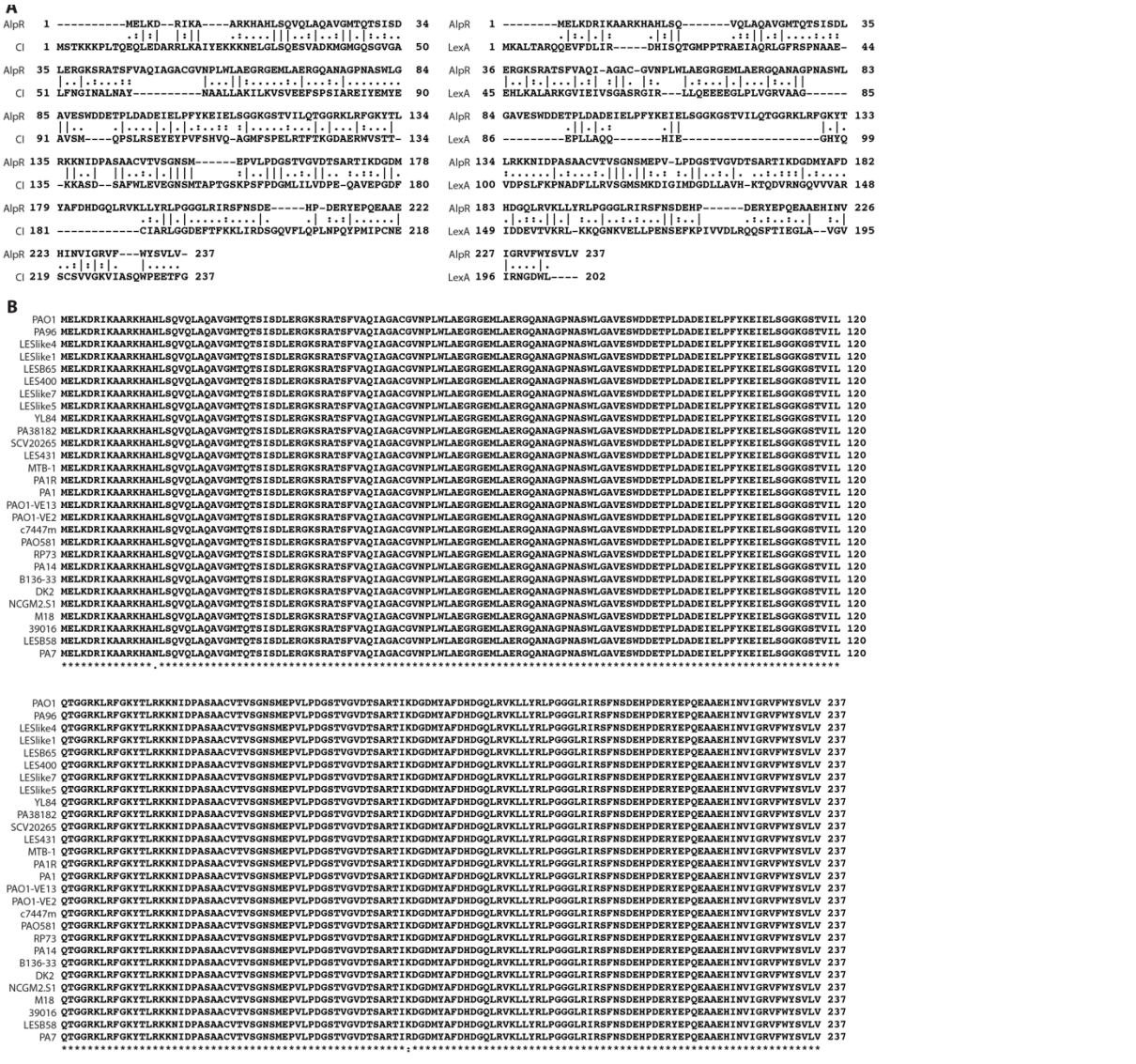

Figure 4.1: AlpR is related to the CI protein from bacteriophage λ (λCI) and to the LexA protein from *E. coli*, and is highly conserved amongst *P. aeruginosa* isolates.

(*A*) Alignment indicating the relatedness of AlpR to LexA and to λCI. AlpR and LexA share 19.9% identity and 34.5% similarity, while AlpR and CI share 21.9% identity and 34.2% similarity. Conserved residues are indicated by a | symbol, while a . (period) and a : (colon) denote similar and highly similar residues, respectively. Gaps are shown with a - (hyphen). Pairwise alignments were produced using EMBOSS Needle using default parameters (43). (*B*) Alignment indicating the degree of conservation of AlpR (PA0906) amongst *P. aeruginosa* isolates. A conserved residue is denoted by an * (asterisk), and a . (period) and a : (colon) denote similar and highly similar residues, respectively. Alignment was generated by T-Coffee using default parameters (44).

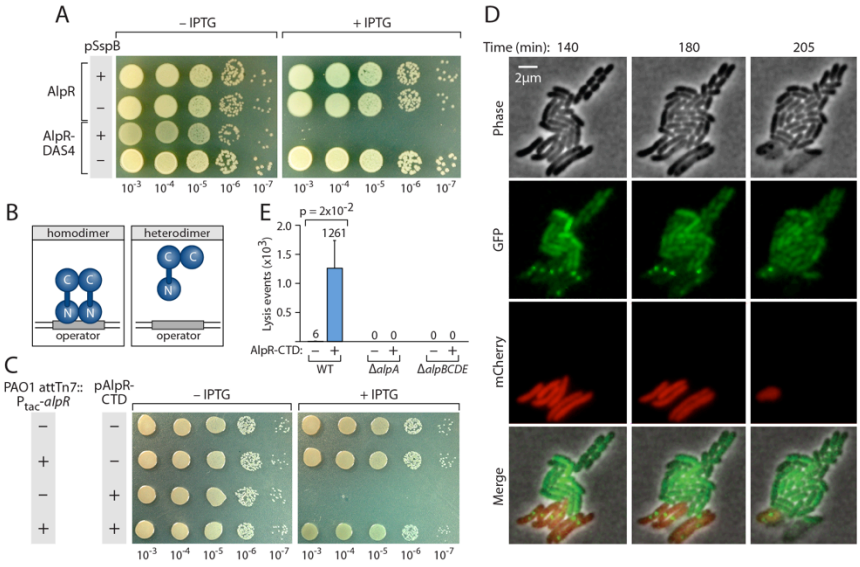

Figure 4.2: Loss of AlpR function results in cell lysis.
(*A*) Depletion of AlpR with a ClpXP-based system. AlpR with a C-terminal DAS4 epitope tag is degraded by the ClpXP protease complex when the ClpXP adaptor protein SspB is supplied. IPTG-induced synthesis of SspB (supplied by pSspB) resulted in inhibition of growth or in cell death only in cells that synthesized AlpR-DAS4. (*B*) Genetic strategy for inhibition of AlpR function with the AlpR-CTD; the AlpR-CTD sequesters full-length AlpR into inactive heterodimers. (*C*) Ectopic synthesis of the AlpR-CTD results in cell death or the inhibition of cell growth in wild-type PAO1 cells but not in cells that contain an additional copy of *alpR* (PAO1 *att*Tn*7*::P_{tac}-*alpR*). Plasmid pAlpR-CTD directs the synthesis of the AlpR-CTD in an IPTG-inducible manner. Wild-type PAO1 cells and PAO1 *att*Tn*7*::P_{tac}-*alpR* cells containing pAlpR-CTD (pAlpR-CTD+) or the empty control vector (pAlpR-CTD –) were serially diluted and incubated on media lacking or containing IPTG. (*D*) Ectopic synthesis of the AlpR-CTD results in cell lysis. Time-lapse fluorescence microscopy (TLFM) image sequence of mCherry-labeled cells (PAO1 *att*Tn*7*::*mCherry*) synthesizing the AlpR-CTD and GFP-labeled control cells (PAO1 *att*Tn*7*::*gfp*) that do not synthesize the AlpR-CTD. Images were acquired at 5 min intervals. (*E*) Quantification of the effect of the AlpR-CTD on the lysis of wild-type, Δ*alpA* mutant, and Δ*alpBCDE* mutant cells. Counting of lysis events in TLFM image sequences of mCherry labeled cells that do or do not synthesize the AlpR-CTD.

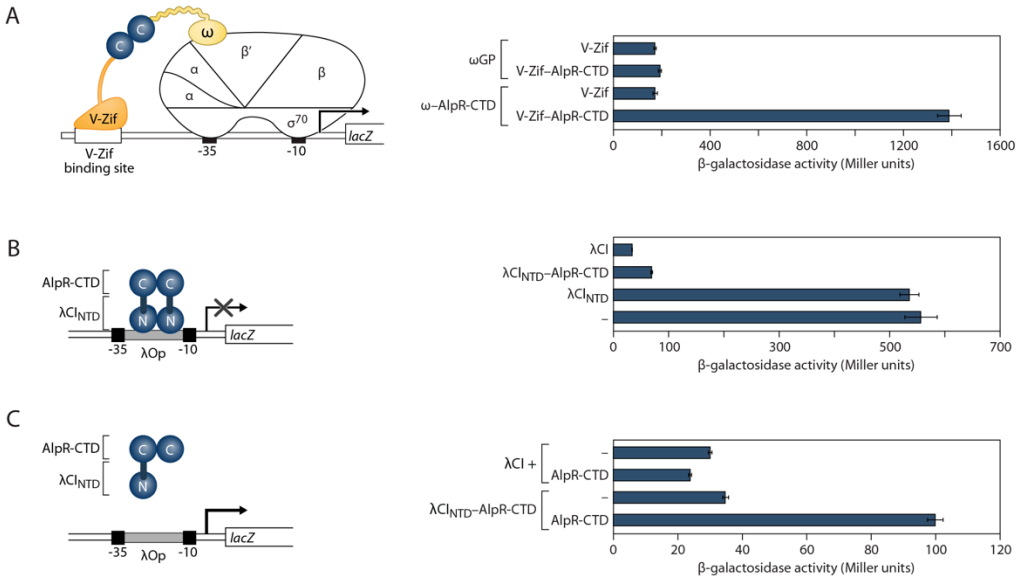

Figure 4.3: The predicted CTD of AlpR contains a dimerization determinant.
(*A*) Bacterial two-hybrid analysis demonstrates interaction between AlpR-CTDs. Contact between AlpR-CTDs (denoted as C) fused to both the ω subunit of *E. coli* RNAP and to V-Zif activates transcription from the test promoter driving expression of *lacZ*. The diagram depicts test promoter p*lacZ*if1, which bears a V-Zif-binding site positioned upstream of the *lac* core promoter. Effect of the ω–Gal11P (indicated ωGP), or ω–AlpR-CTD fusion protein on expression of the *lacZ* reporter in the presence of either the unfused V-Zif, or the V-Zif–AlpR-CTD fusion protein. KDZif1ΔZ cells harbouring compatible plasmids directing the IPTG-inducible synthesis of the indicated proteins were grown in the presence of 50 μM IPTG and assayed for β-galactosidase activity. This indicated that only the AlpR-CTD fusion proteins are capable of interacting. (*B*) The AlpR-CTD can functionally substitute for the dimerization domain of the CI protein from bacteriophage λ (λCI). FW123 cells containing a plasmid directing the IPTG-dependent synthesis of either the N-terminal domain and linker of λCI (λCI_{NTD}), λCI, or the λCI_{NTD}–AlpR-CTD fusion protein were grown in the presence of 5 μM IPTG and assayed for β-galactosidase activity. In this system the AlpR-CTD functionally replaces the dimerization domain of λCI. Occupancy of the λ operator (located between the promoter −35 and −10 elements) by λCI prevents RNAP from binding the promoter and represses transcription. (*C*) Ectopic synthesis of the AlpR-CTD specifically interferes with the ability of the λCI_{NTD}-AlpR-CTD fusion protein to bind the λ operator in *E. coli*, resulting in derepression of the test promoter.

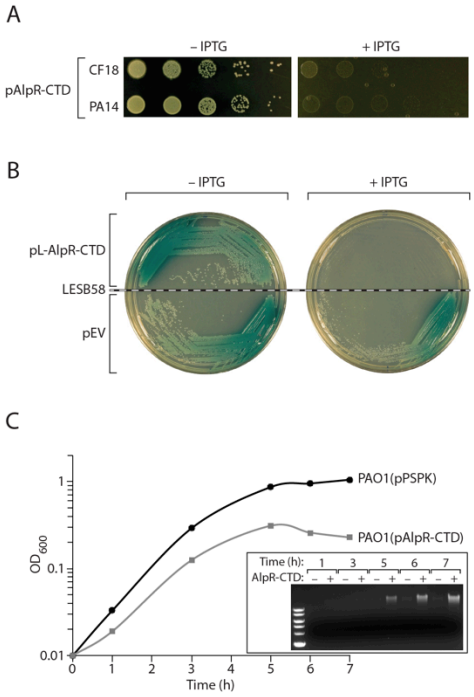

Figure 4.4: Ectopic synthesis of the AlpR-CTD is toxic in cells of clinical *P. aeruginosa* isolates, and causes a decrease in culture density and an increase in DNA in the culture supernatant of strain PAO1.

(*A*) Ectopic synthesis of the AlpR-CTD results in cell death or the inhibition of cell growth in *P. aeruginosa* clinical isolates CF18 and PA14. CF18 and PA14 cells containing pAlpR-CTD were serially diluted and incubated on media lacking or containing IPTG. (*B*) Ectopic synthesis of the AlpR-CTD results in cell death or the inhibition of cell growth in the Liverpool Epidemic Strain, LESB58. LESB58 cells containing pL-AlpR-CTD, (in which synthesis of the AlpR-CTD is under the control of a weaker promoter than in pAlpR-CTD) or the empty control vector (pEV) were streaked and incubated on media lacking or containing IPTG. (*C*) In wild-type PAO1 cells grown in liquid culture, induction of the AlpR-CTD resulted in a decrease in the OD_{600} of the culture over time that corresponded with an increase in the abundance of DNA in the culture supernatant (AlpR-CTD +), in comparison with wild type cells that contained the empty vector control (pPSPK; AlpR-CTD –). Experiments were repeated three times and a representative data set is shown.

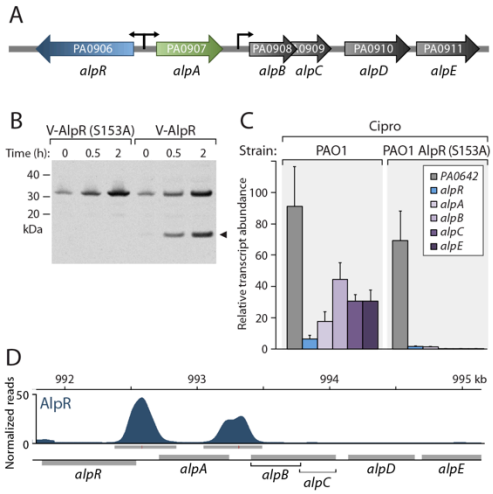

Figure 4.5: AlpR is a repressor that undergoes cleavage in response to DNA damage.
(*A*) Schematic of *alp* gene cluster. (*B*) AlpR is cleaved in cells exposed to ciprofloxacin. Western blot analysis of AlpR with a vesicular stomatitis virus-glycoprotein (VSV-G) epitope tag fused to its N-terminus (V-AlpR) and V-AlpR(S153A) following exposure of cells to ciprofloxacin for the indicated amounts of time. Arrow indicates AlpR cleavage product. (*C*) AlpR represses expression of the *alp* gene cluster. Quantification of transcript abundance by qRT-PCR in cells of the indicated strains following exposure to ciprofloxacin. Relative transcript abundance is shown in cells treated with ciprofloxacin compared to untreated cells. Expression of the *PA0642* gene was induced in both the wild-type and AlpR(S153A) mutant cells indicating that AlpR does not control the expression of all genes that are induced upon exposure to ciprofloxacin. (*D*) ChIP-Seq reveals that AlpR regulates the *alp* genes directly. ChIP-Seq with V-AlpR shows AlpR associates with the *alpR-alpA* and *alpA-alpB* intergenic regions.

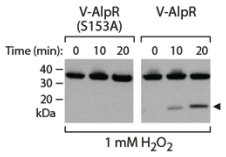

Figure 4.6: AlpR is cleaved in cells exposed to hydrogen peroxide.
Western blot analysis of AlpR with a vesicular stomatitis virus-glycoprotein (VSV-G) epitope tag fused to its N-terminus (V-AlpR) and V-AlpR(S153A) following exposure of cells to hydrogen peroxide for the indicated amounts of time. Arrow indicates AlpR cleavage product.

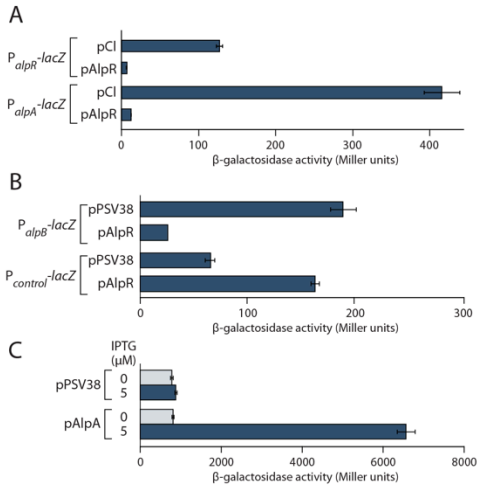

Figure 4.7: Repression of *alp* promoter-*lacZ* fusions by AlpR and activation of the *alpB* promoter-*lacZ* fusion by AlpA.
(*A*) Ectopic synthesis of AlpR in *E. coli* resulted in repression of *alpR* promoter- and *alpA* promoter-*lacZ* reporter fusions, whereas ectopic synthesis of λCI did not. (*B*) Ectopic synthesis of AlpR in *P. aeruginosa* resulted in repression of an *alpB* promoter-*lacZ* reporter fusion, but did not repress a control *orn* promoter-*lacZ* reporter fusion. Plasmid pPSV38 served as an empty vector control. (*C*) Ectopic synthesis of AlpA in *E. coli* resulted in activation of an *alpB* promoter-*lacZ* reporter fusion, whereas activity did not increase in cells that contained the empty vector. Error bars denote standard deviation from the mean.

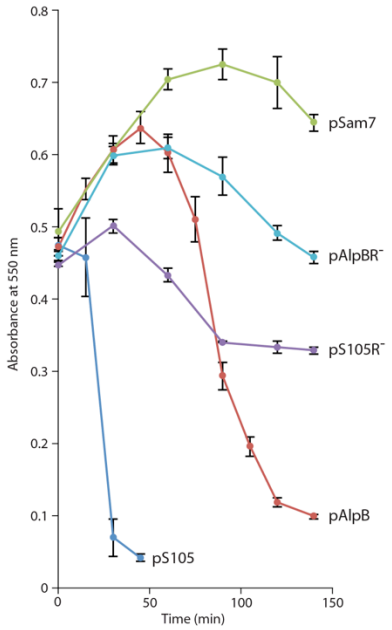

Figure 4.8: AlpB can functionally substitute for the holin from bacteriophage λ.

Plasmid pS105 contains the λ*SRRzRz1* lysis cassette placed downstream from the pR′ promoter. The λ*S105* gene (except the portion that overlaps with the *R* gene) in the plasmids pS105 and pS105R– was replaced with the *alpB* gene to create pAlpB and pAlpBR–. Cultures of MC4100 λΔ(*SR*) carrying the pS105-derived plasmids were grown at 30°C to A_{550} of 0.3, thermally induced for 15 min at 42°C, and aerated at 37°C thereafter. Lysis curves were obtained by measuring A_{550} after thermal induction. Time in minutes is shown. Cells containing pS105 (navy line) undergo rapid lysis after thermal induction, and pAlpB-containing cells also show a drop in turbidity after thermal induction (red line). The drop in turbidity is endolysin dependent, as cells that contain the plasmids pS105R– (purple line) and pAlpBR– (blue line), that lack a functional *R* gene, do not show the same phenotype. Additionally, the lysis is holin dependent, as the cells containing the pSam7 plasmid (green line) that produces a truncated holin also does not undergo lysis.

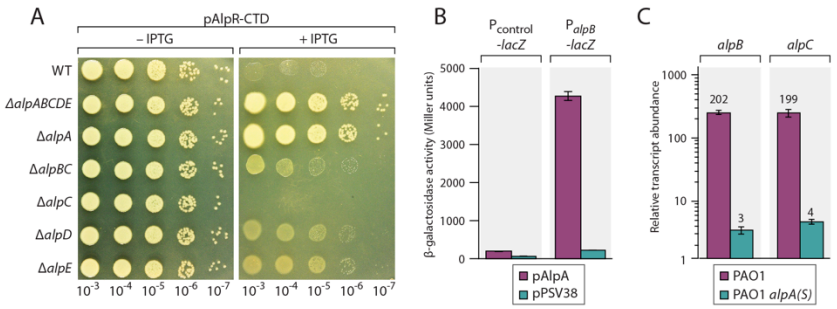

Figure 4.9: The essential function of AlpR is to repress expression of *alpA* which encodes a positive regulator of the *alpBCDE* lysis genes.
A) Effect of ectopic synthesis of the AlpR-CTD. Wild-type and mutant PAO1 cells containing plasmid pAlpR-CTD were serially diluted and incubated on media lacking or containing IPTG. (*B*) AlpA positively regulates expression of an *alpB* promoter-*lacZ* fusion. Cells harboring the indicated promoter-*lacZ* fusions and containing plasmid pAlpA or the empty control plasmid pPSV38 were assayed for β-galactosidase activity. (*C*) AlpA positively regulates expression of the *alpBC* genes. Quantification of transcript abundance by qRT-PCR in cells following exposure to ciprofloxacin. (Cells of the PAO1 *alpA(s)* mutant strain contain a premature stop codon early in the *alpA* ORF.) Relative transcript abundance is shown in cells treated with ciprofloxacin compared to cells of the PAO1 AlpR(S153A) mutant strain treated with ciprofloxacin.

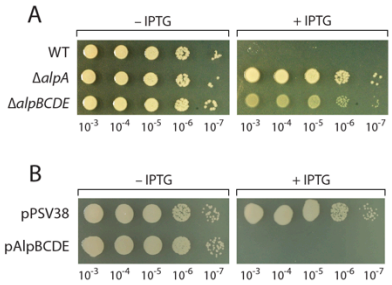

Figure 4.10: Cells lacking *alpBCDE* tolerate ectopic synthesis of the AlpR-CTD and ectopic synthesis of *alpBCDE* results in lethality.
(*A*) Cells lacking *alpBCDE* tolerate ectopic synthesis of the AlpR-CTD almost as well as cells that lack *alpA*. Wild-type PAO1 cells, cells of the PAO1 Δ*alpA* mutant strain, and cells of the PAO1 Δ*alpBCDE* mutant strain containing pAlpR-CTD were serially diluted and incubated on media lacking or containing IPTG. (*B*) Ectopic synthesis of *alpBCDE* results in lethality in strain PAO1. Wild-type PAO1 cells containing the empty vector pPSV38 or the *alpBCDE* expression plasmid pAlpBCDE were serially diluted and incubated on media lacking or containing IPTG.

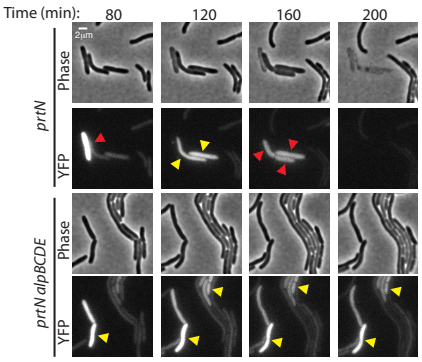

Figure 4.11: Induction of the Alp system occurs in a subset of cells treated with a DNA-damaging agent and results in *alpBCDE*-dependent cell lysis.
Representative cropped regions from TLFM image sequences of Δ*prtN* mutant cells and Δ*prtN* Δ*alpBCDE* mutant cells containing an *alpB* promoter-*yfp* fusion following exposure to ciprofloxacin. The addition of ciprofloxacin resulted in induction of *alpB* promoter activity in a subset of cells. Expression of the *alpB* promoter-*yfp* fusion was not induced in cells that were not exposed to ciprofloxacin (Movie 4.9, Movie 4.11). Yellow arrowheads point to *alp*-induced cells; red arrowheads point to cells that undergo lysis in the subsequent frame. Cells of the Δ*prtN* mutant strain in which the *yfp* reporter was induced lysed (upper panels). Cells of the Δ*prtN* Δ*alpBCDE* mutant strain in which the *yfp* reporter was induced did not lyse (lower panels). Images were normalized for background fluorescence. Scale bar denotes 2 μm.

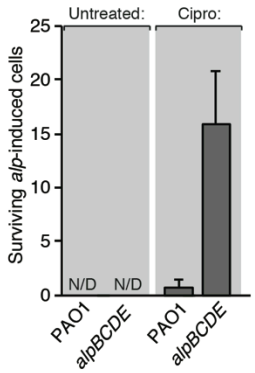

Figure 4.12: The *alpBCDE* genes influence the survival of wild-type cells in which the *alp* genes are induced in response to DNA damage.
Quantification of surviving *alp*-induced cells from time-lapse microscopy sequences taken after a one-hour ciprofloxacin pulse, or taken after no ciprofloxacin treatment. Wild-type and Δ*alpBCDE* mutant strains harbored an *alpB* promoter-*yfp* fusion. Final YFP-positive cells were normalized to the starting cell number. Error bars, standard deviation; n = 3. See also Movies 4.4-4.7.

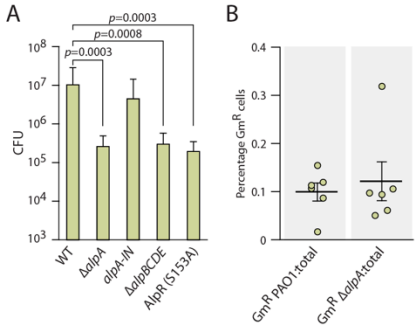

Figure 4.13: The AlpR-regulated PCD pathway promotes *P. aeruginosa* colonization of the murine lung.

(*A*) Ability of the indicated strains to colonize the murine lung. Male C57BL/6 mice were inoculated via the oropharyngeal route with equivalent numbers of wild-type PAO1 cells and the indicated mutant derivatives. Graphs indicate the mean and error bars indicate SD. After 24 hours mice were sacrificed and colony-forming units (CFUs) in the lungs were enumerated. (*B*) Ability of the indicated marked strains to colonize the murine lung when mixed with an excess of wild-type cells. PAO1 cells marked with a gentamicin resistance cassette (Gm^R PAO1) and PAO1 Δ*alpA* cells marked with a gentamicin resistance cassette (Gm^R Δ*alpA*) were each mixed with an excess of unmarked wild-type PAO1 cells and inoculated into male C57BL/6 mice via the oropharyngeal route. After 24 hours mice were sacrificed and the % gentamicin resistant (Gm^R) cells compared to the total number of cells in the lungs was determined. Experiments were performed twice with similar results. A representative data set is shown.

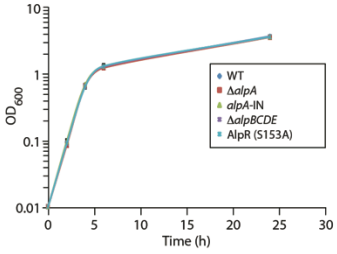

Figure 4.14: Cells of the Δ*alpA* mutant strain, the Δ*alpBCDE* mutant strain, and the AlpR(S153A) mutant strain grow identically to wild-type cells *in vitro*.
Growth curves of cultures of cells of the Δ*alpA* mutant strain, the Δ*alpBCDE* mutant strain, the AlpR(S153A) mutant strain, and the wild-type PAO1 strain. Growth curves were obtained by measurement of the culture OD_{600} over a 24 h period. Error bars denote standard deviation from the mean.

Movie 4.1. TLFM was used to visualize the growth of cells that synthesized mCherry and the AlpR-CTD, alongside control cells that synthesized GFP alone. Following induction of the AlpR-CTD, most red fluorescent cells lysed. Cell lysis did not occur in control cells that synthesized GFP. A 60× objective was used for all movies. Time in minutes is shown.

Movie 4.2. Depletion of AlpR results in cell lysis. Time-lapse microscopy was used to visualize the effects of depleting AlpR-DAS4 using the ClpXP-based degradation system as described in Fig. 4.1A. Following induction with IPTG, pervasive lysis was observed in cells bearing pSspB. (See Movie 4.3 for empty vector control.) Images were acquired at 5-min intervals.

Movie 4.3. AlpR depletion is required for cell lysis. Time-lapse microscopy sequence accompanying Movie 4.2. Following IPTG induction, cells bearing an empty control vector did not undergo lysis. Images were acquired at 5-min intervals.

Movie 4.4. Induction of alpBCDE due to DNA damage leads to cell lysis. Growth of PAO1 alpB-yfp following exposure to ciprofloxacin was visualized by TLFM. Overlays of the phase and YFP channels are displayed; identical scaling was applied to Movies 4.4–4.7.

Movie 4.5. Induction of alpBCDE does not occur in the absence of DNA damage. Growth of PAO1 alpB-yfp in the absence of ciprofloxacin treatment was visualized by TLFM. Overlays of the phase and YFP channels are displayed; identical scaling was applied to Movies 4.4–4.7.

Movie 4.6. AlpBCDE contributes to DNA-damaged induced lysis in wild-type cells. Growth of PAO1 ΔalpBCDE alpB-yfp following exposure to ciprofloxacin was visualized by TLFM. Overlays of the phase and YFP channels are displayed; identical scaling was applied to Movies 4.4–4.7.

Movie 4.7. Induction of alpB does not occur in the absence of DNA damage. Growth of PAO1 ΔalpBCDE alpB-yfp in the absence of ciprofloxacin treatment was visualized by TLFM. Overlays of the phase and YFP channels are displayed; identical scaling was applied to Movies 4.4–4.7.

Movie 4.8. AlpBCDE mediates DNA-damaged induced lysis in the absence of prtN. Growth of PAO1 ΔprtN alpB-yfp following exposure to ciprofloxacin was visualized by TLFM. Lysis is observed for alp-induced cells. Overlays of the phase and YFP channels are displayed; identical scaling was applied to Movies 4.8–4.11.

Movie 4.9. Induction of alpB does not occur in the absence of DNA damage. Growth of PAO1 prtN alpB-yfp in the absence of ciprofloxacin treatment was visualized by TLFM. Overlays of the phase and YFP channels are displayed; identical scaling was applied to Movies 4.8–4.11.

Movie 4.10. AlpBCDE mediates DNA-damaged induced lysis in the absence of prtN. Growth of PAO1 ΔprtN ΔalpBCDE alpB-yfp following exposure to ciprofloxacin was visualized by TLFM. The alp-induced cells (green) do not undergo lysis. Overlays of the phase and YFP channels are displayed; identical scaling was applied to Movies 4.8–4.11.

Movie 4.11. Induction of alpB does not occur in the absence of DNA damage. Growth of PAO1 ΔprtN ΔalpBCDE alpB-yfp in the absence of ciprofloxacin treatment was visualized by time-lapse fluorescence microscopy TLFM. Overlays of the phase and YFP channels are displayed; identical scaling was applied to Movies 4.8–4.11.

Chapter 5. Conclusions and Future Directions

Portions adapted from:

LeRoux M, Peterson S.B., and Mougous J.D. *Bacterial danger sensing*. Journal of Molecular Biology, under review

5.1 Significance

Over the course of my graduate career, our understanding of polymicrobial communities has dramatically improved thanks to high throughput sequencing and inititatives such as the Human Microbiota Project (201). These efforts have catalogued the species present in healthy hosts, highlighted the importance of beneficial microbes to human health, and identified changes in bacterial consortia that are associated with particular disease states, termed dysbioses (202). Currently, there is an interest in restoring dysbiotic communities to a healthy state. An approach that has been successfully used for patients suffering from *Clostridium difficile* infections has been to entirely replace an existing, often depleted, community with one derived from a healthy host in the process of fecal transplantation (203). While this dramatic approach has saved many lives, the next step in this promising field will be to effect more nuanced changes, perhaps by replacing only a few members of a microbial community. As a result, there is a growing need to understand the forces that can alter the composition of microbial communities.

It is well established that bacterial communities are influenced by physical parameters such as nutrient availability, temperature, and pH. Furthermore, microbes can promote or inhibit the growth of other microbes by altering their nutritional environment through the consumption of nutrients and the production of metabolic byproducts (204, 205). Another factor that has gained more attention in recent years are the direct, antagonistic interactions that occur between bacteria and prevent the co-existence of particular species (42). Understanding the mechanisms by which bacteria influence the growth and death of the other microbes in their surroundings may ultimately lead to predictive models that will allow physicians to shift an entire community by adding or eliminating a single organism (206). However, in parallel to such large scale '-omics' and modeling approaches, it is essential that mechanisms of bacterial interactions also be

investigated to inform predictive models. Towards this larger goal, my work has focused on mechanistically characterizing interbacterial behaviors that occur within polymicrobial communities.

Many of the danger response regulons described in the introduction are replete with hypothetical genes and genes of unknown function. This may not be happenstance, but rather a result of the tendency to study bacteria in monoculture or through the lense of pathogenesis. The components of danger response regulons are necessarily factors that function in genetically heterogenous populations and thus may have been systematically overlooked or their evolutionary underpinnings obscured in both of these settings. For example, the Gac/Rsm pathway was interpreted as a quorum-like system owing on its response in monoculture to self-derived signals. However, more recent investigation of the pathway in the presence of competing bacteria offer an alternative explanation for its sensitivity to self-derived cues and provide a physiological context in which to define the function of factors under RsmA control. We suggest that interrogating the components of danger response regulons within mixed communities that more accurately recapitulate the natural setting in which they operate could be a productive approach to reducing the number of currently uncharacterized proteins.

5.2 Quantitative time-lapse fluorescence microscopy tools

Interbacterial interactions have predominantly been characterized at the population level by growth competition assays. These methods are limited by their ability to resolve individual cells, and thus clarify the forces that lead to overall changes in the ratio of two organisms in a co-culture. To address this, I developed techniques to image bacteria with automated time-lapse fluorescence microscopy (TLFM) and computational tools to analyze the resulting datasets.

These tools were developed in collaboration with Paul Wiggins (Physics Department, University of Washington). Pre-existing software developed by the Wiggins group identifies cells, links them between frames, and tabulates fluorescence intensity measurements. I adapted this software by adding modules to distinguish two or more bacterial populations, track lysis, identify contacts between cells, measure cellular fluorescence intensity, and detect fluorescent foci within cells. When combined with conventional microbiology tools such as genetics, biochemistry, and molecular biology, we were able to investigate an entirely new aspect of T6S-dependent interactions.

Prior to my work, the fate of recipient cells and the spatiotemporal requirements for T6S-dependent interactions were largely unknown. In early studies, the competitive index (change in ratio of donor/recipient) following the co-culture of two strains or species was the primary metric used to quantify T6S-dependent fitness. However, this approach does not provide information on how this fitness advantage came about. Monitoring co-cultures at high time resolution by microscopy enables us to observe cellular growth and death, thereby distinguishing among the possibilities that can lead to a reduction in the numbers of bacteria, including reduced growth, stasis, or cell death (e.g. lysis). We discovered that lysis is the principal outcome of *P. aeruginosa* H1-T6SS-dependent intoxication of bacterial competitors, and that it is primarily due to a single effector, Tse1. I also observed that T6S-dependent lysis was not abrogated in a strain lacking all three effectors known at the time, suggesting the existence of additional effectors. As a result of this observation, our laboratory went on to identify three additional H1-T6SS substrates (71). The spatiotemporal requirements for T6S-dependent interactions had previously been inferred from population-level experiments wherein strains were separated by cell-impermeant filters. These experiments led to the model that T6S-dependent intoxication is

contact-dependent, and occurs on a timescale of several hours. However, such experiments could not rule out that lysis is due to high local concentrations of effectors and does not require cells to be in direct contact. My work demonstrated that sustained cell–cell contact was indeed required for effector delivery and that this could occur on a timescale of several minutes.

In addition to characterization of cellular neighborhood and fates, we also examined the subcellular localization of the apparatus itself. To this end, we generated functional translational fluorescent fusions of several T6SS structural components on the chromosome. This allowed the detection of expression levels and activity of the system by visualizing protein localization. We made the intriguing discovery that the apparatus localizes preferentially towards adjacent cells that themselves contain an active T6SS apparatus. Initially, we and others proposed that this spatial localization underlies the observation that susceptible recipients with T6SSs themselves are more susceptible to T6S-dependent intoxication. However, the measurements to date have only been made within populations of genetically identical *P. aeruginosa* cells, not between *P. aeruginosa* and a susceptible recipient. If the T6SS primarily participates in interbacterial antagonism, why it preferentially localizes towards itself is not apparent. One possibility is that it localizes towards any T6SS in its surroundings, and the localization towards self cell is an accidental result of this. However, it is not yet known whether preferential targeting of non-self recipients occurs, and whether this could partially underlie the ability of T6SS-dependent intoxication to be more efficient when a recipient cell has a T6SS as well. To address this, studies are needed to quantify localization of the apparatus towards a non-self recipient, and to directly correlate spatial localization of the apparatus with targeting. A limitation of the current system is that the repeated fluorescent exposure required to capture each apparatus localization

event (~every 2 seconds) cannot be sustained for time scales greater than 5-10 minutes due to bleaching and toxicity of the fluorescent exposure.

Another problem with interpreting localization of fluorescently labeled T6S apparatus components is that, even though their localization correlates well with measures of T6SS activity, the mechanism of effector delivery is not well understood. It is known that a subset of effectors require Hcp1 for stability, and are localized on the interior of homohexameric Hcp rings. Based on these data, the current model is that these Hcp rings stack to form tubules that localize inside of tubules composed of the proteins VipA and VipB. VipA/B tubules have been visualized in an extended and contracted state, and these contractions are thought to propel effectors into recipient cells. ClpV is required for disassembly of tubules composed of VipA/B, but whether effectors actually transit through these tubules has not been directly tested. Neither ClpV and VipA have been directly demonstrated to participate in effector delivery or localization with the membrane-spanning channel. Therefore, precisely what aspect of secretion/translocation of effectors the localization of these proteins corresponds to is not known.

We have established and validated this approach with two bacterial competitors growing in a monolayer; but polymicrobial communities are commonly composed of more than two organisms with diverse, environment-specific spatial configurations. Future work could build on the existing toolkit to enable characterization of increasingly complex bacterial communities, perhaps by combining TLFM with other imaging methods such as in situ hybridization. Our current quantification methodology requires that we restrict bacterial growth to a monolayer for cell identification. Adaptation of cell tracking to spatially complex communities will be a major advance in this field. Currently, our software and similar packages uses the phase image to identify cells. Growth in a third dimension would likely require a confocal system and the use of

fluorescence for cell identification. Alternatively, the measurements made in two-dimensions could be extrapolated to a third dimension, and incorporated into bacterial growth simulations.

5.3 Implications of Gac/Rsm-mediated detection of kin cell lysis.

One mechanism by which eukaryotic innate immune systems sense danger is through detection of DAMPs. We discover an analogous system for detecting cellular damage and mounting a counterattack in the Gram-negative opportunistic pathogen, *Pseudomonas aeruginosa* (Figure 1A) (207). During growth in the presence of an antagonistic competitor, a subset of the *P. aeruginosa* population lyse, releasing cell-associated molecules into the extracellular milieu. One or more of these molecules then stimulates a global regulatory pathway in surrounding cells that raises the fitness of *P. aeruginosa* during interbacterial competition. When considered a danger sensing pathway, the molecules released by lysed cells are the danger signals (analogous to eukaryotic DAMPs) that launch a global response when sensed by the intact cells.

The pathway that responds to lysate from kin cells, and that we propose coordinates the danger response, is the Gac/Rsm pathway. At its foundation, Gac/Rsm consists of a sensor kinase and response regulator pair, GacS and GacA, respectively (208). When GacS is stimulated, GacA positively regulates transcription of the small RNAs (sRNA) *rsmY* and *rsmZ* (209). These sRNAs modulate activity of RsmA and RsmF, RNA binding proteins that interact with recognition sequences in a subset of messenger RNAs (mRNA) and prevent their translation. At sufficient abundance, *rsmY* and *rsmZ* sequester RsmA and RsmF from these mRNA targets, allowing translation to proceed (209, 210). GacS is additionally modulated by upstream orphan sensor kinases (80, 126, 127, 211), one of which, RetS, is required for the

ability of *P. aeruginosa* to detect kin cell lysis (207). A point mutation in a conserved residue in the predicted periplasmic signal binding domain of RetS abrogates the ability of *P. aeruginosa* to sense kin cell lysate, suggesting that this sensor kinase may directly perceive the danger signal(s). Future work will focus on identifying the molecule(s) contained within lysate that RetS detects. This important piece of information will allow us to determine whether other organisms have the capacity to stimulate this response.

Viewing the Gac/Rsm pathway as a danger response, its regulon encompasses offensive factors (e.g. T6SS, hydrogen cyanide) that have been demonstrated to directly antagonize the source of the threat and putative defensive factors (e.g. exopolysaccharide) that may provide resistance to antagonism (80, 125). Many uncharacterized proteins under Gac/Rsm control are secreted or predicted to localize to the cell surface, consistent with their participation in intercellular interactions (125, 137). *P. aeruginosa* cells lacking a functional Gac/Rsm system undergo dramatic cell death in the presence of a bacterial competitor that cannot be attributed to any one component of the pathway, indicating that Gac-mediated danger sensing is a multi-faceted response (207). Though we now appreciate that many factors under Gac/Rsm control mediate bacterial interactions, the pathway has received most attention as a key mediator of the switch between the chronic and acute infectious states of *P. aeruginosa*. As populations of *P. aeruginosa* are predominantly free-living in the environment and not associated with infection, the selective pressure for the duality of factors under Gac/Rsm likely derived from intermicrobial antagonism.

Unlike the core components of the Gac/Rsm pathway, which are broadly conserved among the proteobacteria, the hybrid sensor kinases that modulate GacS activity, including RetS, are found only in the pseudomonads, perhaps as a unique adaptation that confers danger sensing.

Gac/Rsm modulates the ability of *Pseudomonas protegens* (previously *Pseudomonas fluorescens*) to inhibit plant pathogens, thus demonstrating that antibacterial factors are Gac/Rsm controlled in other pseudomonads (80, 212). Outside of this phylogenetic group, the function of the pathway is less clear. In *Escherichia coli*, acetate stimulates the GacS homolog, BarA, pointing to a role in metabolism (213). However, Lapouge and colleagues noted that many Gac regulated factors have relevance to interbacterial interactions: production of antibiotics, extracellular proteases, quorum sensing factors, and exopolysaccharide production (125). Furthermore, the RsmA homolog, CsrA, negatively regulates T6S in *Yersinia pseudotuberculosis* (214). These observations may suggest a more general role for this conserved signalling pathway in mediating danger sensing.

5.4 A *P. aeruginosa* programmed cell death pathway

In Chapter 4 we applied a combination of these methods to an altogether different system to characterize a *P. aeruginosa* programmed cell death pathway. This work was performed in collaboration with the laboratory of Dr. Simon Dove (Boston Children's Hospital). Their laboratory had discovered the existence of a DNA-damage induced pathway that, when stimulated, leads to a reduction in the c.f.u. of a population of *P. aeruginosa* cells. However, it was not clear what the outcome of activating this pathway was on individual cells, or which particular components of the pathway were responsible. Applying our single-cell characterization methods to this system led to the discovery that the primary outcome of this pathway is lysis of a subset of cells. I went on to correlate activation of the pathway – by monitoring a transcriptional fluorescent reporter – with cell lysis, and determine that a single gene within the pathway is responsible for the majority of lysis observed. This single cell

analysis also revealed that Alp expression is bistable. Work from the Hogan laboratory demonstrated that this pathway enhances survival of *P. aeruginosa* in an *in vivo* infection model, consistent with the model that death of some cells promotes the overall success of the organism. This type of multicellular coordination is similar to what we observed in Chapter 3, and together suggests that *P. aeruginosa*, and likely other species, have the capacity for sophisticated behaviors that benefit the population as a whole. Future work will be needed to determine why only a subset of cells is activated and how the death of these cells promotes survival. One intriguing possibility is that Alp-mediated cell death, in response to DNA damage, is another mechanism by which the Gac/Rsm pathway is stimulated.

References

1. Bhaya D, Davison M, & Barrangou R (2011) CRISPR-Cas systems in bacteria and archaea: versatile small RNAs for adaptive defense and regulation. *Annu Rev Genet* 45:273-297.
2. Kono H & Rock KL (2008) How dying cells alert the immune system to danger. *Nat Rev Immunol* 8(4):279-289.
3. Shi Y, Evans JE, & Rock KL (2003) Molecular identification of a danger signal that alerts the immune system to dying cells. *Nature* 425(6957):516-521.
4. Martinon F, Petrilli V, Mayor A, Tardivel A, & Tschopp J (2006) Gout-associated uric acid crystals activate the NALP3 inflammasome. *Nature* 440(7081):237-241.
5. Hayes CS, Aoki SK, & Low DA (2010) Bacterial contact-dependent delivery systems. *Annu Rev Genet* 44:71-90.
6. Gabrielsen C, Brede DA, Nes IF, & Diep DB (2014) Circular bacteriocins: biosynthesis and mode of action. *Appl Environ Microbiol* 80(22):6854-6862.
7. Jamet A & Nassif X (2015) New Players in the Toxin Field: Polymorphic Toxin Systems in Bacteria. *MBio* 6(3).
8. Ruhe ZC, Low DA, & Hayes CS (2013) Bacterial contact-dependent growth inhibition. *Trends Microbiol* 21(5):230-237.
9. Coulthurst SJ, Barnard AM, & Salmond GP (2005) Regulation and biosynthesis of carbapenem antibiotics in bacteria. *Nat Rev Microbiol* 3(4):295-306.
10. Cornforth DM & Foster KR (2013) Competition sensing: the social side of bacterial stress responses. *Nature reviews. Microbiology* 11(4):285-293.
11. Macfarlane EL, Kwasnicka A, Ochs MM, & Hancock RE (1999) PhoP-PhoQ homologues in Pseudomonas aeruginosa regulate expression of the outer-membrane protein OprH and polymyxin B resistance. *Mol Microbiol* 34(2):305-316.
12. Miller SI, Kukral AM, & Mekalanos JJ (1989) A two-component regulatory system (phoP phoQ) controls Salmonella typhimurium virulence. *Proc Natl Acad Sci U S A* 86(13):5054-5058.
13. Garcia Vescovi E, Soncini FC, & Groisman EA (1996) Mg2+ as an extracellular signal: environmental regulation of Salmonella virulence. *Cell* 84(1):165-174.
14. Groisman EA (2001) The pleiotropic two-component regulatory system PhoP-PhoQ. *J Bacteriol* 183(6):1835-1842.
15. Johnson L*, et al.* (2013) Extracellular DNA-induced antimicrobial peptide resistance in Salmonella enterica serovar Typhimurium. *BMC Microbiol* 13:115.
16. Mulcahy H, Charron-Mazenod L, & Lewenza S (2008) Extracellular DNA chelates cations and induces antibiotic resistance in Pseudomonas aeruginosa biofilms. *PLoS Pathog* 4(11):e1000213.
17. Dalebroux ZD & Miller SI (2014) Salmonellae PhoPQ regulation of the outer membrane to resist innate immunity. *Curr Opin Microbiol* 17:106-113.
18. Gunn JS*, et al.* (1998) PmrA-PmrB-regulated genes necessary for 4-aminoarabinose lipid A modification and polymyxin resistance. *Mol Microbiol* 27(6):1171-1182.
19. Courvalin P (2006) Vancomycin resistance in gram-positive cocci. *Clin Infect Dis* 42 Suppl 1:S25-34.

20. Hillen W & Berens C (1994) Mechanisms underlying expression of Tn10 encoded tetracycline resistance. *Annu Rev Microbiol* 48:345-369.
21. Davies J, Spiegelman GB, & Yim G (2006) The world of subinhibitory antibiotic concentrations. *Curr Opin Microbiol* 9(5):445-453.
22. Bernier SP & Surette MG (2013) Concentration-dependent activity of antibiotics in natural environments. *Front Microbiol* 4:20.
23. Romero D, Traxler MF, Lopez D, & Kolter R (2011) Antibiotics as signal molecules. *Chem Rev* 111(9):5492-5505.
24. Hoffman LR*, et al.* (2005) Aminoglycoside antibiotics induce bacterial biofilm formation. *Nature* 436(7054):1171-1175.
25. Colvin KM*, et al.* (2011) The pel polysaccharide can serve a structural and protective role in the biofilm matrix of Pseudomonas aeruginosa. *PLoS Pathog* 7(1):e1001264.
26. Kharel MK*, et al.* (2004) Isolation and characterization of the tobramycin biosynthetic gene cluster from Streptomyces tenebrarius. *FEMS Microbiol Lett* 230(2):185-190.
27. Bleich R, Watrous JD, Dorrestein PC, Bowers AA, & Shank EA (2015) Thiopeptide antibiotics stimulate biofilm formation in Bacillus subtilis. *Proc Natl Acad Sci U S A* 112(10):3086-3091.
28. Wang W*, et al.* (2014) Angucyclines as signals modulate the behaviors of Streptomyces coelicolor. *Proc Natl Acad Sci U S A* 111(15):5688-5693.
29. Perez J*, et al.* (2011) Myxococcus xanthus induces actinorhodin overproduction and aerial mycelium formation by Streptomyces coelicolor. *Microb Biotechnol* 4(2):175-183.
30. Muller S, Strack SN, Ryan SE, Kearns DB, & Kirby JR (2015) Predation by Myxococcus xanthus induces Bacillus subtilis to form spore-filled megastructures. *Appl Environ Microbiol* 81(1):203-210.
31. Muller S*, et al.* (2014) Bacillaene and sporulation protect Bacillus subtilis from predation by Myxococcus xanthus. *Appl Environ Microbiol* 80(18):5603-5610.
32. Straight PD, Willey JM, & Kolter R (2006) Interactions between Streptomyces coelicolor and Bacillus subtilis: Role of surfactants in raising aerial structures. *J Bacteriol* 188(13):4918-4925.
33. Draper LA, Cotter PD, Hill C, & Ross RP (2015) Lantibiotic resistance. *Microbiol Mol Biol Rev* 79(2):171-191.
34. Peschel A & Sahl HG (2006) The co-evolution of host cationic antimicrobial peptides and microbial resistance. *Nat Rev Microbiol* 4(7):529-536.
35. Li M*, et al.* (2007) Gram-positive three-component antimicrobial peptide-sensing system. *Proc Natl Acad Sci U S A* 104(22):9469-9474.
36. Prost LR & Miller SI (2008) The Salmonellae PhoQ sensor: mechanisms of detection of phagosome signals. *Cell Microbiol* 10(3):576-582.
37. McPhee JB, Lewenza S, & Hancock RE (2003) Cationic antimicrobial peptides activate a two-component regulatory system, PmrA-PmrB, that regulates resistance to polymyxin B and cationic antimicrobial peptides in Pseudomonas aeruginosa. *Mol Microbiol* 50(1):205-217.
38. Fernandez L*, et al.* (2010) Adaptive resistance to the "last hope" antibiotics polymyxin B and colistin in Pseudomonas aeruginosa is mediated by the novel two-component regulatory system ParR-ParS. *Antimicrob Agents Chemother* 54(8):3372-3382.

39. Fernandez L*, et al.* (2012) The two-component system CprRS senses cationic peptides and triggers adaptive resistance in Pseudomonas aeruginosa independently of ParRS. *Antimicrob Agents Chemother* 56(12):6212-6222.
40. Macfarlane EL, Kwasnicka A, & Hancock RE (2000) Role of Pseudomonas aeruginosa PhoP-phoQ in resistance to antimicrobial cationic peptides and aminoglycosides. *Microbiology* 146 (Pt 10):2543-2554.
41. Li M*, et al.* (2007) The antimicrobial peptide-sensing system aps of Staphylococcus aureus. *Mol Microbiol* 66(5):1136-1147.
42. Hibbing ME, Fuqua C, Parsek MR, & Peterson SB (2010) Bacterial competition: surviving and thriving in the microbial jungle. *Nat Rev Microbiol* 8(1):15-25.
43. He YW & Zhang LH (2008) Quorum sensing and virulence regulation in Xanthomonas campestris. *FEMS Microbiol Rev* 32(5):842-857.
44. Twomey KB*, et al.* (2012) Bacterial cis-2-unsaturated fatty acids found in the cystic fibrosis airway modulate virulence and persistence of Pseudomonas aeruginosa. *ISME J* 6(5):939-950.
45. Ryan RP*, et al.* (2008) Interspecies signalling via the Stenotrophomonas maltophilia diffusible signal factor influences biofilm formation and polymyxin tolerance in Pseudomonas aeruginosa. *Mol Microbiol* 68(1):75-86.
46. Chandler JR, Heilmann S, Mittler JE, & Greenberg EP (2012) Acyl-homoserine lactone-dependent eavesdropping promotes competition in a laboratory co-culture model. *ISME J* 6(12):2219-2228.
47. Subramoni S & Venturi V (2009) LuxR-family 'solos': bachelor sensors/regulators of signalling molecules. *Microbiology* 155(Pt 5):1377-1385.
48. Lee JH, Lequette Y, & Greenberg EP (2006) Activity of purified QscR, a Pseudomonas aeruginosa orphan quorum-sensing transcription factor. *Mol Microbiol* 59(2):602-609.
49. Poole SJ*, et al.* (2011) Identification of functional toxin/immunity genes linked to contact-dependent growth inhibition (CDI) and rearrangement hotspot (Rhs) systems. *PLoS Genet* 7(8):e1002217.
50. Prudhomme M, Attaiech L, Sanchez G, Martin B, & Claverys JP (2006) Antibiotic stress induces genetic transformability in the human pathogen Streptococcus pneumoniae. *Science* 313(5783):89-92.
51. Slager J, Kjos M, Attaiech L, & Veening JW (2014) Antibiotic-induced replication stress triggers bacterial competence by increasing gene dosage near the origin. *Cell* 157(2):395-406.
52. Claverys JP, Martin B, & Havarstein LS (2007) Competence-induced fratricide in streptococci. *Mol Microbiol* 64(6):1423-1433.
53. Kreth J, Merritt J, Shi W, & Qi F (2005) Co-ordinated bacteriocin production and competence development: a possible mechanism for taking up DNA from neighbouring species. *Mol Microbiol* 57(2):392-404.
54. Claverys JP & Havarstein LS (2007) Cannibalism and fratricide: mechanisms and raisons d'etre. *Nat Rev Microbiol* 5(3):219-229.
55. Cornejo OE, McGee L, & Rozen DE (2010) Polymorphic competence peptides do not restrict recombination in Streptococcus pneumoniae. *Mol Biol Evol* 27(3):694-702.
56. Carrolo M, Pinto FR, Melo-Cristino J, & Ramirez M (2009) Pherotypes are driving genetic differentiation within Streptococcus pneumoniae. *BMC Microbiol* 9:191.

57. Takemura AF, Chien DM, & Polz MF (2014) Associations and dynamics of Vibrionaceae in the environment, from the genus to the population level. *Front Microbiol* 5:38.
58. Martinez-Urtaza J*, et al.* (2012) Ecological determinants of the occurrence and dynamics of Vibrio parahaemolyticus in offshore areas. *ISME J* 6(5):994-1006.
59. Yamamoto S, Morita M, Izumiya H, & Watanabe H (2010) Chitin disaccharide (GlcNAc)2 induces natural competence in Vibrio cholerae through transcriptional and translational activation of a positive regulatory gene tfoXVC. *Gene* 457(1-2):42-49.
60. Borgeaud S, Metzger LC, Scrignari T, & Blokesch M (2015) The type VI secretion system of Vibrio cholerae fosters horizontal gene transfer. *Science* 347(6217):63-67.
61. Unterweger D*, et al.* (2014) The Vibrio cholerae type VI secretion system employs diverse effector modules for intraspecific competition. *Nat Commun* 5:3549.
62. Hauser AR, Jain M, Bar-Meir M, & McColley SA (2011) Clinical significance of microbial infection and adaptation in cystic fibrosis. *Clin Microbiol Rev* 24(1):29-70.
63. Gjodsbol K*, et al.* (2006) Multiple bacterial species reside in chronic wounds: a longitudinal study. *Int Wound J* 3(3):225-231.
64. Rudkjobing VB*, et al.* (2012) The microorganisms in chronically infected end-stage and non-end-stage cystic fibrosis patients. *FEMS Immunol Med Microbiol* 65(2):236-244.
65. Li J*, et al.* (2015) SecReT6: a web-based resource for type VI secretion systems found in bacteria. *Environ Microbiol*.
66. Russell AB, Peterson SB, & Mougous JD (2014) Type VI secretion system effectors: poisons with a purpose. *Nature reviews. Microbiology* 12(2):137-148.
67. Hood RD*, et al.* (2010) A type VI secretion system of Pseudomonas aeruginosa targets a toxin to bacteria. *Cell Host Microbe* 7(1):25-37.
68. Russell AB*, et al.* (2011) Type VI secretion delivers bacteriolytic effectors to target cells. *Nature* 475(7356):343-347.
69. Hachani A, Allsopp LP, Oduko Y, & Filloux A (2014) The VgrG proteins are "a la carte" delivery systems for bacterial type VI effectors. *J Biol Chem* 289(25):17872-17884.
70. Silverman JM*, et al.* (2013) Haemolysin Coregulated Protein Is an Exported Receptor and Chaperone of Type VI Secretion Substrates. *Mol Cell* 51(5):584-593.
71. Whitney JC*, et al.* (2014) Genetically distinct pathways guide effector export through the type VI secretion system. *Molecular microbiology* 92(3):529-542.
72. Shneider MM*, et al.* (2013) PAAR-repeat proteins sharpen and diversify the type VI secretion system spike. *Nature* 500(7462):350-353.
73. Brunet YR, Henin J, Celia H, & Cascales E (2014) Type VI secretion and bacteriophage tail tubes share a common assembly pathway. *EMBO Rep* 15(3):315-321.
74. Bonemann G, Pietrosiuk A, Diemand A, Zentgraf H, & Mogk A (2009) Remodelling of VipA/VipB tubules by ClpV-mediated threading is crucial for type VI protein secretion. *The EMBO journal* 28(4):315-325.
75. Kapitein N*, et al.* (2013) ClpV recycles VipA/VipB tubules and prevents non-productive tubule formation to ensure efficient type VI protein secretion. *Molecular microbiology* 87(5):1013-1028.
76. Jiang F, Waterfield NR, Yang J, Yang G, & Jin Q (2014) A Pseudomonas aeruginosa type VI secretion phospholipase D effector targets both prokaryotic and eukaryotic cells. *Cell Host Microbe* 15(5):600-610.

77. Russell AB*, et al.* (2013) Diverse type VI secretion phospholipases are functionally plastic antibacterial effectors. *Nature* 496(7446):508-512.
78. Silverman JM, Brunet YR, Cascales E, & Mougous JD (2012) Structure and Regulation of the Type VI Secretion System. *Annu Rev Microbiol* 66:453-473.
79. Lesic B, Starkey M, He J, Hazan R, & Rahme LG (2009) Quorum sensing differentially regulates Pseudomonas aeruginosa type VI secretion locus I and homologous loci II and III, which are required for pathogenesis. *Microbiology* 155(Pt 9):2845-2855.
80. Goodman AL*, et al.* (2004) A signaling network reciprocally regulates genes associated with acute infection and chronic persistence in Pseudomonas aeruginosa. *Dev Cell* 7(5):745-754.
81. Hsu F, Schwarz S, & Mougous JD (2009) TagR promotes PpkA-catalysed type VI secretion activation in Pseudomonas aeruginosa. *Mol Microbiol* 72(5):1111-1125.
82. Mougous JD, Gifford CA, Ramsdell TL, & Mekalanos JJ (2007) Threonine phosphorylation post-translationally regulates protein secretion in Pseudomonas aeruginosa. *Nature cell biology* 9(7):797-803.
83. Casabona MG*, et al.* (2013) An ABC transporter and an outer membrane lipoprotein participate in posttranslational activation of type VI secretion in Pseudomonas aeruginosa. *Environ Microbiol* 15(2):471-486.
84. Fuqua C, Parsek MR, & Greenberg EP (2001) Regulation of gene expression by cell-to-cell communication: acyl-homoserine lactone quorum sensing. *Annu Rev Genet* 35:439-468.
85. Waters CM & Bassler BL (2005) Quorum sensing: cell-to-cell communication in bacteria. *Annu Rev Cell Dev Biol* 21:319-346.
86. Blango MG & Mulvey MA (2009) Bacterial landlines: contact-dependent signaling in bacterial populations. *Curr Opin Microbiol* 12(2):177-181.
87. Pathak DT*, et al.* (2012) Cell contact-dependent outer membrane exchange in myxobacteria: genetic determinants and mechanism. *PLoS Genet* 8(4):e1002626.
88. Aoki SK*, et al.* (2010) A widespread family of polymorphic contact-dependent toxin delivery systems in bacteria. *Nature* 468(7322):439-442.
89. Russell AB*, et al.* (2012) A widespread bacterial type VI secretion effector superfamily identified using a heuristic approach. *Cell Host Microbe* 11(5):538-549.
90. Li M*, et al.* (2012) Structural basis for type VI secretion effector recognition by a cognate immunity protein. *PLoS Pathog* 8(4):e1002613.
91. Chou S*, et al.* (2012) Structure of a Peptidoglycan Amidase Effector Targeted to Gram-Negative Bacteria by the Type VI Secretion System. *Cell Rep* 1(6):656-664.
92. Schwarz S*, et al.* (2010) Burkholderia type VI secretion systems have distinct roles in eukaryotic and bacterial cell interactions. *PLoS Pathog* 6(8).
93. MacIntyre DL, Miyata ST, Kitaoka M, & Pukatzki S (2010) The Vibrio cholerae type VI secretion system displays antimicrobial properties. *Proc Natl Acad Sci U S A* 107(45):19520-19524.
94. Murdoch SL*, et al.* (2011) The opportunistic pathogen Serratia marcescens utilises Type VI Secretion to target bacterial competitors. *J Bacteriol*.
95. Locke JC & Elowitz MB (2009) Using movies to analyse gene circuit dynamics in single cells. *Nat Rev Microbiol* 7(5):383-392.

96. Sliusarenko O, Heinritz J, Emonet T, & Jacobs-Wagner C (2011) High-throughput, subpixel precision analysis of bacterial morphogenesis and intracellular spatio-temporal dynamics. *Mol Microbiol* 80(3):612-627.
97. Klein J*, et al.* (2012) TLM-Tracker: Software for cell segmentation, tracking and lineage analysis in time-lapse microscopy movies. *Bioinformatics*.
98. Brencic A & Lory S (2009) Determination of the regulon and identification of novel mRNA targets of Pseudomonas aeruginosa RsmA. *Mol Microbiol* 72(3):612-632.
99. Basler M & Mekalanos JJ (2012) Type 6 Secretion Dynamics Within and Between Bacterial Cells. *Science* 337(6096):815.
100. Hachani A*, et al.* (2011) Type VI secretion system in Pseudomonas aeruginosa: secretion and multimerization of VgrG proteins. *J Biol Chem* 286(14):12317-12327.
101. Mougous JD*, et al.* (2006) A virulence locus of Pseudomonas aeruginosa encodes a protein secretion apparatus. *Science* 312(5779):1526-1530.
102. Leiman PG*, et al.* (2009) Type VI secretion apparatus and phage tail-associated protein complexes share a common evolutionary origin. *Proc Natl Acad Sci U S A* 106(11):4154-4159.
103. Basler M, Pilhofer M, Henderson GP, Jensen GJ, & Mekalanos JJ (2012) Type VI secretion requires a dynamic contractile phage tail-like structure. *Nature* 483(7388):182-186.
104. Zheng J & Leung KY (2007) Dissection of a type VI secretion system in Edwardsiella tarda. *Mol Microbiol* 66(5):1192-1206.
105. Bohne J, Yim A, & Binns AN (1998) The Ti plasmid increases the efficiency of Agrobacterium tumefaciens as a recipient in virB-mediated conjugal transfer of an IncQ plasmid. *Proc Natl Acad Sci U S A* 95(12):7057-7062.
106. Stover CK*, et al.* (2000) Complete genome sequence of Pseudomonas aeruginosa PA01, an opportunistic pathogen. *Nature* 406(6799):959-964.
107. Rietsch A, Vallet-Gely I, Dove SL, & Mekalanos JJ (2005) ExsE, a secreted regulator of type III secretion genes in Pseudomonas aeruginosa. *Proc Natl Acad Sci U S A* 102(22):8006-8011.
108. Choi KH & Schweizer HP (2006) mini-Tn7 insertion in bacteria with single attTn7 sites: example Pseudomonas aeruginosa. *Nature protocols* 1(1):153-161.
109. Cummings LA, Wilkerson WD, Bergsbaken T, & Cookson BT (2006) In vivo, fliC expression by Salmonella enterica serovar Typhimurium is heterogeneous, regulated by ClpX, and anatomically restricted. *Mol Microbiol* 61(3):795-809.
110. Vance RE, Rietsch A, & Mekalanos JJ (2005) Role of the type III secreted exoenzymes S, T, and Y in systemic spread of Pseudomonas aeruginosa PAO1 in vivo. *Infection and immunity* 73(3):1706-1713.
111. Russell AB*, et al.* (2012) A widespread type VI secretion effector superfamily identified using a heuristic approach. *Cell Host Microbe* in press.
112. Palmer KL, Aye LM, & Whiteley M (2007) Nutritional cues control Pseudomonas aeruginosa multicellular behavior in cystic fibrosis sputum. *J Bacteriol* 189(22):8079-8087.
113. Martinez-Garcia E, Calles B, Arevalo-Rodriguez M, & de Lorenzo V (2011) pBAM1: an all-synthetic genetic tool for analysis and construction of complex bacterial phenotypes. *BMC Microbiol* 11:38.

114. Castang S & Dove SL (2012) Basis for the essentiality of H-NS family members in Pseudomonas aeruginosa. *J Bacteriol* 194(18):5101-5109.
115. Little AE, Robinson CJ, Peterson SB, Raffa KF, & Handelsman J (2008) Rules of engagement: interspecies interactions that regulate microbial communities. *Annu Rev Microbiol* 62:375-401.
116. Linares JF, Gustafsson I, Baquero F, & Martinez JL (2006) Antibiotics as intermicrobial signaling agents instead of weapons. *Proceedings of the National Academy of Sciences of the United States of America* 103(51):19484-19489.
117. Andersson DI & Hughes D (2014) Microbiological effects of sublethal levels of antibiotics. *Nature reviews. Microbiology* 12(7):465-478.
118. Konovalova A & Sogaard-Andersen L (2011) Close encounters: contact-dependent interactions in bacteria. *Mol Microbiol* 81(2):297-301.
119. Coulthurst SJ (2013) The Type VI secretion system - a widespread and versatile cell targeting system. *Res Microbiol* 164(6):640-654.
120. Leroux M*, et al.* (2012) Quantitative single-cell characterization of bacterial interactions reveals type VI secretion is a double-edged sword. *Proceedings of the National Academy of Sciences of the United States of America* 109(48):19804-19809.
121. Durand E, Cambillau C, Cascales E, & Journet L (2014) VgrG, Tae, Tle, and beyond: the versatile arsenal of Type VI secretion effectors. *Trends in microbiology* 22(9):498-507.
122. Benz J & Meinhart A (2014) Antibacterial effector/immunity systems: it's just the tip of the iceberg. *Curr Opin Microbiol* 17:1-10.
123. Russell AB*, et al.* (2014) A type VI secretion-related pathway in Bacteroidetes mediates interbacterial antagonism. *Cell Host Microbe* 16(2):227-236.
124. Mougous JD*, et al.* (2006) A sulfated metabolite produced by stf3 negatively regulates the virulence of Mycobacterium tuberculosis. *Proc Natl Acad Sci U S A* 103(11):4258-4263.
125. Lapouge K, Schubert M, Allain FH, & Haas D (2008) Gac/Rsm signal transduction pathway of gamma-proteobacteria: from RNA recognition to regulation of social behaviour. *Mol Microbiol* 67(2):241-253.
126. Goodman AL*, et al.* (2009) Direct interaction between sensor kinase proteins mediates acute and chronic disease phenotypes in a bacterial pathogen. *Genes Dev* 23(2):249-259.
127. Ventre I*, et al.* (2006) Multiple sensors control reciprocal expression of Pseudomonas aeruginosa regulatory RNA and virulence genes. *Proc Natl Acad Sci U S A* 103(1):171-176.
128. Laville J*, et al.* (1992) Global control in Pseudomonas fluorescens mediating antibiotic synthesis and suppression of black root rot of tobacco. *Proceedings of the National Academy of Sciences of the United States of America* 89(5):1562-1566.
129. Dubuis C & Haas D (2007) Cross-species GacA-controlled induction of antibiosis in pseudomonads. *Appl Environ Microbiol* 73(2):650-654.
130. Silverman JM*, et al.* (2011) Separate inputs modulate phosphorylation-dependent and -independent type VI secretion activation. *Mol Microbiol* 82(5):1277-1290.
131. Basler M, Ho BT, & Mekalanos JJ (2013) Tit-for-tat: type VI secretion system counterattack during bacterial cell-cell interactions. *Cell* 152(4):884-894.
132. Ho BT, Basler M, & Mekalanos JJ (2013) Type 6 secretion system-mediated immunity to type 4 secretion system-mediated gene transfer. *Science* 342(6155):250-253.

133. Felisberto-Rodrigues C*, et al.* (2011) Towards a structural comprehension of bacterial type VI secretion systems: characterization of the TssJ-TssM complex of an Escherichia coli pathovar. *PLoS Pathog* 7(11):e1002386.
134. Cascales E & Cambillau C (2012) Structural biology of type VI secretion systems. *Philos Trans R Soc Lond B Biol Sci* 367(1592):1102-1111.
135. Koskiniemi S*, et al.* (2013) Rhs proteins from diverse bacteria mediate intercellular competition. *Proceedings of the National Academy of Sciences of the United States of America* 110(17):7032-7037.
136. Marden JN*, et al.* (2013) An unusual CsrA family member operates in series with RsmA to amplify posttranscriptional responses in Pseudomonas aeruginosa. *Proceedings of the National Academy of Sciences of the United States of America* 110(37):15055-15060.
137. Robert-Genthon M*, et al.* (2013) Unique features of a Pseudomonas aeruginosa alpha2-macroglobulin homolog. *MBio* 4(4).
138. Jimenez PN*, et al.* (2012) The multiple signaling systems regulating virulence in Pseudomonas aeruginosa. *Microbiology and molecular biology reviews : MMBR* 76(1):46-65.
139. Jing X, Jaw J, Robinson HH, & Schubot FD (2010) Crystal structure and oligomeric state of the RetS signaling kinase sensory domain. *Proteins* 78(7):1631-1640.
140. Vincent F*, et al.* (2010) Distinct oligomeric forms of the Pseudomonas aeruginosa RetS sensor domain modulate accessibility to the ligand binding site. *Environ Microbiol* 12(6):1775-1786.
141. Subramanian A*, et al.* (2005) Gene set enrichment analysis: a knowledge-based approach for interpreting genome-wide expression profiles. *Proc Natl Acad Sci U S A* 102(43):15545-15550.
142. Mootha VK*, et al.* (2003) PGC-1alpha-responsive genes involved in oxidative phosphorylation are coordinately downregulated in human diabetes. *Nature genetics* 34(3):267-273.
143. Pansegrau W*, et al.* (1994) Complete nucleotide sequence of Birmingham IncP alpha plasmids. Compilation and comparative analysis. *Journal of molecular biology* 239(5):623-663.
144. Waters VL, Strack B, Pansegrau W, Lanka E, & Guiney DG (1992) Mutational analysis of essential IncP alpha plasmid transfer genes traF and traG and involvement of traF in phage sensitivity. *Journal of bacteriology* 174(20):6666-6673.
145. Kaczmarek A, Vandenabeele P, & Krysko DV (2013) Necroptosis: the release of damage-associated molecular patterns and its physiological relevance. *Immunity* 38(2):209-223.
146. Matzinger P (1994) Tolerance, danger, and the extended family. *Annu Rev Immunol* 12:991-1045.
147. Lee VT*, et al.* (2007) A cyclic-di-GMP receptor required for bacterial exopolysaccharide production. *Molecular microbiology* 65(6):1474-1484.
148. Irie Y*, et al.* (2012) Self-produced exopolysaccharide is a signal that stimulates biofilm formation in Pseudomonas aeruginosa. *Proceedings of the National Academy of Sciences of the United States of America* 109(50):20632-20636.
149. Colvin KM*, et al.* (2011) The pel polysaccharide can serve a structural and protective role in the biofilm matrix of Pseudomonas aeruginosa. *PLoS pathogens* 7(1):e1001264.

150. Billings N*, et al.* (2013) The extracellular matrix Component Psl provides fast-acting antibiotic defense in Pseudomonas aeruginosa biofilms. *PLoS pathogens* 9(8):e1003526.
151. Barrow K & Kwon DH (2009) Alterations in two-component regulatory systems of phoPQ and pmrAB are associated with polymyxin B resistance in clinical isolates of Pseudomonas aeruginosa. *Antimicrobial agents and chemotherapy* 53(12):5150-5154.
152. Korgaonkar A, Trivedi U, Rumbaugh KP, & Whiteley M (2013) Community surveillance enhances Pseudomonas aeruginosa virulence during polymicrobial infection. *Proceedings of the National Academy of Sciences of the United States of America* 110(3):1059-1064.
153. Cascales E*, et al.* (2007) Colicin biology. *Microbiol Mol Biol Rev* 71(1):158-229.
154. Borgeaud S, Metzger LC, Scrignari T, & Blokesch M (2015) Bacterial evolution. The type VI secretion system of Vibrio cholerae fosters horizontal gene transfer. *Science* 347(6217):63-67.
155. Yu Y*, et al.* (2006) Genomic patterns of pathogen evolution revealed by comparison of Burkholderia pseudomallei, the causative agent of melioidosis, to avirulent Burkholderia thailandensis. *BMC Microbiol* 6:46.
156. Ren Y*, et al.* (2010) Complete genome sequence of Enterobacter cloacae subsp. cloacae type strain ATCC 13047. *Journal of bacteriology* 192(9):2463-2464.
157. Panicker MM & Minkley EG, Jr. (1985) DNA transfer occurs during a cell surface contact stage of F sex factor-mediated bacterial conjugation. *Journal of bacteriology* 162(2):584-590.
158. Chandler JR*, et al.* (2009) Mutational analysis of Burkholderia thailandensis quorum sensing and self-aggregation. *J Bacteriol* 191(19):5901-5909.
159. Hoang TT, Kutchma AJ, Becher A, & Schweizer HP (2000) Integration-proficient plasmids for Pseudomonas aeruginosa: site-specific integration and use for engineering of reporter and expression strains. *Plasmid* 43(1):59-72.
160. Choi KH*, et al.* (2005) A Tn7-based broad-range bacterial cloning and expression system. *Nature methods* 2(6):443-448.
161. Datsenko KA & Wanner BL (2000) One-step inactivation of chromosomal genes in Escherichia coli K-12 using PCR products. *Proceedings of the National Academy of Sciences of the United States of America* 97(12):6640-6645.
162. Liu H, Sadygov RG, & Yates JR, 3rd (2004) A model for random sampling and estimation of relative protein abundance in shotgun proteomics. *Analytical chemistry* 76(14):4193-4201.
163. Yuan J & Kroemer G (2010) Alternative cell death mechanisms in development and beyond. *Genes Dev* 24(23):2592-2602.
164. Raff M (1998) Cell suicide for beginners. *Nature* 396(6707):119-122.
165. Brinkmann V & Zychlinsky A (2007) Beneficial suicide: why neutrophils die to make NETs. *Nat Rev Microbiol* 5(8):577-582.
166. Pearson JS*, et al.* (2013) A type III effector antagonizes death receptor signalling during bacterial gut infection. *Nature* 501(7466):247-251.
167. Engelberg-Kulka H, Amitai S, Kolodkin-Gal I, & Hazan R (2006) Bacterial programmed cell death and multicellular behavior in bacteria. *PLoS Genet* 2(10):e135.
168. Bayles KW (2014) Bacterial programmed cell death: making sense of a paradox. *Nat Rev Microbiol* 12(1):63-69.

169. Hazan R & Engelberg-Kulka H (2004) Escherichia coli mazEF-mediated cell death as a defense mechanism that inhibits the spread of phage P1. *Mol Genet Genomics* 272(2):227-234.
170. Rice KC*, et al.* (2007) The cidA murein hydrolase regulator contributes to DNA release and biofilm development in Staphylococcus aureus. *Proc Natl Acad Sci U S A* 104(19):8113-8118.
171. Ma L*, et al.* (2009) Assembly and development of the Pseudomonas aeruginosa biofilm matrix. *PLoS Pathog* 5(3):e1000354.
172. Erental A, Kalderon Z, Saada A, Smith Y, & Engelberg-Kulka H (2014) Apoptosis-like death, an extreme SOS response in Escherichia coli. *MBio* 5(4):e01426-01414.
173. Erental A, Sharon I, & Engelberg-Kulka H (2012) Two programmed cell death systems in Escherichia coli: an apoptotic-like death is inhibited by the mazEF-mediated death pathway. *PLoS Biol* 10(3):e1001281.
174. Lyczak JB, Cannon CL, & Pier GB (2002) Lung infections associated with cystic fibrosis. *Clin Microbiol Rev* 15(2):194-222.
175. Chastre J & Fagon JY (2002) Ventilator-associated pneumonia. *Am J Respir Crit Care Med* 165(7):867-903.
176. Winsor GL*, et al.* (2011) Pseudomonas Genome Database: improved comparative analysis and population genomics capability for Pseudomonas genomes. *Nucleic Acids Res* 39(Database issue):D596-600.
177. Sauer RT, Jordan SR, & Pabo CO (1990) Lambda repressor: a model system for understanding protein-DNA interactions and protein stability. *Adv Protein Chem* 40:1-61.
178. Jacobs MA*, et al.* (2003) Comprehensive transposon mutant library of Pseudomonas aeruginosa. *Proc Natl Acad Sci U S A* 100(24):14339-14344.
179. Liberati NT*, et al.* (2006) An ordered, nonredundant library of Pseudomonas aeruginosa strain PA14 transposon insertion mutants. *Proc Natl Acad Sci U S A* 103(8):2833-2838.
180. Castang S, McManus HR, Turner KH, & Dove SL (2008) H-NS family members function coordinately in an opportunistic pathogen. *Proc Natl Acad Sci U S A* 105(48):18947-18952.
181. Luo Y*, et al.* (2001) Crystal structure of LexA: a conformational switch for regulation of self-cleavage. *Cell* 106(5):585-594.
182. Goldman SR*, et al.* (2011) NanoRNAs prime transcription initiation in vivo. *Mol Cell* 42(6):817-825.
183. Wang IN, Smith DL, & Young R (2000) Holins: the protein clocks of bacteriophage infections. *Annu Rev Microbiol* 54:799-825.
184. Pang X*, et al.* (2011) Active Bax and Bak are functional holins. *Genes Dev* 25(21):2278-2290.
185. Kropinski AM (2000) Sequence of the genome of the temperate, serotype-converting, Pseudomonas aeruginosa bacteriophage D3. *J Bacteriol* 182(21):6066-6074.
186. Nakayama K*, et al.* (2000) The R-type pyocin of Pseudomonas aeruginosa is related to P2 phage, and the F-type is related to lambda phage. *Mol Microbiol* 38(2):213-231.
187. Matsui H, Sano Y, Ishihara H, & Shinomiya T (1993) Regulation of pyocin genes in Pseudomonas aeruginosa by positive (prtN) and negative (prtR) regulatory genes. *J Bacteriol* 175(5):1257-1263.
188. Nathan C & Cunningham-Bussel A (2013) Beyond oxidative stress: an immunologist's guide to reactive oxygen species. *Nat Rev Immunol* 13(5):349-361.

189. Fang FC (2004) Antimicrobial reactive oxygen and nitrogen species: concepts and controversies. *Nat Rev Microbiol* 2(10):820-832.
190. Wagner PL*, et al.* (2002) Bacteriophage control of Shiga toxin 1 production and release by Escherichia coli. *Mol Microbiol* 44(4):957-970.
191. Whitchurch CB, Tolker-Nielsen T, Ragas PC, & Mattick JS (2002) Extracellular DNA required for bacterial biofilm formation. *Science* 295(5559):1487.
192. Thomas VC*, et al.* (2014) A central role for carbon-overflow pathways in the modulation of bacterial cell death. *PLoS Pathog* 10(6):e1004205.
193. Cirz RT, O'Neill BM, Hammond JA, Head SR, & Romesberg FE (2006) Defining the Pseudomonas aeruginosa SOS response and its role in the global response to the antibiotic ciprofloxacin. *J Bacteriol* 188(20):7101-7110.
194. Hamilton JJ*, et al.* (2014) A holin and an endopeptidase are essential for chitinolytic protein secretion in Serratia marcescens. *J Cell Biol* 207(5):615-626.
195. Wolfgang MC*, et al.* (2003) Conservation of genome content and virulence determinants among clinical and environmental isolates of Pseudomonas aeruginosa. *Proc Natl Acad Sci U S A* 100(14):8484-8489.
196. Whipple FW (1998) Genetic analysis of prokaryotic and eukaryotic DNA-binding proteins in Escherichia coli. *Nucleic Acids Res* 26(16):3700-3706.
197. Vallet-Gely I, Donovan KE, Fang R, Joung JK, & Dove SL (2005) Repression of phase-variable cup gene expression by H-NS-like proteins in Pseudomonas aeruginosa. *Proc Natl Acad Sci U S A* 102(31):11082-11087.
198. Ramsey KM*, et al.* (2015) Ubiquitous promoter-localization of essential virulence regulators in Francisella tularensis. *PLoS Pathog* 11(4):e1004793.
199. Jackson AA*, et al.* (2013) Anr and its activation by PlcH activity in Pseudomonas aeruginosa host colonization and virulence. *J Bacteriol* 195(13):3093-3104.
200. Castang S & Dove SL (2010) High-order oligomerization is required for the function of the H-NS family member MvaT in Pseudomonas aeruginosa. *Mol Microbiol* 78(4):916-931.
201. Group NHW*, et al.* (2009) The NIH Human Microbiome Project. *Genome Res* 19(12):2317-2323.
202. Clemente JC, Ursell LK, Parfrey LW, & Knight R (2012) The impact of the gut microbiota on human health: an integrative view. *Cell* 148(6):1258-1270.
203. Gough E, Shaikh H, & Manges AR (2011) Systematic review of intestinal microbiota transplantation (fecal bacteriotherapy) for recurrent Clostridium difficile infection. *Clin Infect Dis* 53(10):994-1002.
204. Lee SM*, et al.* (2013) Bacterial colonization factors control specificity and stability of the gut microbiota. *Nature* 501(7467):426-429.
205. Mahowald MA*, et al.* (2009) Characterizing a model human gut microbiota composed of members of its two dominant bacterial phyla. *Proc Natl Acad Sci U S A* 106(14):5859-5864.
206. Greenblum S, Chiu HC, Levy R, Carr R, & Borenstein E (2013) Towards a predictive systems-level model of the human microbiome: progress, challenges, and opportunities. *Curr Opin Biotechnol* 24(4):810-820.
207. LeRoux M*, et al.* (2015) Kin cell lysis is a danger signal that activates antibacterial pathways of Pseudomonas aeruginosa. *Elife* 4.

208. Reimmann C*, et al.* (1997) The global activator GacA of Pseudomonas aeruginosa PAO positively controls the production of the autoinducer N-butyryl-homoserine lactone and the formation of the virulence factors pyocyanin, cyanide, and lipase. *Mol Microbiol* 24(2):309-319.
209. Brencic A*, et al.* (2009) The GacS/GacA signal transduction system of Pseudomonas aeruginosa acts exclusively through its control over the transcription of the RsmY and RsmZ regulatory small RNAs. *Mol Microbiol* 73(3):434-445.
210. Marden JN*, et al.* (2013) An unusual CsrA family member operates in series with RsmA to amplify posttranscriptional responses in Pseudomonas aeruginosa. *Proc Natl Acad Sci U S A* 110(37):15055-15060.
211. Kong W*, et al.* (2013) Hybrid sensor kinase PA1611 in Pseudomonas aeruginosa regulates transitions between acute and chronic infection through direct interaction with RetS. *Mol Microbiol* 88(4):784-797.
212. Kay E, Dubuis C, & Haas D (2005) Three small RNAs jointly ensure secondary metabolism and biocontrol in Pseudomonas fluorescens CHA0. *Proc Natl Acad Sci U S A* 102(47):17136-17141.
213. Chavez RG, Alvarez AF, Romeo T, & Georgellis D (2010) The physiological stimulus for the BarA sensor kinase. *J Bacteriol* 192(7):2009-2012.
214. Avican K*, et al.* (2015) Reprogramming of Yersinia from virulent to persistent mode revealed by complex in vivo RNA-seq analysis. *PLoS Pathog* 11(1):e1004600.

Vita

Michele LeRoux was born in Johannesburg, South Africa, and moved to the United States at the age of 13. Following graduation from Sharon High School in Sharon, Massachusetts in 2002, she attended Colgate University where she received a B.A. in Molecular Biology in 2007. In 2015, she received a Doctor of Philosophy degree from the Molecular and Cellular Biology Program at the University of Washington in Seattle where she investigated interbacterial interactions in the laboratory of Dr. Joseph Mougous in the Department of Microbiology.